POLITECNICO DI MILANO

School of Industrial and Information Engineering

Department of Chemistry, Materials and Chemical Engineering
"Giulio Natta"

Master's Degree Thesis in Chemical Engineering

Magnetically controlled microdevices for pH triggered drug release from hydrogels

Advisor: Ing. Filippo Rossi

Co-advisors: Ing. Roberto Bernasconi
Ing. Stefano Rimondo

Albano Filippo, 877259

Gaibotti Davide, 875892

Academic Year 2018/2019

Alle nostre famiglie.

Index

List of Figures

List of Tables

Abstract

The development of novel drug delivery systems is a field subjected to an increasing interest by the scientific community, due to the growing request of more effective therapies, on-demand and tailored disease treatments and drug patents expirations. In this field, a lot of efforts are dedicated to rate-controlled release of drugs, and on-target delivery of drugs.

This double objective might be achieved with the aid of composite materials, i.e. materials that have the best properties of two or more very different systems. This multidisciplinary approach, typical of the drug delivery field, allows exploiting the best features of a lot of different technologies.

In this thesis work, we investigated the possibility of using 3D-printed magnetic microdevices, coated with drug loaded hydrogels, in order to have both the on-target delivery and the controlled and pH-triggered release.

In collaboration with +LAB of Politecnico di Milano the basic scaffold structure of the microdevices has been 3D printed in DL260 resin. With SEE Lab of Politecnico di Milano the metallization procedures have been carried out according to a layer by layer logic, in order to turn them both magnetically actuable and biocompatible.

Once metallized, they have been properly coated with the hydrogel Sodium Alginate, which we loaded together with a mimic drug for 2 different set of tests:

- Steric loading of 2 mimic drugs with very different steric hinderance: Rhodamine B and Dextran 70k Da.
- Chemical loading of Rhodamine B to the alginate chains via 2 different kind of bonds: amidic-bond and ester-bond.

At last, in collaboration with ETH of Zurich, the magnetic actuation of the final hydrogel coated microdevices have been tested with the OctoMag technology.

The effect of the hydrogel coating on the mobility of the microdevices has

been tested in apposite arenas by comparing the relationship velocity – frequency of rotation of the magnetic field with the ones of the uncoated microdevices. In this work we were able to obtain both the movement of the samples, and the pH-triggered drug release in the case of chemical loading of the mimic drug.

Sommario

Lo sviluppo di nuovi sistemi di *drug delivery* è un campo di grande interesse da parte della comunità scientifica, a causa della crescente richiesta di terapie più efficaci, trattamenti su misura delle malattie e per le scadenze dei brevetti esistenti. In questo campo, un grande sforzo è dedicato al rilascio controllato nel tempo dei farmaci e alla loro somministrazione mirata nelle zone d'interesse per la cura della malattia.

Questo doppio obiettivo può essere raggiunto con l'aiuto di materiali compositi, cioè aventi le migliori proprietà di due o più sistemi molto diversi. Questo approccio multidisciplinare consente di sfruttare le migliori caratteristiche di tecnologie differenti.

In questo lavoro di tesi, ci siamo occupati di valutare la possibilità di utilizzare microdispositivi magnetici stampati in 3D, rivestiti con un idrogel a sua volta caricato con un farmaco, per avere sia la somministrazione mirata che il rilascio controllato e attivato da pH.

In collaborazione con + LAB del Politecnico di Milano, la struttura di base dei microdispositivi è stata stampata in 3D in resina DL260. Insieme al laboratorio SEE Lab del Politecnico di Milano le procedure di metallizzazione sono state eseguite secondo una logica *layer-by-layer*, al fine di renderle sia magneticamente attuabili che biocompatibili.

Una volta metallizzati, sono stati rivestiti con l'idrogel Alginato di Sodio insieme ad un farmaco mimetico per 2 diversi set di test:

- Caricamento sterico di 2 farmaci mimici con impedenza sterica molto diversa: rodamina B e Destrano 70k Da.
- Caricamento chimico di rodamina B alle catene di alginato tramite 2 tipi di legami: amidico e estere.

  Infine, con la collaborazione dell'ETH di Zurigo, l'attuazione magnetica dei

microdispositivi rivestiti in idrogel è stata testata con la tecnologia OctoMag. L'effetto del rivestimento sulla loro mobilità è stato testato in apposite arene confrontando la relazione velocità – frequenza di rotazione del campo magnetico con quelle dei microdispositivi non rivestiti. In questo lavoro siamo stati in grado di ottenere sia il movimento dei campioni, sia il rilascio del farmaco attivato dal pH nel caso di caricamento chimico del farmaco.

1 Introduction

One of the most important issues in modern medicine is the developing of new and smarter therapeutic strategies to have better efficiencies in diseases treatments while improving patient compliance.

In many cases, the efficiency of newly developed drugs is strongly limited by the inefficiencies related to the administration routes by which they are inserted within the organism so, even if the best medicine is invented from a pharmacodynamic point of view, it is not straightforward that it would be able to achieve the best treatment efficacy.

Conventional drug delivery exploits a non-selective approach, in which the active substance is transported in the whole organisms through physiological systems, such as the blood circulation. Typically, in this case there are issues related to high administration frequencies, and the risk of overdosage and underdosage.

To solve these problems research is focused on targeted drug delivery, through which drugs are released in a controlled way only in correspondence of their target site, thus these technologies exploit a selective and controlled approach resulting in:

- Increasing patient compliance, by decreasing both therapy invasiveness and administration frequencies.
- Increasing the duration of the therapeutic effect while minimizing side-effects.
- Optimized usage of medicines, which can be very expensive.

The topic of this thesis work was to achieve a controlled and targeted drug delivery by coupling the ability of magnetically controlled microdevices to be moved within the organism and the capability of hydrogel to have an enviro-stimuli responsive drug release behaviour.

In the following chapters the microdevices fabrication, the coating

technologies and the functionalizations of hydrogels will be treated both theoretically and practically.

In particular, the work will be composed of the following parts:

- The 3D printing of the basic microdevice's scaffolds, performed in +LAB of Politecnico di Milano, by exploiting the high precision and flexibility of micro stereolithography (μSLA) technique with DL260 resin.
- The metallization of the printed scaffolds, performed in SEE Lab of Politecnico di Milano, by wet metallization techniques to achieve both the biocompatibility and the magnetic actability of the devices exploiting a layer by layer electroless technology.
- The adhesion of different hydrogel types on metallic surfaces, specifically AC1, AC6, AC-PEG and Sodium Alginate where investigated in order to identify the best solution in terms of adhesion, mechanical properties and drug loading effectiveness onto the magnetic microdevices.
- The coating methods, to obtain the best hydrogel coating on a point of view of quantity and homogeneity.
- Hydrogel functionalizations, to make it able to have a pH triggered release behaviour of the Rhodamine B mimic drug.
- Release studies of the sterically loaded mimic drugs, Rhodamine B and Dextran 70k, and the chemically loaded drug (Rhodamine B) in different pH conditions to mimic the physiological conditions of the gastrointestinal system.
- Remote magnetic actuation tests, performed in ETH Zurich with the OctoMag technology, to study the mobility of the hydrogel coated microdevices.

The adhesion tests have been performed on planar samples to avoid the influence of the microdevice's geometry and underline only the metal-hydrogel interaction, studied both in dry conditions and immersed in water, in different

physiological conditions, for different timings.

The coating methods have been analysed in terms of timings, operational steps, cycles and dipping bath composition with different dipping and gelling technological solutions.

The Rhodamine B mimic drug has been chemically loaded into the hydrogel by two different functionalization types, called ester-bond functionalization and amide-bond functionalization. This choice of bonds is based in the fact that, according to literature, they should sever only at low pH, achieving the pH triggered release [1].

The drug release profiles have been analysed at different timings to underline the influence of the functionalization type on the controlled release of the drug.

The release behaviour of the two sterically loaded drugs, Rhodamine B and Dextran 70k, have been investigated in order to underline the influence of the drug size on the release profile, being the Dextran 70k molecule about 100 times bigger than Rhodamine B.

Furthermore, the starting polymer, the functionalized ones, the mimic drug and its synthetized derivatives have been characterized by FT-IR analysis. The release profiles have been obtained by spectrophotometric analysis and the magnetic actuation studies have been performed using apposite built arenas with the OctoMag technology.

2 3D printing and metallization for magnetic actuation

2.1 3D printing

3D printing is a process that creates a 3D object by adding material one layer at a time. It is a very versatile technique that allows to build an object of almost any shape and dimension. 3D printers can be purchased easily for a cheap price and used in a lot of different fields: from homemade objects production to advanced technology applications, like organ or bone printing, scaffolds for biomedical applications [2] and rapid prototyping [3].

2.1.1 Process

The process always starts with a digital model, created with some CAD (computer aided design) package. A STL (Surface Tessellation Language) file is created, then the mesh data are further sliced into a build file of 2D layers and sent to the 3D printing machine [2]. 3D printing technique can differ. In our work the scaffolds are fabricated by means of stereolithography (SLA) [4]. Stereolithography uses photopolymers that can be cured by UV laser, which is controlled in a desired path to shoot in the resin reservoir. Then the photocurable resin polymerizes into a 2D patterned layer. After each layer is cured, the platform lowers, and another layer of uncured resin is applied to be patterned.

Typical polymers used in SLA are acrylic and epoxy resins. Also, photo initiators and UV absorbers can be added to the polymer in order to control the speed and the quality of polymerization.

This 3D printing method presents some advantages: high resolution and

possibility to avoid nozzle clogging. This is in fact a nozzle free technique. On the other hand, a main concern (even more in biological applications) is the possible cytotoxicity of the residual photo initiator and uncured resin [2].

SLA is a method that belongs to the Light polymerized family. Other important families are Material extrusion and Powder Bed.

In Material extrusion (figure 2.1), a thermoplastic polymer is heated and extruded through a nozzle onto the support. There it rapidly hardens. The nozzle moves in the plane while extruding, depositing the polymer in the desired shape. Then either the platform goes down or the nozzle goes up in order to deposit the successive layer.

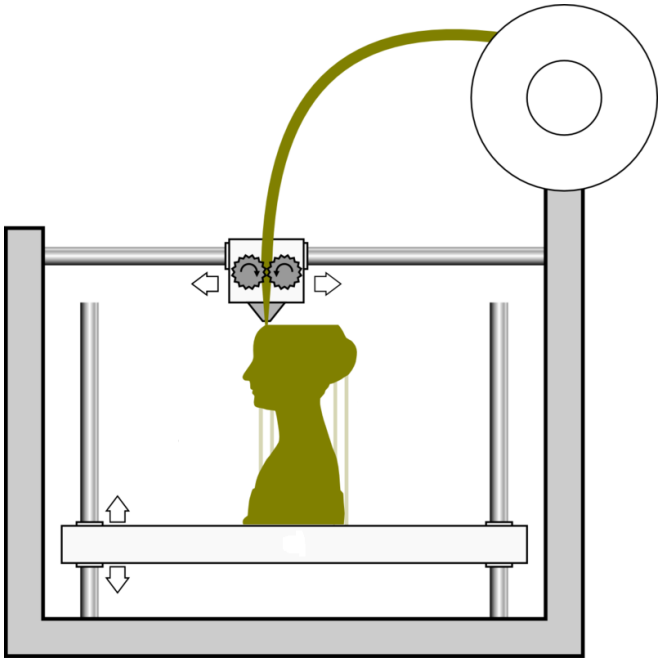

Figure 2.1 - 3D printing via Material extrusion

In powder bed there is a continuous layer of granules. A moving head acts by selectively binding (by laser sintering or gluing) a part of the surface. Then another layer of granules is added, and the process continue in the following layer.

2.2 Electrodeposition

Electrodeposition is the industrial technique used to electrolytically deposit a metallic coating onto a conductive or semi conductive surface. With this process single metals, alloys or composites can be deposited. The aim of this process can be to improve corrosion resistance, superficial hardness or to act on the surface of a metallic piece, turning it magnetic.

2.2.1 The mechanism

The involved reaction is a reduction of metal ions (positive) dispersed in an aqueous solution. The electrons needed for this reduction are provided by an external power supply.

$$M^{n+}(aq) + ne^{-} \rightarrow M(s)$$

As shown in figure 2.2 the object to be plated is the cathode of the circuit, the metal can be (not necessarily) made of the metal to be deposited. Anode and cathode are immersed in a solution called electrolyte, which is an aqueous solution containing ions of the metal to be plated, together with one or more other salts. The purposes of these salts are to permit adequate flow of electricity in the solution and

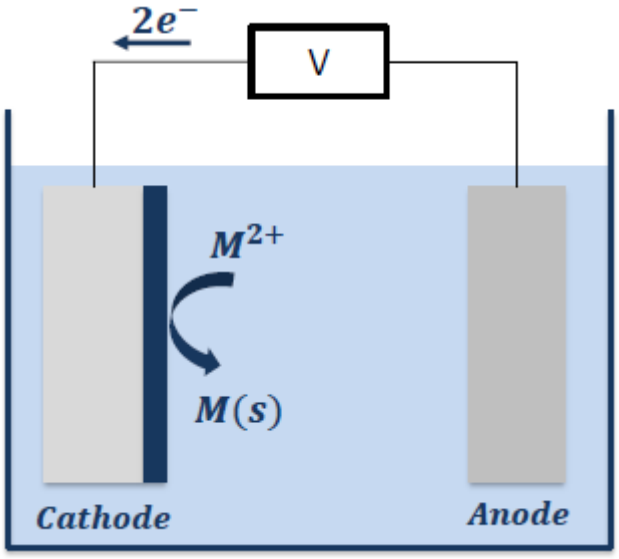

Figure 2.1 - Electrochemical cell

to guarantee the formation of a better deposited layer in terms of strength, brightness and adhesion [5]. Anode and cathode are linked by the solution and by the power source (thus closing the circuit).

Every chemical species has its own reduction potential, i.e. the tendency to acquire electrons and thus be reduced. The more positive the potential, the grater the tendency to be reduced. Therefore, when two metals are placed in a conductive medium and linked by a metal wire, the difference in this potential leads to a difference in cell potential and thus current starts to circulate. The metal with higher reduction potential (cathode) rip electrons off the other one (anode). So negative charge accumulates at the cathode and positive ions in solution migrate towards it. Once there, they take the electrons, reduce to metallic state and stick to the surface of the cathode. On the anode, lack of electrons causes the oxidation of atoms on the surface, consequentially they detach and become positive ions in the liquid medium. The overall result is the transfer of atoms from the surface of the anode to the surface of the cathode. This process is called Electroless deposition. By adding a battery, the potential and the flowing current in the cell can be changed according to thermodynamics and kinetics considerations.

2.2.2 Governing equations

The most important parameter we are concerned with in electrodeposition is the current flowing in the system, because this is directly linked to the rate of electrodeposition via the Faraday's law.

$$\Delta n_i = \frac{\nu_i}{\nu_e} \frac{I * t}{F}$$

Where Δn_i is the number of moles of substance reacted, ν_i and ν_e are respectively the stoichiometric numbers of the product of the reaction and the amount of electrons required per atom of substance reacted. F is the faraday's constant, t is the time and I the circulating current. In order to estimate these current,

other variables, which are now going to be introduced, must be taken into consideration. Anyway, by knowing the number of moles deposited over time, one can estimate both the deposited mass and the thickness variation of the deposit over time.

When there is another potential in the circuit, applied by a battery (in figure 2.2 the rectangular shape with letter V inside), the potential of each electrode (anode and cathode are called electrodes) changes by a value called overpotential. In the following formula E is the new potential, Eeq is the potential without the battery (equilibrium potential) and η is the overpotential.

$$E = Eeq + \eta$$

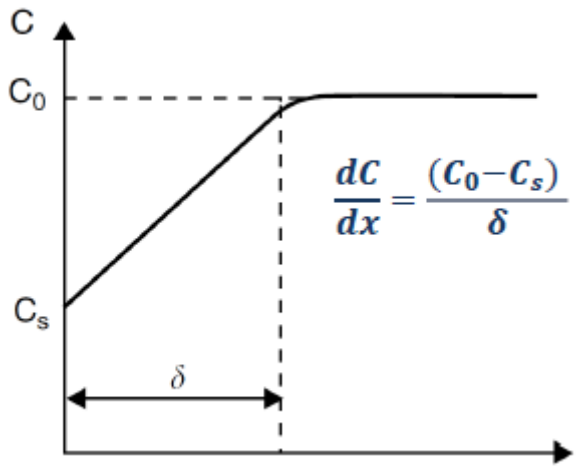

Figure 2.2 - Concentration of the reactive species from bulk to the surface of the electrode

Without the battery, at overpotential zero, the net circulating current is zero. At each electrode the rate of dissolution equals the rate of deposition of atoms, so there is a continuous flow of electrons at the interface. In these conditions the ongoing current in both directions is called exchange current density, here denoted as i_0.

There are basically three different asymptotical behaviours that describe the amount of current flowing in the circuit:

- At low overpotential (<0.01)

$$i = i_0 * \frac{F * \eta}{R * T}$$

- At medium overpotential (around 0.01)

$$i = i_0 * e^{\frac{-\alpha * F * \eta}{R * T}}$$

- At high overpotential (i.e. when E>>Eeq)

$$i = i_{lim}$$

The last case means that when E>>Eeq the reaction is limited by the diffusion of ions towards the electrode surface. The surface reaction is way faster than the diffusion process. So, the current reaches a limit which is called limiting current (i_{lim}).

In figure 2.3 the correlation between concentration and distance from the surface is approximated as linear up to the bulk, where it becomes constant. In the formula contained in the figure, δ is the thickness of the diffusion layer (usually around 0.3-0.5 mm), C_0 and C_s are respectively the bulk and the surface concentration of the reactive species.

$$i_{lim} = n * F * D\frac{dC}{dx}$$

So, by integrating the previous formula, when C_s goes to 0:

$$i_{lim} = n * F * D\frac{C_0}{\delta}$$

2.2.3 Bath formulations

Solutions for electroplating are composed by various components:

- Metal ions of the species to be deposited: they can come from the anode or be added as salts to the solution.
- Other electrolytes: improve conductivity and act as a pH buffer (pH influence deposition).
- Complexing agents: they surround the ions to be deposited, thus preventing them from forming other oxides and unexpected compounds.
- Organic additives: usually they are molecules with high molecular weight. These compounds are used for making the deposit brighter, reducing the

grain size, improve smoothness, reducing stress and pitting [6].

2.2.4 Deposit properties

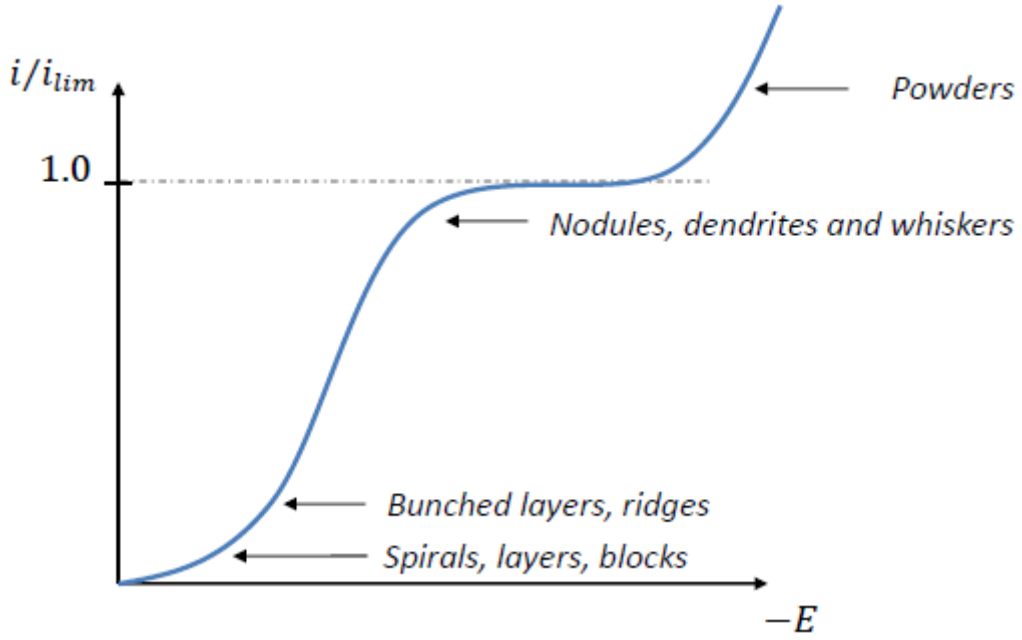

Figure 2.4 - Deposit morphology as a function of the circulating current

Deposit morphology depends mainly on the deposition rate, which depends on the circulating current.

As shown in figure 2.4 and 2.5, by raising the overvoltage (or the circulating current, since they are directly linked, as stated before) the grain size shrinks. This is due to the fact that with the increase in deposition rate, there is not enough time to let the single crystals grow, instead more smaller crystals are formed. Moreover, by increasing the circulating current, a plateau corresponding to the limiting current is reached. After that, by continuously increasing the overvoltage the current starts

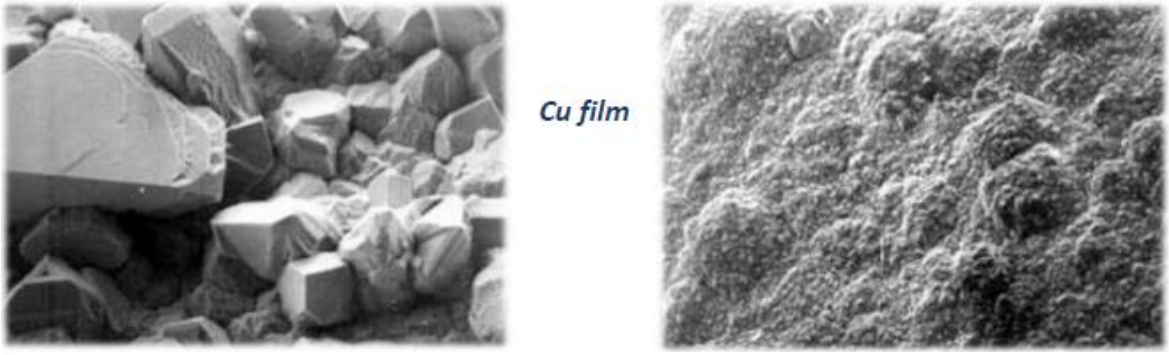

Figure 2.5 - Relationship between overvoltage and grain size

to increase again. This is due to the start of another reaction: the hydrogen evolution.

$$2H^+ + 2e^- \rightarrow H_2$$

This reaction, competitive to the metal ion reduction, cause the formation of gas bubbles on the surface of the growing film. These bubbles grow and then detach from the surface while the film is growing, leaving empty spaces. This complex phenomenon causes the resulting film to look porous or powdery-like.

Another interesting possibility is depositing a composite. By adding for example ceramic particles to the plating bath and maintaining a strong mixing, is possible to entangle these particles in the growing film. As a result, is possible to obtain increasing in hardness, in wear resistance and in corrosion resistance.

2.3 Electroless deposition

Electroless deposition is the industrial technique used to deposit a metallic coating onto a conductive or semi conductive surface, without the application of an external current source. With this process single metals, alloys or composites can be deposited. The aim of this process, as in electrodeposition, can be to improve corrosion resistance, superficial hardness or to turn the surface of a metallic piece magnetic.

This process is only a chemical process, based on redox (reduction-oxidation) reactions. This means that it can take place only if $\Delta G<0$.

$$\Delta G = -zFE$$

Where z is the number of exchanged electrons, F is the faraday's constant and E the standard electrode potential.

There are two different mechanisms through which this process can take place: Galvanic displacement and Autocatalytic deposition.

2.3.1 Galvanic displacement

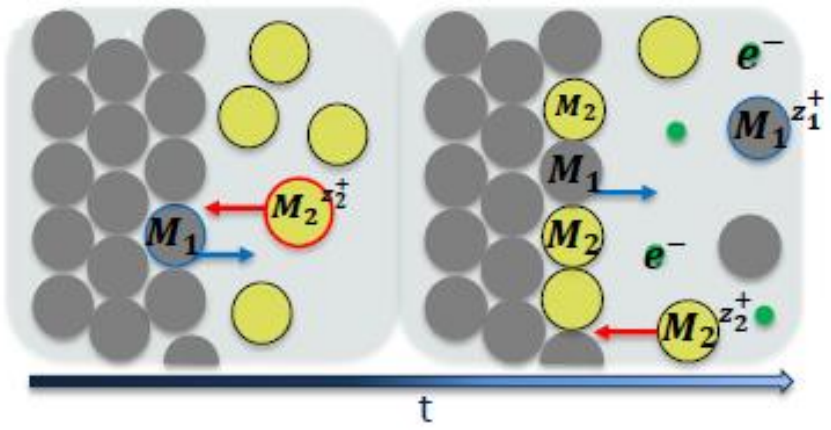

Figure 2.6 - Mechanism of galvanic displacement

It happens when a less noble metal is immersed in a solution containing ions of a more noble metal. The reactions are that of a redox and can be written as follows:

$$M_2^{n+} + ne^- = M_2 \text{ Reduction}$$

$$M_1 = M_1^{n+} + ne^- \text{ Oxidation}$$

Where M_1 is the less noble metal and M_2 is the more noble metal. As a result, the first layer of atoms on the surface of the less noble metal is replaced with atoms of the more noble metal. Intuitively, in theory only a monolayer can be deposited with this method. In practice thicker deposits can be obtained because: deposited metal can be porous or because there is a difference in dissolution and deposition rate between the two metals. In the first case, if the deposited film is porous, the ions of the more noble metal can still penetrate, and redox reaction can continue (figure 2.6).

2.3.2 Autocatalytic deposition

In this process there is still a Redox reaction, the metal to be deposited is dissolved as positive ions in the solution, while there is another chemical species, called reducing agent, which oxidises, providing the electrons for the reduction. Examples of reducing agents are: Formaldehyde, Hydrazine, Sodium Borohydride and Sodium Hypophosphite. The reaction is catalysed by the depositing film itself, hence the name of autocatalytic deposition. This is the overall reaction:

$$M^{n+} + RedAg^{m-} = M + RedAg^{n-m}$$

Where M is the metal to be deposited and RedAg the reducing agent. As opposite to galvanic displacement, with autocatalytic deposition the film thickness has no theoretical limitations.

2.3.3 Comparison between electro and electroless deposition

Deposits from electroless deposition are more uniform in thickness. This is due to the fact that the electrical field is stronger at the edges of object the to be plated. Thus, the deposit is thicker in these parts. Electrodeposition baths are more stable and work at lower temperatures: since the process is controlled by an external source of electrons, there is no need to raise the temperature to favour kinetics.

Another important difference is that with electroless deposition it is possible to deposit also on non-conducting materials. This is possible by prior activation of the non-conducting surface with one of the following methods:

- Immersion in a Colloidal Palladium Suspension
- Immersion in Palladium Chloride Solution
- Immersion in Tin Chloride Solution

2.4 Magnetism in metals and alloys

A magnetic field is produced either by moving electric charges or by the intrinsic magnetic moments of elementary particles (electrons in particular). In the first case, the magnetic field is completely defined by the position and velocity vector of all the electric charges in the system. In the second case, the magnetic moment of each elementary particle is a fixed number, so it depends on the atom or considered molecule. Usually, each electron in a solid generates a magnetic moment pointing in a different random direction, so the material in its whole does not show any magnetic behaviour. Sometimes, spontaneously, or due to the applications of an external electrical (or magnetic) field, the magnetic moments are all lined up, causing the object to generate a coherent magnetic field. Magnetic behaviour of materials can be summarized in the following categories:

- Diamagnetism. Objects repelled by a magnetic field. When an external magnetic field is applied, they produce a magnetic field in the opposite direction. When no magnetic field is applied, they show no sign of magnetism.
- Paramagnetism. Every atomic orbital possesses a permanent dipole, but they are not orientated in any direction. When an external magnetic field is applied, they align in the same direction of the field, reinforcing it.
- Ferromagnetism. Materials that have a magnetic moment without any external magnetic field applied. They originally possess no magnetic field. They are divided into domains of about 10^{12} atoms which possess uniform magnetization in a random direction. When a strong magnetic field is applied and then removed, the domains orientate themselves following the field. When the field is then removed, the domains remain aligned in the same direction as before, so the object will still produce a clear magnetic field. Ferromagnetism is associated with Iron, Cobalt, Nickel and some alloys of

these elements.

2.4.1 CoNiP

There is a big research concerning the realization of high performance, magnetic films used in various fields, like data storage and MEMS actuation [7]. Of particular interest is the electroless deposition of the alloy Cobalt-Nickel-Phosphorous (CoNiP), which shows excellent magnetic properties, together with hardness and a good corrosion resistance.

Electroless CoNiP bath can be made in the following way: "NiSO4·6H2O and CoSO4·6H2O were used as the source of nickel and cobalt, respectively. NaH2PO2·H2O was used as a reducing agent, which also forms the source of phosphorus in the deposit. Na3C6H5O7 was used as the complexing agent to control the rate of release of free metal ions for the reduction reaction. In addition to other constituents, ammonia solution was added to control the bath pH and the bath was operated at a constant temperature 35 ± 1 °C during the deposition process." [7].

2.5 Microrobots

Technically a microrobot is a mechanical device, able to do some trivial operations, which has the characteristic lengths in the order of micrometers. Nowadays there is a great interest in this field due to the advancement in 3D printing technology and metallization, which made easier, and cheaper, the creation of such devices.

2.5.1 Motion

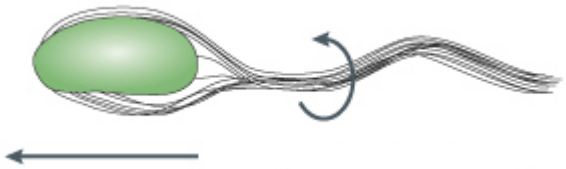

Figure 2.7 - E. Coli bacteria and how they swim

Very challenging, in the size of microscale, is to find a way to effectively move and control these devices. Energy storage is not feasible due to limited dimensions, so they have to be somewhat activated via an external power source. Moreover, in liquids, when the sizes are so low, Reynolds number (which is directly proportional to the characteristic length of the object) can go from 0.1 to 0.0001, i.e. the viscous forces are way more dominant than the inertia forces. Direct consequence of this fact is that, in this condition, swimming by executing geometrically reciprocal motion will not make one move forward.

A common path in order to overcome this problem is to "reverse engineer" microrobots starting by looking at the way bacteria move around in similar conditions. At the end of the nineteen century scientist concluded that all microorganisms use some kind of rotating cilia or flagella to move around, by performing nonreciprocal movements. So, in the same way, artificial magnetic microrobots can rotate under a rotating magnetic field, and with a helical shape flagellum, they can translate this rotational motion in a translational motion [8] (figure 2.7). Otherwise, a microrobot can "roll" on a surface due to the application of a rotating magnetic field. Since these fields are harmless for tissues and cells, this seems to be a promising way to power up these microdevices in biological applications. Other external sources of energy to impress motion to the microrobots can be chemical reaction, ultrasound or light.

2.5.2 Uses

Microrobots can be used for a lot of operations when the direct human intervention is difficult due to danger or due to the human size. An interesting application of these devices is the biomedical one: minimally invasive surgery, cell manipulation and controlled drug delivery [8]. Researchers have designed a device which can be placed into the human eye and moved inside the eye cavity with a magnetic field. The body of the microrobot is dyed in a specific material, which has a luminescent response, proportional to the quantity of oxygen in the surrounding area. It can reveal the levels of oxygen within the eye and thus diagnosticate diseases correlated to oxygen deficit (diabetic retinopathy, glaucoma, and age-related macular degeneration) [9].

Magnetic-actuated biocompatible micro scaffolds can be used to host drugs or cells for transport and release inside the human body in specific locations. 3D printed objects can be enclosed in a magnetic alloy (CoNiP for example), and then in a biocompatible material such as gold or platinum (figure 2.8).

Another application is the so called “swarm of microrobots”. It is a group of small robots in which units interact with each other like a swarm of insects. They can be used for example to search for people inside a collapsed building, swim inside the human body repairing damages or administrating drugs, or to find dangerous chemicals in the air or in the water.

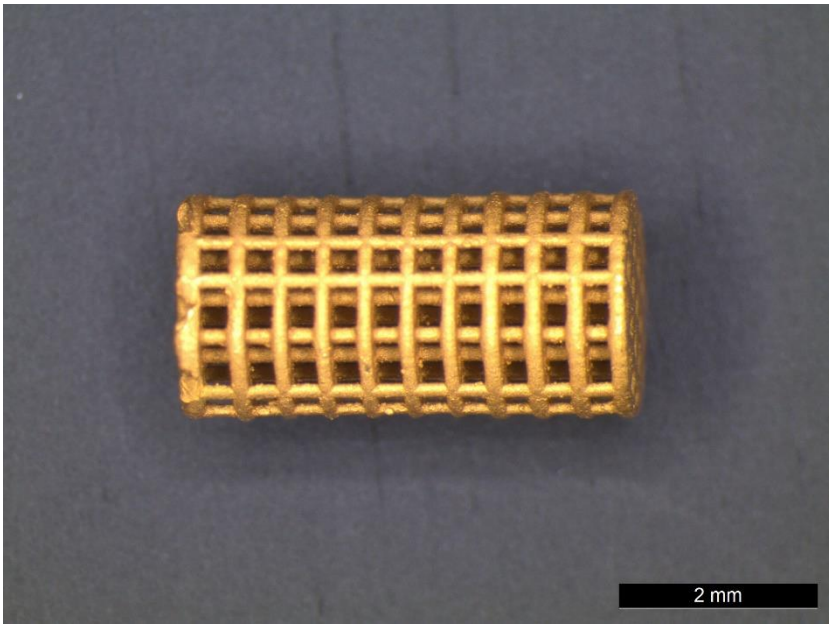

Figure 2.8 - Gold plated magnetic micro scaffold

3 Hydrogels

3.1 Structure

Hydrogels are cross-linked polymers that have the ability to retain a significative quantity of water within their structure without dissolving in the liquid. The ability to avoid dissolution is guaranteed by the cross-linking between the polymeric chains. These chains form a 3-dimensional matrix which entangle the liquid inside [10, 11].

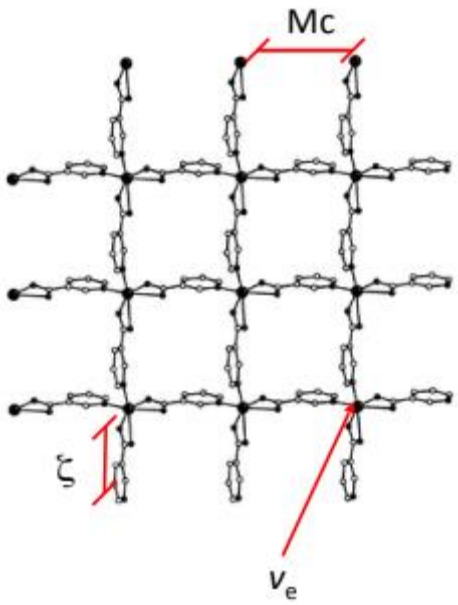

Figure 3.1 - Characteristics of the gel matrix

Figure 3.1 shows an example of this matrix, M_c is the average molecular weight between two following crosslinks, ξ is the mesh size and ν_e is the density of cross-links. M_c depends on X, which is the degree of cross linking of the gel, and M_o, which is the molecular weight of the monomer unit, via the following formula:

$$M_c = \frac{M_o}{2X}$$

The mesh size ξ is the distance between two sequential points of cross-linking and thus, is useful to estimate the space in which a drug or a cell can

eventually diffuse inside the gel:

$$\xi = v_s^{-\frac{1}{3}} * C \left(\frac{M_c}{M_o}\right)^{\frac{1}{2}} = v_s^{-\frac{1}{3}} * C \left(\frac{1}{2X}\right)^{\frac{1}{2}}$$

Where C is a constant depending the polymer and the solvent, and v_s is the polymer volume fraction in the swollen state, defined as the ratio between the volume of the polymer and the volume of the swollen gel.

At last, the density of cross-links ν_e represents the ratio between the density of the polymer and the molecular weight between two following crosslinks:

$$\nu_e = \frac{\rho_p}{M_c} = \frac{2\rho_p X}{M_o}$$

Where ρ_p is the density of the dry polymer.

3.1.1 Swelling

The main characteristic of the hydrogels is the swelling behaviour, i.e. the amount of water it can retain. An indicative parameter called volumetric swelling ratio (Q) can be estimated as follows:

$$Q = \frac{V_{wet}}{V_{dry}}$$

Where V_{wet} is the volume of the hydrogel when completely filled with water, and V_{dry} is the volume when the hydrogel is dry. The volumetric swelling ratio depends on temperature, osmosis and pH. As order of magnitude Q can vary from 0.1 to 100 [12]. Swelling starts by putting a dry hydrogel inside water. Some water molecules will interact directly with the hydrophilic groups of the polymer, these

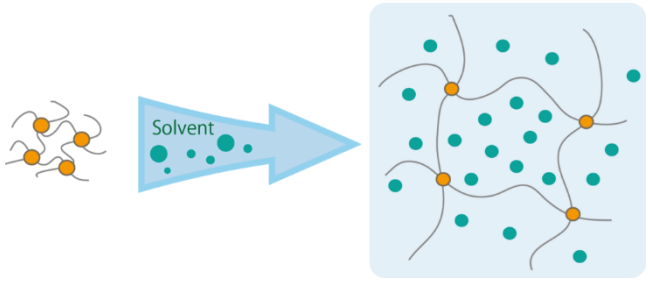

Figure 3.2 - Hydrogel Swelling

molecules compose the primary bound water. Then, the hydrophobic groups are also exposed, and are able to interact with the water molecules forming hydrophobically-bound water, called also secondary bound water. At last, the osmotic driving force of the network chains towards infinite dilution, will cause the adsorption of additional water, called free water, since it is assumed to be filling the pores inside the gel matrix while not being bonded by it (figure 3.2). After some time, a swelling equilibrium is reached. it is important to notice that this equilibrium is given by the balance between the two forces acting against each other: elastic retraction force of the gel and osmotic force causing stretching of the gel matrix.

3.1.2 Degradation

Another important feature is the possibility, and rate, of hydrogel degradation. It can be due to temperature, pH or enzymatic hydrolysis. It can occur on the chains or at the cross-linking points (figure 3.3).

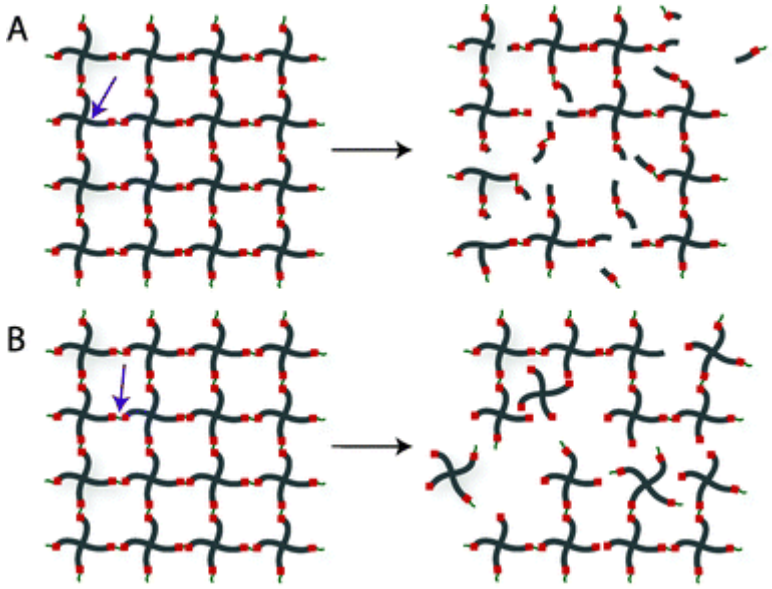

Figure 3.3 - Hydrogel degradation mechanisms: cleavage of the polymer bone (A), cleavage of the cross-linker (B)

Particularly in biomaterial engineering, where hydrogels can be used as artificial tissues, artificial parts of organs, or drug delivery systems, biodegradation is a key characteristic. This is due to the fact that surgical removal of the hydrogel

inside the body, once it has fulfilled its role, is not a trivial operation: at best is painful and annoying for the host. Moreover, in tissue engineering, degradation provides space for cell migration and proliferation, while in drug delivery applications, the progressive decay allows control over the release of charged molecules in terms of space and time. In this case, release kinetics are determined by surface or bulk erosion. Surface erosion occurs when the degraded reaction is faster than the diffusion rate into the network, so the water is adsorbed on the surface before it diffuses into the bulk of the gel. On the contrary, the bulk erosion is characterized by a rate of water diffusion faster than the hydrolysis reaction (This concept will be further discussed later on).

Biodegradation might be achieved by the introduction of labile bonds in the gel matrix. A variety of these kinds of bonds include: esters, imine, acetal, ketal, polyanhydrides and enzymatically labile peptides. These links can be with time cleaved by simple hydrolysis. Of course, also the remains of the hydrogel after hydrolysis needs to be non-toxic and biocompatible, to avoid inflammation, immunological response or cytotoxicity [13].

3.1.3 Porosity

Pore size, distribution and interconnection are three fundamental parameters in hydrogels that are not of easy estimation. This is due to the fact that often, methods to estimate these parameters require solvent or temperature to be changed, causing the hydrogel to shrink or swell, altering the results. Alternatively, this estimation requires mathematical tools, so approximations and assumptions are involved.

Pore size, distribution and interconnections influence mechanical resistance but are also important in other applications. When hydrogels are used for tissue engineering, controlling these parameters means allowing a correct and

homogeneous cell distribution, and diffusion of the nutrients necessary for the cell's growth [13]. At last, when a hydrogel is loaded with a drug, porosity controls the rate of diffusion of this compound outside the gel matrix.

Concerning porosity, gels can be divided in the following categories:

- Non-porous hydrogels.
- Micro-porous hydrogels. Pore size between 100 and 1000 Å.
- Macro-porous hydrogels. Pore size between 0.1 and 1 μm.
- Super-porous hydrogels. Pore size of several hundred of micrometers.

3.2 Preparation

Formation of a hydrogel occurs with polymerization of a monomer and cross-linking between chains. By controlling the degree of cross-linking is possible to regulate almost every other property of the hydrogel. Cross-linking can occur via chemical or physical mechanism [10, 11].

3.2.1 Physical cross-linking

Advantage in physical cross-linking is the ease of production and the advantage of not using a cross-linking agent, which may affect the integrity of the gel, may be toxic, and also needs to be removed after application. While chemical cross-linked hydrogels are usually more stable because physical interactions are usually not so strong.

- Via hydrogen bonds. Complexes formed between polyacrylic acid or polymethacrylic acid with polyethylene glycol. The bond is formed between the oxygen of the polyethylene glycol and the carboxylic group of polyacrylic acid or polymethacrylic acid.
- From amphiphilic graft and block polymers. Amphiphilic graft and block

polymers have ability to self-assemble in aqueous media to form hydrogels and polymeric micelles.

- Via crystallization. Polyvinyl alcohol in water at room temperature create a gel with very poor mechanical strength. When the solution is frozen and then thawed out a very though and elastic gel is formed.
- Via ionic interactions. Sodium alginate can be cross-linked with calcium ions. This occurs at pH 7 and room temperature.
- Via protein interactions.

3.2.2 Chemical cross-linking

- Via chemical reaction of complementary groups. Hydrophilic polymers having -OH groups or polymers having -amine groups bay be cross-linked with glutaraldehyde. This include also addition and condensation reactions.
- Via energy radiation. It can polymerize unsaturated substances.
- Via free radical polymerization. Using energy in the form of temperature of light, radicals are formed. These radicals start a propagation reaction that form the polymeric matrix.
- Via enzymes.

3.2.3 Environmentally responsive hydrogels

Some hydrogels can be considered environmentally responsive, meaning they can turn from solution to gel and vice versa when specific environmental conditions are met [15].

Gel whose gelation behaviour is determined by temperature changes are defined Thermoresponsive. Their sensitivity to temperature is useful in biomedical applications because gelation will occur without the introduction of another chemical and in absence of another environmental treatment. Some Thermoresponsive hydrogels begin gelation above a certain temperature, defined lower critical solution temperature (LCST). Above the LCST, they start to become hydrophobic leading to separation from the solution and then to gel formation. On the other hand, some hydrogels start to form when their temperature goes below an upper critical solution temperature (UCST). When a polymer is dissolved in water, there are three types of interactions that take place: polymer-polymer, polymer-water and water-water. For polymers with an LCST, temperature increase results in a negative free energy of the system, which makes polymer-water association unfavorable, favouring the other two kinds of interaction. For polymers with an UCST the mechanism is the exact opposite. An example of a Thermoresponsive hydrogel is a cellulose derivative: Methylcellulose. Methylcellulose gelation happens when its temperature raises up to 60-80 °C, and it turns back into a solution upon cooling.

Another parameter effecting hydrogels, and in particular their swelling behaviour is the pH. This applies in particular to ionic gels, where acidity enhances swelling in acid hydrogels, due to repulsion between ions of the same charge. In the same way basicity cause an acid gel to shrink. The opposite mechanism happens for basic hydrogels.

3.3 Classifications

- Based on the source: natural (collagen, fibrin, hyaluronic acid, alginate, chitosan), synthetic (polyethylene glycol diacrylate, polyacryl amide) or hybrid.
- Based on composition. In particular referring to the monomers: homopolymeric (single monomeric species), copolymeric (two or more polymeric species arranged at blocks, at random or alternated) or multipolymer interpenetrating polymeric hydrogel (two independent polymers are cross-linked to form the hydrogel matrix).
- Based on configuration: amorphous, semicrystalline or crystalline.
- Based on the type of cross-linking.
- Based on physical appearance: matrix, film or microsphere.
- Based on electrical charge: ionic, non-ionic, amphoteric or zwitterionic.
- Biocompatible or not.

3.4 Applications

Hydrogels are used in a lot of different fields, one of the most famous application is represented by contact lens. In this case main characteristics of the hydrogel are flexibility, biocompatibility and high oxygen permeability. Hydrogel characteristics like high permeability and high retainment of water can also be exploited for the production of super adsorbent diapers. Unlike sponges, which trap liquid in their pores, and then push it out when compressed, hydrogels can hold water inside while also remaining dry on surface.

Other fields in which hydrogels can be exploited are agriculture, where they can hold water and nutrients for the plants without losing it in the ground like normal culture, and cosmetics. Cosmetics is a field in which many innovative

hydrogel applications can be engineered and produced, but, unlike medical devices, the path of approval is way shorter. So, innovations are more common, and progress is faster.

Hydrogels can be a support for bacterial cultures or microorganisms (algae). These bacteria can for example be used for water cleaning or living biosensors for toxic substances [16]. Chlorella and Spirulina are bacteria already used for removing pollutants from water. Their growth can be controlled and protected inside a gel matrix. A second way to solve the problem of water pollution is to modify the hydrogel in order to make it capable to adsorb and retain pollutants. This can be done for example to deal with traces of heavy metals [17] or oil [18] inside the water, both very pressing issues.

Hydrogels can be used in tissue engineering. In this case a hydrogel scaffold is combined with cells from the patient. These cells are growth on the scaffold, which then is used to replace the original tissue that was lost or damaged. Similarly, there is the study to engineer biocompatible hydrogels for bone regeneration [19]. Way more than tissue, bone self-healing is limited, and demands an external aid to make the bone recover completely as it was before. Currently various materials are used, like metal implants (titanium), of calcium phosphate cements. Hydrogels scaffolds can be used to provide a support for cells adhesion and proliferation and can incorporate bioactive growth factors that promote bone repair. Also, being biodegradable these gels will with time be demolished and substituted completely with the host bone cells.

Lastly, and even more important for this particular work, is the possibility to use hydrogels to administrate drug delivery. This topic will be discussed in detail later on.

3.5 Sodium Alginate

Sodium alginate is a polymer typically extracted from seaweed of the class of the Phaeophyceae (brown algae). The alga is treated with NaOH and then filtered. Sodium or calcium chloride is added to precipitate alginate salt. This salt undergoes various other purifications to obtain dry sodium alginate powder [20].

3.5.1 Structure and gelation

Alginate is composed of D-mannuronate (M) and L-guluronate (G). these two components can be arranged in blocks of consecutive G, consecutive M or

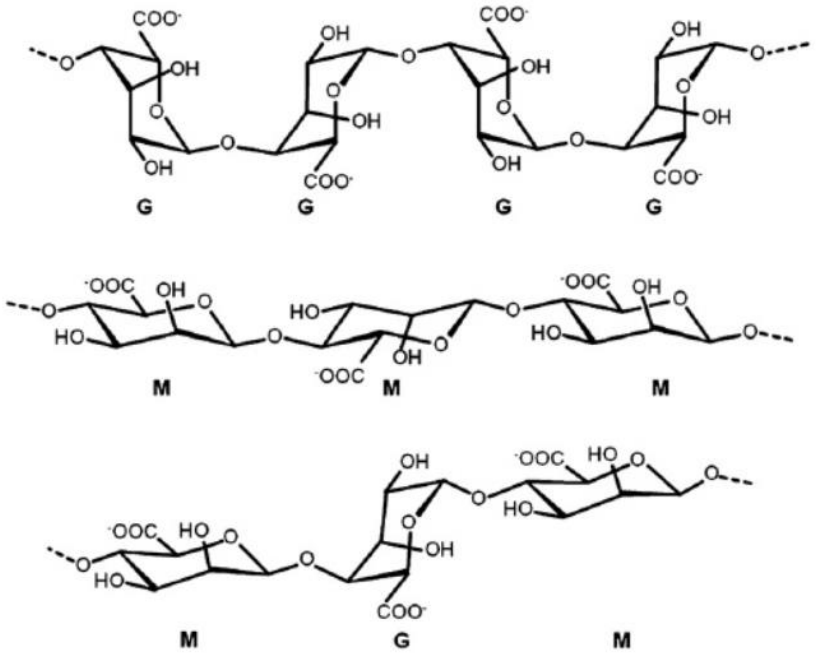

Figure 3.4 - Chemical structures of G-block, M-block, and alternating block in alginate

alternating G and M components (figure 3.4). The content of the two compounds as well as their arrangement depends on the source of the alginate. Only the G components seem to be responsible of cross linking in presence of divalent cations to form hydrogels.

The molecular weight of sodium alginates range between 32,000 and 400,000

g/mol. A sodium alginate with a very high molecular weight can attain an alginate hydrogel with better physical properties, compared to one with lower molecular weight. But, on the other hand, it will also produce a very viscous alginate-water solution (before gelation), which can be bad depending on the process.

Sodium alginate is soluble in aqueous solution, because it has many polar groups. For the same reason it is very difficult to dissolve it in an organic media. Solubility depends on the degree of protonation of the carboxyl groups. Sodium alginate can be protonated by adding HCl, forming Alginic acid, which is insoluble in a polar solvent. Adding a base, like NaOH, to alginic acid cause it to transform back to Sodium alginate.

Typically, alginate gelation is performed by introducing in a sodium alginate aqueous solution an ionic cross-linking agent. This is usually a divalent cation like Ca^{2+}. This method is called Ionic cross-linking. As previously stated, divalent cations bind with the carboxylate groups of the Guluronate blocks in the polymer chain, through a mechanism which is called egg-box model of gelation (figure 3.5).

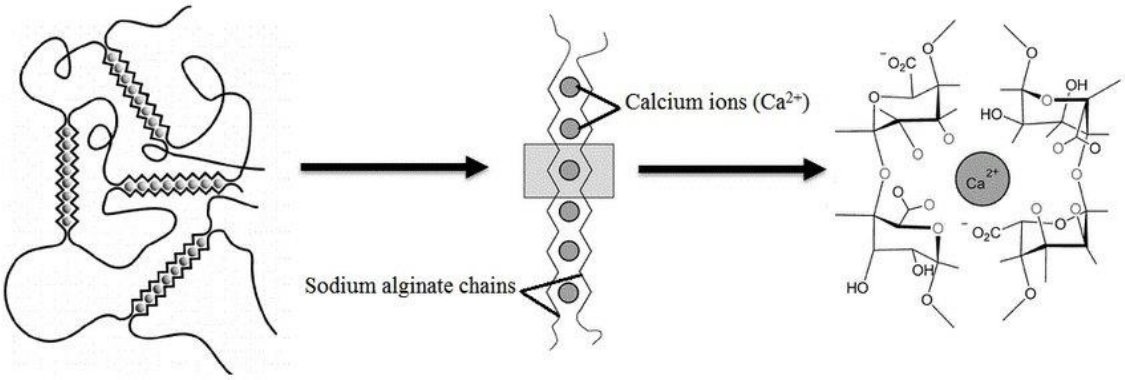

Figure 3.5 - Sodium alginate gelation

The source of Calcium cations is generally Calcium Chloride, or Calcium Acetate (in the food industry), but the high solubility in water of these two compounds may lead to an uncontrolled gelation kinetics due to the rapid availability of many Calcium cations. So, a buffer with the ability to compete with the reaction of the carboxylate groups in alginate with Calcium, thus slowing the gelation, can be used when needed. Another factor influencing gelation rate is temperature. At low

temperatures reactivity of cations is lower, so the gelation is slower and thus the resulting hydrogel network has greater order, so better mechanical properties. A main drawback in ionic cross-linking is that the cross-links dissociate and reform somewhere else in time, causing plastic deformation in the gel and loss of some of the water retained inside the gel matrix. This problem may be avoided if the alginate is cross-linked via some other method, like Covalent cross-linking.

Covalent cross-linking is performed by using Polyethylene glycol diamines (PEG diamines) to link the sodium alginate chains. Concerning the mechanical properties, elastic modulus of the gel increases initially with the weight fraction of the PEG diamine in the gel, then decrease when the molecular weight between each cross-link became smaller than the molecular weight of the PEG diamine. The properties of this gel can also be tuned by varying the molecular weight of the PEG diamine cross-linker chosen. The problem in Covalent cross-linking is that the cross-linking agent might be toxic and thus unreacted cross-linker has to be completely removed from the gel.

3.5.2 Biocompatibility and Biodegradation

Alginate hydrogel has proven to show no sign of foreign body reaction when implanted into mammals [21], but only when it was a high purity alginate in terms of composition. Being this polymer, something extracted from algae (not something synthesized in the lab), it may retain traces of impurities like heavy metals, endotoxins, proteins and polyphenolic compounds. So, an accurate multi step purification is compulsory especially for biomedical applications.

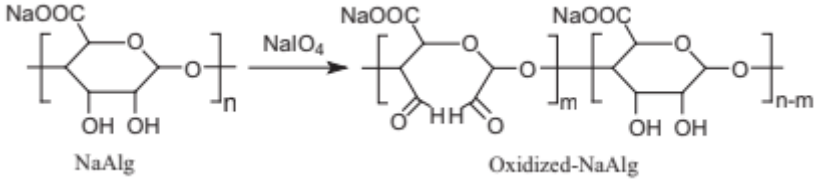

Figure 3.6 - Oxidation of sodium alginate

Alginate polymer is nondegradable by the human body, because humans lack alginase, i.e. the enzyme that destroys this polymer. Ionically cross-linked alginate hydrogel can be dissolved in time, by exchange reactions of calcium ions (which is divalent) with some monovalent cation (like sodium). This process dismantles the hydrogel matrix but doesn't affect the integrity of the polymer chains. Moreover, the molecular weight of these chains is, most of the times, higher than the clearance threshold of the kidneys, meaning they can't be completely removed from the body through urine [23]. A way to make alginate hydrogel degradable by the human body is to partially oxidise the alginate chains (with sodium periodate), thus they can dissolve in water (figure 3.6).

3.5.3 Chemical modification of alginate

Raw alginate hydrogels can be used in a lot of different fields. They have shown the capacity to hold and shield cells that need protection in order to grow, they can be used for drug delivery, controlled release, they can have dental applications, in the food industry they are used as thickeners and gelling agents and are also used in the paper and textiles industry [22]. Chemical modification allows to improve this already great potential by tuning existing properties or adding new ones.

In order to modify alginates, it is necessary to understand the reactivity of the functional groups of the alginate monomers. In particular, each monomer possesses two hydroxyl groups and one carboxyl group. Difference in reactivity between these different groups allows for chemoselective reactions.

Chemical modifications include:

- Acetylation
- Esterification
- Phosphorylation

- Sulfation
- Oxidation
- Carbodiimide coupling
- Nucleophilic substitution
- End-group modification [24].

4 Drug Delivery

4.1 Introduction

Drug delivery is a very broad subject, as underlined in figure 4.1. The term "drug delivery" refers to all the technologies, formulations and systems designed to have a targeted and controlled way of drug administration. It involves the transportation of the drug within the body to the desired location and the improvement of both the pharmacokinetics and pharmacodynamics. Control over these two variables permits to avoid the dangers and side effects of under and over dosage and makes the therapy more effective.

Typical solutions can be the modification of the pharmaceutical formulation (i.e. acting on the Pharmacodynamics) or the administration techniques (i.e. acting on the Pharmacokinetics).

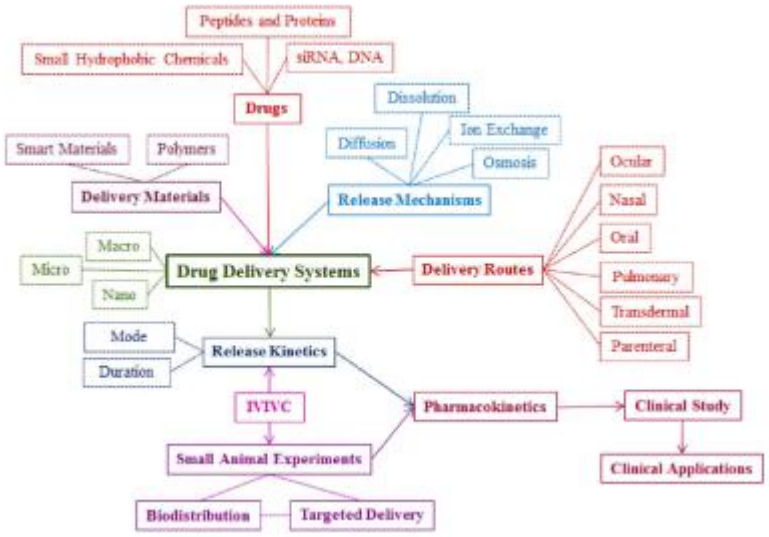

Figure 4.3 - Scheme of all the terms related to drug delivery

The most important advantages of a targeted and controlled drug delivery are:

- Increase the duration of the therapeutic effect [25]

- Lower administration frequency [26] while increasing patient compliance. [27, 28]
- On-target drug release, to have the presence of the drug where it's needed
- Optimized usage of pharmaceutical compounds, which can be very expensive
- Minimize side effects [29]

To be most effective, and to minimize the risk for side effects, the drug level in the plasma has to be maintained between the MEC (minimum effective concentration) an the MTC (minimum toxic concentration). Below the MEC the drug will be almost ineffective, and above MTC there is high risk of undesirable side effects. This result might be obtained by classical administration methods like pills, injections and so on (figure 4.2), but in this case, the concentration of the drug in the blood will not be easy to maintain inside these boundaries. Every time a new dose is introduced inside the body the concentration of the drug in the blood will skyrocket, reach a peak and then drop. At this time another dose is introduced, which cause another increase in concentration and so on. Problem is, with these sudden changes in concentration it is easy to drop below the MEC line. Moreover,

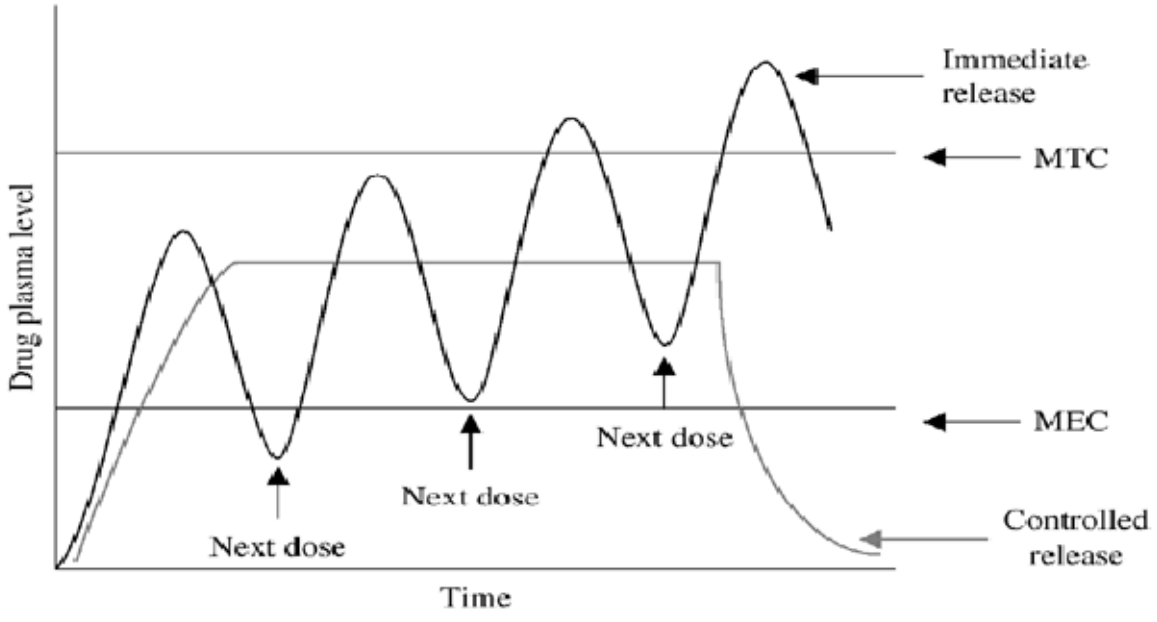

Figure 4.4 - Immediate versus Controlled release

with each new dose, some of the drug accumulates inside the body due to not perfect disposal of it and it can lead to an overdosage.

The best way to solve these problems can be having a controlled drug delivery. By controlling the drug delivery, it is possible to maintain the drug level perfectly in between the two critical drug levels for a longer time, thus reducing the drug administration frequency (allowing higher patient compliances), avoiding the side effects of overdosage and avoid wasting precious drug.

4.2 Drug design

The most important aspects to be considered in drug design are Pharmacodynamics and Pharmacokinetics.

Pharmacodynamics is the study of what the drug does to the body. The interaction of the drug with its specific receptor triggers a sequence of events. These events happen on various levels (molecular, cellular, physiological) and all together characterize the pharmacodynamic response. The effect of the drug is correlated to its concentration near the receptor.

Pharmacokinetics. On the contrary, Pharmacokinetics is the study of what the body does to a drug, in terms of Adsorption, Distribution, Metabolism, and Excretion. Pharmacokinetics deals with the optimization of the capacity of the drug to reach the target site and to have an acceptable lifetime within the organism. It might seem of secondary importance with respect to the first point but actually it is not.

In medicine, there is no guarantee that the compound with the best drug-binding site interaction properties would be the best drug to be used. There are several barriers in the organism that drugs should pass to reach its target in the body in an efficient way (absorption and distribution in the body). There are many solutions to let the drug pass unscathed these barriers, such as encapsulating it into

an appropriate matrix, link it to a polymer or polymeric carriers, and transdermal injection strategies. All these obstacles should be overcome while ensuring an appropriate lifetime of the drug inside the body. This means that the drug has to be able to survive the metabolism during the journey to the target, and also have appropriate elimination characteristics in order to not accumulate inside the body, situation that is potentially dangerous for the patient health.

4.2.1 Absorption

The absorption behaviour of a drug in the organism is mostly governed by its hydrophilic/hydrophobic properties, which in turn are determined by other properties like the polarity and ionization. Depending on the absorption behaviour it is possible to choose the right method to administer the drug.

For example, drugs which are too polar have difficulties in passing through the gut wall barrier and so they are better absorbed if administered via injections rather than administered in an oral way. On the other hand, non-polar drugs cannot be administered via injections because they're absorbed only by the fat tissues due to the fact that they are poorly soluble in aqueous solutions.

Typically, the polarity and the ionization properties of a drug can be tuned by modifying its substituents. The most common techniques are:

- Modification of alkyl/acyl substituents to modify the polarity. It is possible to reduce the drug polarity by adding extra lipophilic groups or by masking a polar functional group with an alkyl/acyl group. This has to be done without masking the functional groups of the pharmacophore, which are the ones active for the interaction with the binding site.
- Variation of the polar functional group to change the drug polarity.
- Variation of N-alkyl substituents to vary pKa. It is possible to modify the ionization properties by adding extra alkyl substituents near the EDG

(electron donating group) functional groups to carry the pKa in the range between 6 and 9 (if required by the specific case).

- Variation of the aromatic substituents to vary the pKa. It is possible to tune the pKa, based on the specific needs, by adding EDG or EWG (electron withdrawing groups). The more EDG are added, the higher pKa and so the more basicity. On the contrary, the more EWG are added, the lower pKa and so the higher acidity.
- Use of bioisosteres as substitutes for important functional groups. Typically, if there is the need of a specific functional group in the drug molecule for the pharmacodynamics, but, the same group, creates problems from a pharmacokinetics point of view, it is possible to use a related bioisostere to overcome the pharmacokinetics problems while ensuring the appropriate pharmacodynamics. A bioisostere of a functional group is another functional group with similar physiochemical properties of the one that has to be substituted. Examples of bioisosteres are carboxylic acid group and 5-substituted tetrazoles (they have similar physiochemical properties but different ionizations). The purpose of exchanging one bioisostere for another is to enhance the desired biological or physical properties of a compound without making significant changes in chemical structure.

4.2.2 Metabolism

With the concept of "improving the drug metabolism" is intended to tune the drug resistance to the chemical and enzymatic degradation, based on the specific need. For example, if a drug is too resistant we have to make it more susceptible to the degradation in order to avoid high concentrations of the compound within the body, else, if a drug is poorly resistant we might have to reduce its degradation susceptibility in order to increase its life time and give the drug the right time to be active. Typical techniques to tune the metabolic behaviour of a drug can be:

- Steric shields. Some functional groups are more susceptible than others to the chemical and enzymatic attack. It's possible to tune the degradation of the susceptible functional groups by adding a steric shield, which is a functional group that is more resistant and can protect the susceptible one with their steric hinderance by the degrading agent.
- Exploit the electronic stabilization effect of bioisosteres. Some bioisosteres are able to stabilize the drug molecule from an electronic point of view. For example, -NH2 instead of -CH3. They have similar dimensions and valence, but the -NH2 group make the molecule more resistant to the hydrolysis (because of its electronic effect).
- Metabolic blockers. Knowing the degradation mechanism of the drug it's possible to hinder it by adding appropriate functional groups in suitable positions (typically near the susceptible groups).
- Removal of susceptible groups. If it's possible to remove the susceptible functional groups without compromising the effectiveness of the drug, this is an easy solution for the improving the metabolic behaviour of the drug itself.
- Shifting the functional group susceptible to the degradation within the drug molecule, to make them less accessible for the degrading agents.

- Modification of rings. Some ring systems are susceptible to metabolism and so varying the ring can often improve metabolic stability.
- Use of prodrugs. Prodrugs are a class of drugs administered in a pharmacologically inactive form, which is then transformed by the body in a pharmacologically active form. This is a strategy to chemically modify pharmacologically active molecules in order to overcome problems like absorption barrier, difficulty in administration, fast degradation, slow excretion and toxicology [30, 31].

4.3 Drug delivery systems

The controlled drug delivery technology has been subjected to an increasing interest over the past decades. It has made many improvements in the medical field

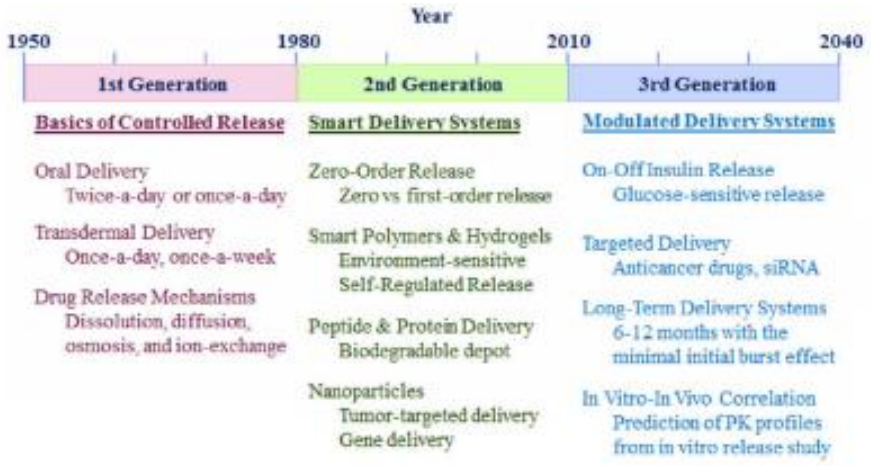

Figure 4.5 - History of drug delivery systems

and it's supposed to continue in this way. According to studies [32], The global drug delivery systems market was valued approximately 510 billion US dollars in 2016 and is anticipated to expand at a CAGR (Compound Annual Growth Rate) of over 6.9% from 2017 to 2025 to reach approximately 900 billion US dollars by 2025. Key companies operating in the global drug delivery systems market include AstraZeneca plc., Bayer AG, Pfizer, Inc., Novartis AG, Amgen Inc., Johnson and

Johnson Services, Inc., Baxter International, Inc., Boston Scientific Corporation, and Becton, Dickinson & Company.

Due to the complexity and the wide spectrum of topics covered by the drug delivery field, it is difficult to classify the drug delivery technologies univocally. In fact, there are a lot of possible classifications such as by release mechanism, delivery route, drug type and so on. However, it is easier to divide the time evolution of these technologies into three generations of drug delivery systems [33], as shown also in figure 4.3:

- First generation. It was focused on developing oral and transdermal sustained release systems and establishing the controlled drug release mechanisms.
- Second generation. It was focused on the development of zero order release systems. Zero order release means that a drug is released at a constant rate. This is the ultimate goal of all controlled-release drug delivery mechanisms. In the second part of this period, the attention has been focused on the so-called "smart" polymers. Hydrogels started to be developed among the path to achieve environmental responsive drug delivery systems, which means controlling the release of the drug as response to an environment change, like pH [34] or temperature [35].
- Third generation. This period starts in 2010 and is not over yet. Since then the most explored topic in the drug delivery field has been nanoparticles that can be administered directly to the blood stream. This is of particular importance in tumour treatment, since the effectiveness of any cure depends largely on the ability of drug delivery systems to reach their intended targets.
- The future. In the near future the demand for developing modulated insulin delivery systems will continue to increase as the number of patients with diabetes continues to rise, as well as the research in targeted drug delivery to fight tumours. Another important topic will be achieving a long term like delivery system (like at least 6 months) to treat chronic diseases.

4.4 Drug delivery routes

4.4.1 Ocular

Therapies for eye diseases prefers the ocular delivery route but it is not that easy due to the numerous physiological barriers present in the eye, which are called precorneal, dynamic and static. Also, being a very sensitive part of the body there are difficulties in maintaining the desired drug level in the target tissue. Drug delivery to the anterior segment of the eye has been improved by modulation of conventional drop administration with permeation and viscosity enhancers, and by the development in the effectiveness of formulations such as suspensions and emulsions. On the other hand, for posterior ocular delivery, research has been focused towards development of drug releasing devices and nanoformulations for treating chronic vitreoretinal diseases. These new devices and formulations may help to surpass ocular barriers and avoid side effects of conventional topical drops [36 - 39].

4.4.2 Pulmonary and nasal

Mainly used to treat nasal and pulmonary diseases. Typically targeting drug delivery into the lungs happens either with pressurized metered dose inhalers or with dry powder inhalers. In order to let a sufficient dose of a drug into the lungs specific carriers are required. These carriers can be solid, liquid, or gaseous. Examples of pharmaceutical carriers that have been successfully used to target drugs into lungs are liposomes, microparticles, cyclodextrins, microemulsions, micelles and suspensions [40, 41].

4.4.3 Dermal and transdermal

Dermal and transdermal Depending on the application it is possible to have dermal, in which the drug is active within locally within a small thickness of penetration, or transdermal, in which the drug needs to enter in the systemic distribution to be effective. The most problematic aspect related to the dermal and transdermal drug delivery is the physiological barrier related to the skin. For a drug to be delivered via the skin it needs to have adequate lipophilicity and also a molecular weight of less than 500 Da. The research efforts in this field are divided in passive methods, like ointments, creams, gels and patches, and active methods like Iontophoresis, Electroporation, Abrasion, Ablation, Perforation, Ultrasounds or Needless Injection [42].

4.4.4 Parenteral

This term is referred to those administration techniques which involve the direct injection of the drug, typically intravenous, intramuscular and subcutaneous. It is typically preferred over the other administration techniques in case of emergency situations or generally whenever there's the need of a fast action of the drug itself with high bioavailability and high reliable dosage. This due to the fact that the drug bypass all absorption barriers and enters directly into the general circulation. Being the delivery medical device established, research efforts have been focused mainly in the formulation field, in particular, to improve the drug solubility in aqueous solutions, allowing them to be administered in the blood, which is indeed an aqueous solution [43, 44].

4.4.5 Oral

Among all the various delivery routes, the oral one is the most commonly adopted in the pharmaceutical field. Particularly due to the easiness of access and patient compliance. But the development of oral controlled release is rather difficult

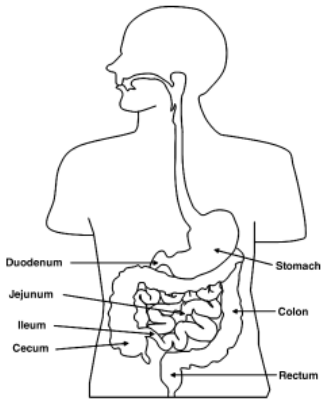

Anatomical Site	pH	Transit Time (h)
Stomach	1–3.5	0.25
Duodenum	5–7	0.26
Jejunum	6–7	1.7
Ileum	6.6–7.4	1.3
Cecum	6.4	4.5
Colon	6.8	13.5

Figure 4.6 - pH at different parts of gastrointestinal tract.

due to the properties of the gastrointestinal tract such as the different length, diameter, absorbing surface, characteristic residence time and pH of each tract. As an example, figure 4.4 represents all the different pH in the various part of the gastrointestinal tract.

For most drugs, there is a better drug absorption in the upper tract due to its higher absorption area, but it's possible to have the optimum absorption of the specific drug in another part of the gastrointestinal tract by tuning the release from the drug delivery system, taking into account of the previously mentioned properties.

4.5 Materials for drug delivery

4.5.1 Mechanisms of drug release from polymers

Drug release from polymers can occur in different ways and is affected by different parameters. These considerations are schematized in table 4.1 and 4.2.

Mechanism	**Variations**
Osmosis [20]	• Elementary osmotic pump • Multichambered and modified osmotic pumps (ex. push-pull) • Controlled porosity osmotic pump
Ion exchange	• Ion-exchange resins (anion/cation) • Polymeric coatings (release rate control) • Relation between small-scale design (particle size) and big-scale design (final utilization form)
Diffusion	• Basic diffusion, monolithic system • Diffusion with rate controlling membrane • Swelling and diffusion • Matrix degradation and diffusion

Table 4.1 - Mechanisms of drug release from polymers

Material matrix	**Release medium**	**Drug compounds**
• Composition • Structure • Swelling • Degradation	• pH • Temperature • Ionic strength • Enzymes	• Solubility • Stability • Charges • Interaction with matrix

Table 4.2 - Main factors affecting drug release from polymers

4.5.1.1 Osmosis

Drug release via osmotic force is based on devices, represented in figure 4.5, constituted by a central core which contains drug, surrounded by a semi-permeable polymeric membrane with one hole. When the devices are immersed in water, the

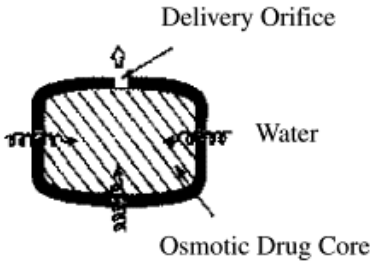

Figure 4.7 - Device for osmotic-driven release

fluid goes across the hole, or diffuses across the polymer, and dissolves the drug. Then, the mixture of drug and water goes out of the orifice. Of course, the drug needs to be sufficiently soluble in water.

4.5.1.2 Ion exchange

Drug release via ion exchange exploits the electrostatic interaction between an ionic drug and a water-insoluble polymeric material containing ionic groups with opposite charge, typically ion-exchange resins [45, 46], as shown in figure 4.6. The drug is released from the ion-exchange resin because it's going to be replaced by other electrolytes present in the surrounding environment, typically Na+ or K+

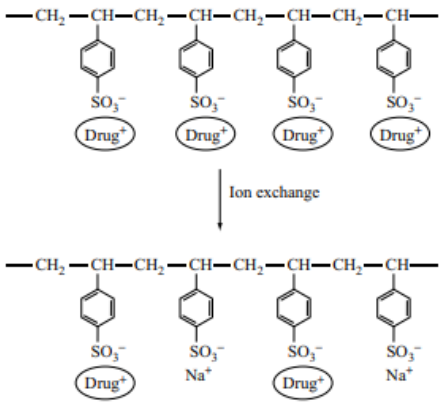

Figure 4.8 - Mechanism of ion exchange release

for cationic drugs and mainly Cl- for anionic drugs. The release rate depends on the surface of diffusion of the device, cross-linking density of the resin and ionic strength of the drug-resin link and can be additionally tuned by applying an external polymeric membrane. Ion-exchange based drug delivery can be done via matrix tables [47], or fast disintegrating tablets [48]. An example of the first way is the Nicorette chewing gum, which is a nicotine-cation-exchange resin complex incapsulated in a sorbitol-based matrix which release the nicotine slowly during chewing.

4.5.1.3 Diffusion

Drug release via diffusion is driven by a difference in concentration between the inside and outside of the device. These systems can be either formed by a bulk drug surrounded by a polymer or monolithic, meaning that the drug is uniformly dispersed in the polymer matrix. Drug release, or drug diffusion, depends on steric hindrance, temperature, pH, concentration gradient, viscosity and so on. However, in general, due to the high clearance of the human body, the complete release of the drug from the device is fairly quick.

In case the drug is uniformly dispersed, drug release obeys the Fick's law so the driving force is the drug concentration gradient between the inside and the outside of the device according to the following law.

$$\frac{\partial C_i}{\partial t} = \nabla(D \nabla C_i)$$

Where D is the diffusion coefficient and Ci is the concentration of the i-th species. It describes the dynamic release of a generic drug from a polymeric matrix, assuming that the polymeric matrix does not undergo any change in terms of chemo-physical properties and does not erode or degrade on a time scale comparable with the one related to the diffusion process, and using the appropriate assumptions and approximations, like the geometry of the device, the diffusion

coefficient of the drug within the polymeric matrix etc. It's possible to end up with diffusion-based release models such as the Peppas equations:

$$\frac{M_t}{M_0} = kt^n$$

Where M_t is the amount of drug released at time t, M_0 is the total amount of drug loaded in the device at time t=0, k is the release kinetic constant, it's mainly a function of the geometrical parameters of the object itself and of the drug diffusion coefficient within the polymeric matrix, n is the geometrical parameter, depending on the geometry of the device it can be 0.5 (thin-film), 0.45 (cylindrical geometry) or 0.43 (spherical geometry). When the exponent n has a value of 1.0, the drug release rate is independent of time and that case corresponds to zero-order release kinetics, in which the drug release rate is constant. When n is equal to 0.5 and the diffusion is pure-Fickian, the law is called Higuchi equation. It's important to underline the presence of a wide variety of release models, each one with its own assumptions and approximations, but the Higuchi power-law based empirical model is the easiest to use specially for short release times, or low M_t/M_0 ratios. It's also important to underline the fact that, going to the high release times, the simple Higuchi equation becomes more complicated and the functional dependence of the drug release on the geometrical parameter changes. A typical example is the release from a slab or disk type drug delivery system made by undegradable polymeric matrix, of generic thickness h, in which the release equation has different expressions depending on the release time and the ratio M_t/M_0 changes its

functional dependence on both time and geometrical parameter according to:

- $\frac{M_t}{M_0} = 4\left[\frac{D\,t}{\pi\,h^2}\right]^{1/2}$ when $0 \leq M_t/M_0 \leq 0.6$
- $\frac{M_t}{M_0} = 1 - \left(\frac{8}{\pi^2}\right)\exp\left[\frac{-\pi^2\,D\,t}{h^2}\right]$ when $0.4 \leq M_t/M_{0z} \leq 1.0$

Diffusion can be tuned with different methods, summarized in figure 4.7.

- Diffusion with rate controlling membrane, also known as reservoir type. Reservoir type devices are those having an inert coating material, which has the function of rate-controlling polymeric membrane, which can be coated-type or microencapsulation-type, on a drug-loaded core. Typically, with these devices it's possible to load a high amount of drug in the coated core and the release rate can be tuned by an appropriate selection of the coating membrane. The more widely used coating polymers are ethyl cellulose, acrylates and polyvinyl acetate. The drug release in polymeric coated reservoir systems undergoes a complex behaviour, mainly due to coating type and thickness, core type and drug type, which can be assumed as the combination of one or more of the basic mechanisms [49]: Diffusion across the polymeric layer, release through water-filled pores and osmotic effect. First of all, the water penetrates through the coating and reaches the core,

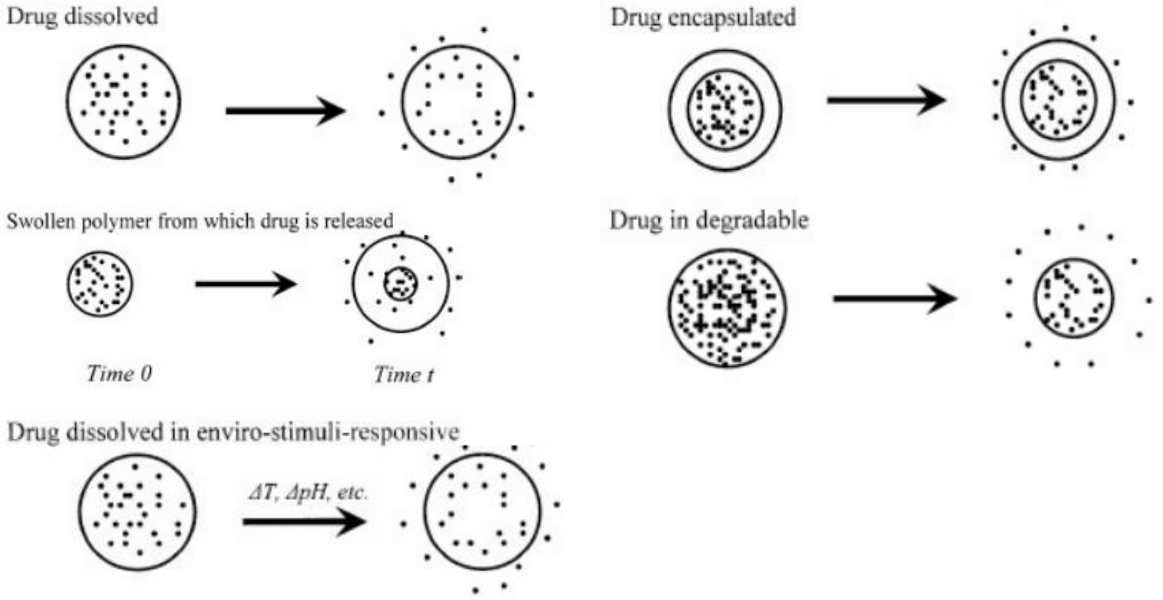

Figure 4.9 - Diffusion driven drug release

after that the drug is dissolved and released due to the concentration gradient. There is the creation of an osmotic pressure related to the water entering and the generation of a stress/strain field due to the different core and polymer swelling properties, these generates the next two mechanisms.

$$\frac{dm_i}{dt} = D_{app}\, A\, K\, \frac{C_i}{d}$$

1D-model balance equation, where D_{app} is the apparent diffusion coefficient of the drug in the polymeric film, A the surface available for diffusion, K the partition coefficient of the drug between aqueous phase and polymeric phase, and d the thickness of the coating. Release through water-filled pores, which are present in the polymeric coating layer due to several reasons for example due to cracks formed by the hydrostatic pressure generated inside these systems by water.

$$\frac{dm_i}{dt} = D_p\, A\, \frac{\varepsilon}{\tau}\, \frac{C_i}{d}$$

Where Dp is the diffusion coefficient of the drug in the aqueous phase present inside the pores, ε the volume fraction of the pores, τ the tortuosity of the pores. Osmotic effect, which tend to push the drug out from the drug delivery device. This release can be described as:

$$\frac{dV}{dt} = \frac{A\, \theta\, \Delta\pi}{l}$$

Where dV/dt denotes the water flow, A the membrane surface area, l the membrane thickness, θ the permeability of the polymeric membrane, and Δπ the difference in osmotic pressure, neglecting the counteracting hydrostatic pressure. These mechanisms can proceed lonely on in combination, but an important role on the release rate is played also by the core/coat swelling behaviour.

- Swelling. In the controlled drug delivery applications of swellable polymers, the drug is dispersed into the polymeric phase and when the latter is contacted with an appropriate solvent, swelling occurs starting the drug

release in the surrounding fluid. This happens because typically in the non-swelled configuration the drug is unable to diffuse through the polymer network in any appreciable extent but when the swell reaches an appropriate extent the network hinderance decreases because of the polymer chains kind of "relax" and tends to elongate between the network junctions thanks to the solvent-polymer interactions, so the drug starts to be released. The swelling behaviour of a polymeric device can be defined as its ability to increase its volume when in presence of an appropriate solvent, or in response to a change in the surrounding environment conditions, such as pH or temperature.

- Degradation and diffusion. These devices are characterized by the degradation of the polymer carrier, which is designed to degrade into biocompatible, and progressively smaller, compounds. Generally, biodegradable polymer chains contain ester, amide and/or anhydride bonds that are susceptible to degradation within the organism, commonly via hydrolysis or enzymatic. The typical parameter used to quantify the degradation process over time is the change in average molecular mass of the polymer due to the breakage of its chains on the labile bonds, the most widely used degradation kinetic equations are:

  Zero-order $MW_r(t) = MW_{r0}k_{degr}t$

  Pseudo first-order $MW_r(t) = MW_{r0}\exp(-k_{degr}t)$

  Where $MW_r(t)$ and MW_{r0} are the average polymer molecular mass at time t and time zero, k_{degr} is the apparent degradation rate constant of the polymer.

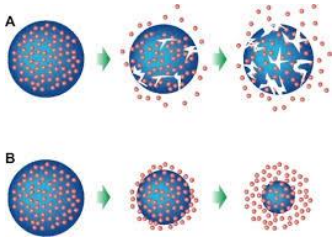

Figure 4.10 - A bulk degradation, B surface degradation

It's possible to distinguish two basic degradation mechanisms according to the characteristic times of water diffusion and polymer degradation, Schematized in figure 4.8. In bulk degradation ($\tau_{diff} \ll \tau_{degr}$), degradation occurs homogeneously throughout the material and the drug is released progressively. Devices based in this type of degradation have a wide variety of possible configurations, such as porous matrices and non-porous matrices, which are in turn configurable into pure diffusion-driven devices and multiple mechanisms-driven devices [50, 51]. On the other hand, surface degradation ($\tau_{diff} \gg \tau_{degr}$), is characterized by a degradation confined to the outer surface of the device and the drug is released continuously as the erosion process proceeds to the centre of the object. Typically, these releases are easier to model and predict than the bulk degradation ones, for example because of the assumption of a "layer by layer" degradation or the hypothesis of a moving "degradation front". In literature there are a lot of release models, but the easiest is the Hopfenberg's model which is based on the following formula:

$$\frac{M_t}{M_0} = 1 - \left(1 - \frac{k_0 t}{C_0 a}\right)^n$$

Where M_t and M_0 are the amounts of drug released respectively at time t and

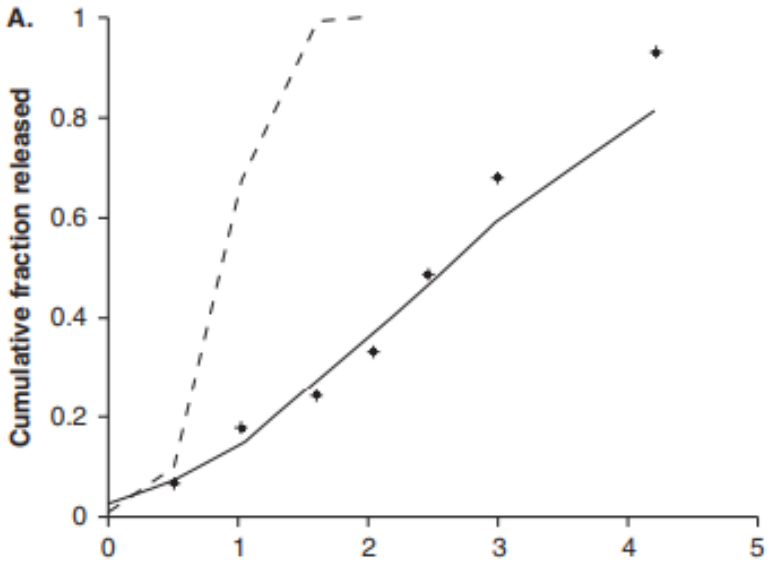

Figure 4.11 - Degradation-based release rate

at infinite time, k_0 refers to the erosion rate constant, C_0 the initial drug concentration within the matrix, a is the radius of a cylinder or sphere or the half-thickness of a slab; and n is a 'shape factor' representing spherical (n = 3), cylindrical (n = 2) or slab geometry (n = 1). The general trend in the degradation-based release rate is reported in figure 4.9 where it's possible to notice that the surface erosion release (dotted line) is much faster than the bulk degradation one (solid line). This is mostly due to the fact that in the surface degradation release mechanism the characteristic time of degradation is much smaller than the one related to the solvent diffusion, so from these devices the drug is released in a faster way than in those devices based on a bulk-degradation mechanism.

- Stimuli responsive release. In this class of devices, it's possible to classify all drug delivery systems which release drugs in response to a change in the surrounding environment conditions, such as pH and T. There are mainly two class of stimuli responsive release devices: physical or chemical. In the first case, the change in the environmental conditions causes a polymer chain expansion or contraction so that the drug diffusion may be facilitated or impeded depending on the drug molecular radius (steric hinderance), with respect to the network mesh size. With these devices it's possible to release drugs in a constant way over a long period, in a cyclical way, or triggered by the environment or other external events. In the chemical release the drug is still released in response to a change in the environment conditions, but due to a chemical reaction. For example, the polymer chain has been functionalized by creating a bond between the polymer chain and the drug. This bond breaks in particular environmental conditions while is stable in other conditions. This aspect is further investigated in the following chapters.

4.5.2 Polymers functionalization

Post-polymerization modification can be used when polymer bear chemoselective groups that are inert toward the polymerization conditions but can be quantitatively bonded in a subsequent step with some other functional groups.

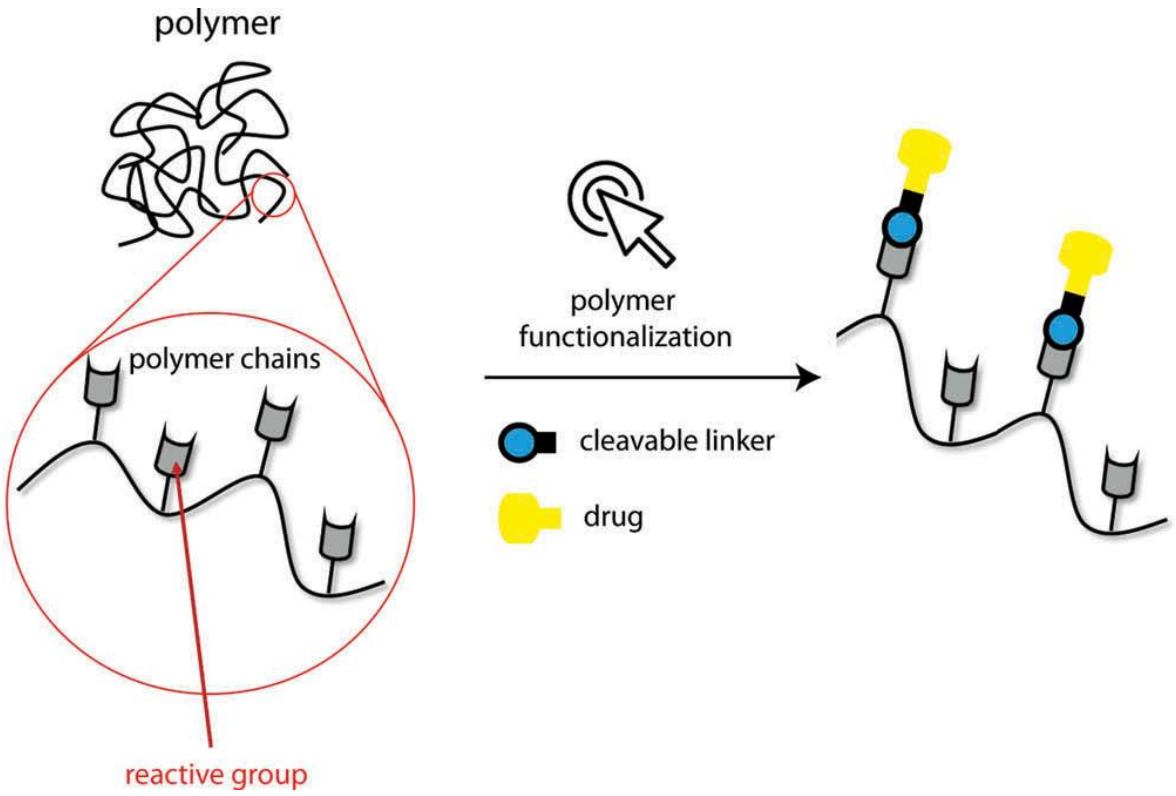

Figure 4.12 - Polymer functionalization

All the successes achieved with this approach can be used to functionalize polymers with drugs, with bonds that can be broken under some particular environmental conditions. Figure 4.10 shows the presence of the reactive groups on the polymer and the functionalization that happens via cleavable link. The cleavable bond that links drug and polymer can delay the release of a drug, by a factor directly proportional to the strength of the bond. Examples of chemical strategies to couple reactive functional groups are:

- Diels–Alder reaction.
- Esterification.
- Hydrazone and imine formation.

- Michael addition.
- Oxime reactions.
- Thiol–ene reaction.

The chemical procedures listed above can be considered efficient methods to cover different kinds of functionalizations [52].

4.5.3 Functionalized hydrogels

As previously stated, hydrogels can be loaded with cells for tissue engineering application or with hydrophilic drugs for targeted drug release. The main problem, as already explained, is due to the high concentration gradient that does not allow the control of drug release rates for a long period. In order to overcome this problem, a strategy has been utilized, which is based on the synthesis of hydrogels prepared with functionalized polymer chains. Obtained gels show lower release if compared to analog formulation of gels without functionalization [52]. In particular, the use of different binding strategies ensures different rate of release: faster release is obtained from network with weak binder than from strong binder structure. In this way, it is possible to generate polymeric systems that permit minimally invasive and localized delivery of therapeutic agents with tunable and extended release profiles. It has also been demonstrated that release can also be tuned upon different physiological pH conditions, due to the different hydrolytic cleavability of the bonds at different pH.

The possibility to deliver drugs from a single device with different release kinetics would be significant to adjust drug level according to biomedical and therapeutic needs. These hydrogels could be used as pH-sensitive drug delivery systems entrapping and then releasing low steric hindrance molecules or even high steric hindrance one.

Polymer functionalization could also be used to have multiple drug delivery:

one physically loaded that could escape due to concentration gradient and one covalently bonded, with potential for dual action for the treatment of various illnesses [52].

Figure 4.11 shows an example of obtained release over time [52]: (a) In vitro release profile of rhodamine delivered from hydrogel (black), hydrogel-drug ester bond at pH 7.4 (blue) and hydrogel-drug ester bond at pH 8.5 (red) hydrogels. (b) In vitro release profile of rhodamine delivered from hydrogel (black), hydrogel-drug hydrazone bond at pH 7.4 (blue) and hydrogel-drug hydrazone bond at pH 8.5 (red) hydrogels.

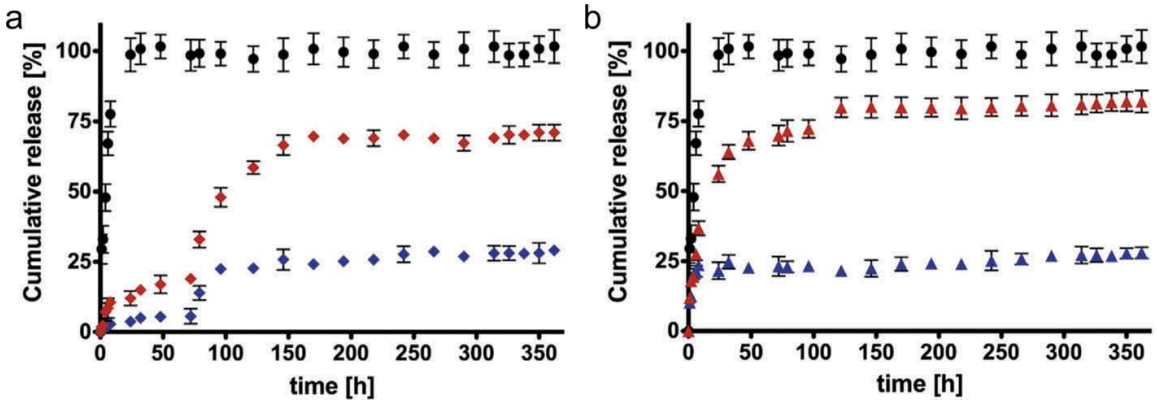

Figure 4.13 - Drug release over time in different conditions

5 Materials and methods

5.1 Microdevices fabrication

The aim was to obtain a micro electromechanical system (MEMS) able to be magnetically actuated in order to perform a targeted drug delivery within the body without causing any biocompatibility issue.

The geometrical design of the MEMS has been chosen to be:

- Cylindrical, to have a well-controlled rolling motion
- Porous mesh-like, to ensure an overall good mechanical resistance, allow a proper surface-active gelation of hydrogel and make the microdevices able to retain enough hydrogel, maximising the ratio between the total weight (hydrogel plus device) and the weight of the device. Moreover, the porosity is also essential for the surface tension, to hold the hydrogel in place during the gelification.

The first step in the microdevices fabrication procedure is the creation of the basic microdevice structure itself. There are many possible technological solutions to build up these structures [53], but the 3D printing has been chosen because of:

- The low costs related to both the system and the materials.
- The high flexibility of the constructing method itself, which allows the creation of geometrical structures impossible to create with other construction technologies.
- The great scalability.

Once the MEMS structure has been built, the microdevices must be made magnetically actuable and biocompatible. While the former property was ensured by the presence of a semi-hard magnetic CoNiP layer, the latter was given by an external finishing Au layer.

5.1.1 3D printing

5.1.1.1 Technology selection

The state of art in the 3D printing field has a wide variety of different techniques, which are basically distinguishable each other depending on the "resolution" of the part that can be built.

Since it's hard to obtain bulk metallic MEMS directly by 3D-printing due to the mismatching between those printing techniques' low resolution and the required low dimensions of the MEMS itself, the best choice is to print them from a polymeric precursor and then to metallize only their surface to give them the required properties.

In this work has been chosen, based on the Carrara's and Cuneo's works [59, 69], the SLA technology to 3D-print the microrobots from a photocurable resin using a UV laser source, computer-controlled by Galvano-mirrors. [54]

5.1.1.2 Experimental section

The 3D printing of the microdevices was performed by +LAB, the 3D Printing Laboratory of Politecnico di Milano, using the commercial stereolithography printer by DWS (Digital Wax Systems) model 028J Plus (shown in figure 5.1), which main characteristic are:

- Mounts a monochromatic actinic laser Solid State Bluedge BE-1500A/BE-1500AHR with galvanometric control.
- Wavelength of 405 nm.
- Emitting power of 30mW.
- Beam spot diameter of 22 μm

Figure 5.14 - DWS 028J Plus 3D printer

- Vertical resolution of 10 μm.

The design of the microdevices was performed on Solidworks software (by Dassault Systèmes), the CAD output is processed by Nauta+ software (the parametric editor, by DWS) and then is sent to Fictor software (by DWS) which directly controls the 028J Plus printer and executes the printing operations, a conceptual procedure is reported in figure 5.2.

Figure 5.15 - Conceptual sequence of operations to obtain a 3D printed object from a computer model

Parameter setup:

- Laser speed between 250 and 4300 mm/s
- Layer thickness between 10 and 25 μm
- Hatching of 20 μm

Two resins types [55] were available for the printing step:

- DL260, a commercial version by DWS based on urethane-acrylate resin filled with 20% m/m silica-alumina powder (propertary formulation).
- SR349, a custom-made resin free of particles, by +LAB.

Figure 5.16 - As printed microdevices

The microdevices were produced using the DWS DL260 resin because it gives optimal finishing results, good dimensional control and doesn't show curing issues. After the printing step there are remains of unreacted resin onto the microdevice's surface, so the device needs to be washed in ethanol to remove them and, after the washing step, a drying step is performed with nitrogen flux. The resin's reticulation is then finished by the exposure of the microdevices to light for 30 min in an UV-curing unit coupled with the printer (λ = 405 nm, Model S Ultraviolet Curing Unit by DWS).

The physical appearance of the microdevices after the SLA printing, already connected to the printing support, is shown in figure 5.3 in which are shown the microdevices printed according to an horizontal logic, but it's possible (and better) to adopt a vertical logic to have less printing support connections because they lead to non-uniformities and critical points for the metallization steps, which has to be as uniform as possible and must avoid any partially or non-coated area, mainly because of biocompatibility issues arisen by the presence of the materials under the final gold layer.

Two types of microdevices have been printed, with the same geometrical design (the 3D model is shown in figure 5.4) but different dimensions, as reported in table 5.1:

- S-type (small)

- L-type (large)

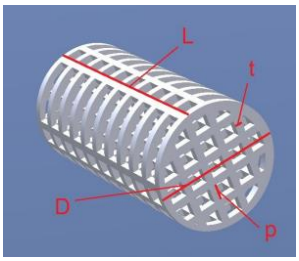

Figure 5.17 - 3D model of the microdevices

Dimension	L-type	S-type
D [μm]	2400	1600
L [μm]	4500	3000
t [μm]	150	100
p [μm]	290	190

Table 5.3 - Design parameters of L- and S-type microdevices

Results after the UV post-curing step have been investigated using optical microscopy, as shown in figure 5.5 (S-type microdevice).

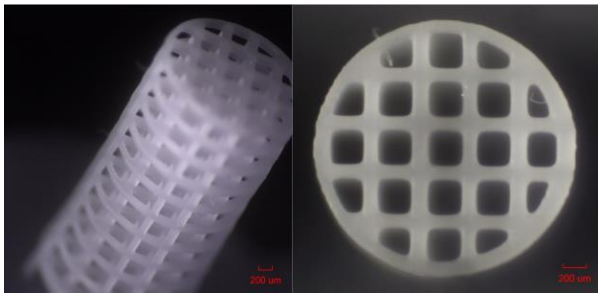

Figure 5.18 - Optical microscopy appearance of the microdevices

It's possible to notice the good matching between the design dimensions and the final results, the structure integrity and the well-connected geometry.

In this thesis work only the L-type have been used because of easier manipulation, but the adaptation to the S-type of all the experimental procedures is immediate. The sizes of the microdevices are mainly related to the 3D-printer resolution and to the resin type, in principle it's possible to obtain smaller devices but, for the purposes of this thesis, these dimensions are enough.

5.1.2 Metallization of microdevices

As stated in the previous chapter, it's better and easier to 3D-print a bulk resin than a bulk metallic microdevice, so once the microdevices are printed from the polymeric precursor, there is the problem to give them the required magnetic and biocompatibility properties.

As reported in the Cuneo's thesis work [59], the solutions adopted are:

- For the magnetic actuation, the deposition on the microdevices surface of a semi-hard magnetic alloy, specifically a CoNiP layer.
- For the biocompatibility, the application of an external finishing Au layer which avoid the contact between the body environment and the inner materials during the drug delivery.

In principle there are a lot of magnetic alloys with which it's possible to plate the microdevices giving them magnetic properties, for example NiP, NiFe and CoP, but CoNiP has been chosen because the main characteristics required for the magnetic actuation system used are:

- High magnetic coercivity, preferably higher than 200 Oe in both parallel and

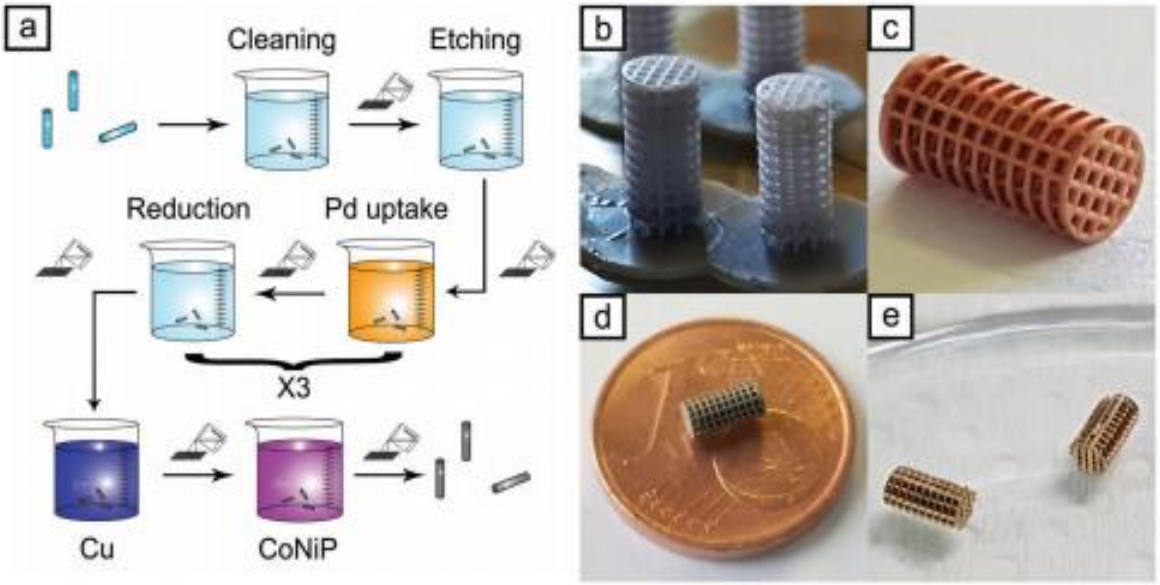

Figure 5.19 - a) Conceptual operations sequence up to the CoNiP layer, b) As printed microdevices, with the vertical logic, c) Cu plated microdevice appearance, d) CoNiP plated microdevice, e) Appearance after Au plating

perpendicular directions, referred to the cylindrical axis of the devices.

- Good remanence, in the order of 100-150 emu/cm^3 both in parallel and perpendicular directions.

In this thesis has been adopted the wet metallization sequences used in Cuneo's thesis [59] and Bernasconi paper [54]:

- Electroless base Cu layer to have good adhesion of the CoNiP layer on the microdevices.
- Electroless CoNiP layer for the reasons previously mentioned.
- The finishing Au layer applied following a complete ENIG (Electroless Nickel Immersion Gold) process directly on the magnetic alloy layer.

The metallization steps and procedures will be described in the following chapters, but is visually schematized in figure 5.6, with the images of the results after each metallization step up to the CoNiP layer.

5.1.2.1 Resin preliminary step

After the UV post-curing step, the microdevices are not ready to be plated with the base Cu layer, the surface firstly needs to be cleaned from any contaminant

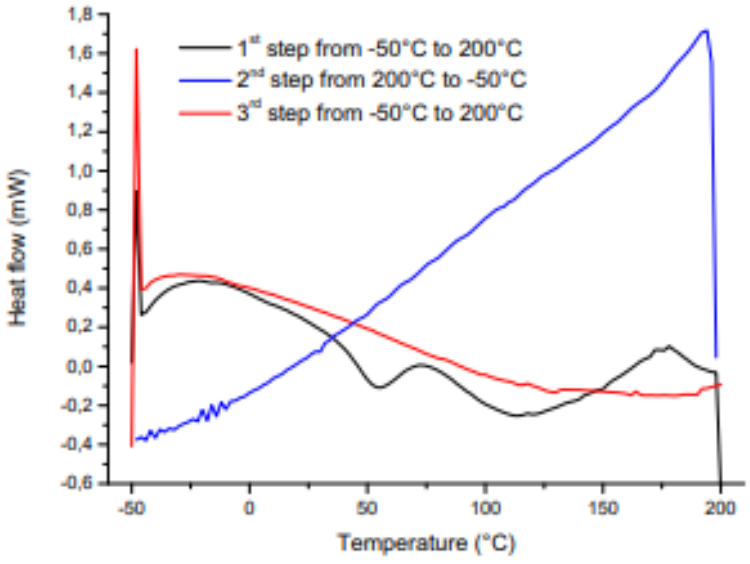

Figure 5.20 - DSC analysis of DL260 resin

and then to be treated to favour the electroless copper layer deposition. This is due to the fact that one of the most critical issues in metallizing a non-conductive surface, such as the DL260 resin, is the adhesion between the metallic layer that has to be deposited and the non-conductive surface.

One of the possible solutions can be the improvement of the cured DL260 resin's surface roughness through the immersion of the samples in an alkaline etching solution, in temperature lower than the glassy transition temperature of the resin (50°C, as reported in figure 5.7) to avoid degradation and changes in material properties and dimension stability.

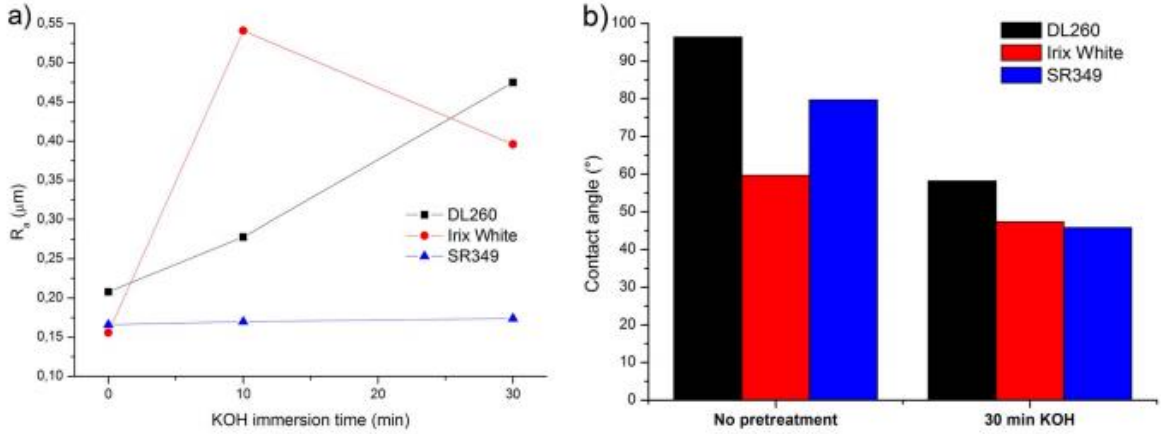

Figure 5.21 - Surface roughness (a) and contact angle (b) of 3D-printed resins treated with alkaline KOH solution

The alkaline solution partially dissolves the cured resin creating cavities on the surface and making the silica particles present in the resin more exposed on the surface, therefore the mechanical interlocking with the metal is favoured.

There's also a chemical effect related to the alkaline dissolution, the urethane-acrylate based polymeric surface undergoes to a chemical modification leading to a decreasing in contact angle (as reported in figure 5.8), which in turn leads to an improvement of the hydrophilicity of the surface itself that becomes more compatible with the aqueous solutions used in the wet plating steps [55] having an overall beneficial effect on the electroless processes.

The improvements in hydrophilicity of the surface is due to the creation of polar functional groups (-COOH and -OH) related to exposure of the acrylates

(which exhibit ester bond) presents in the resin to the alkaline bath, according to the general degradation reaction [55]:

$$R_1 - CO - O - R_2 + OH^- \rightarrow R_1 - CO - OH + R_2 - OH$$

All the experimental conditions adopted in this part are chosen as optimal parameters directly from the Cuneo thesis work [59] and Roberto Bernasconi's paper [55] and the laboratory work was performed in the seeLab of Politecnico di Milano. All chemicals used were purchased from Sigma-Aldrich or Carlo Erba and used without further purifications.

5.1.2.2 Experimental section

- Ethanol cleaning. The microdevices are cleaned in ethanol under sonication to remove contaminants from the surface, then are washed in demineralized water.
- ABS solution cleaning [55]. The microdevices in order to degrease the surface and remove further unreacted resin are washed under sonication (4 minutes at room temperature) in a neutral solution (ABS) with composition reported in table 5.2, and then washed in deionized water and dried.

Compound	Concentration [g/l]
Sodium Carbonate	50
Disodium metasilicate	35
Sodium laurilsulphate	3

Table 5.4 - ABS solution cleaning composition

- Resin dissolution. The microdevices are immersed in a KOH solution (200 g/l) for 30 min at 45°C without sonication, then washed in deionized water. The resin dissolution time (etching time) for a general polymeric material, in these working conditions, influences the metal adhesion according to a plateau trend of the adherent after peel test (which is given by the percentage of coating not removed by the peel test) [56].

The preliminary step can be resumed in table 5.3.

Step		Solution	Sonication	T	t
1	Ethanol cleaning	CH3CH2OH	V	Room temperature	4 min
2	ABS cleaning	ABS	V	Room temperature	4 min
3	Resin dissolution (etching)	KOH	X	45°C	30 min

Table 5.5 - Resin preliminary step

At this point the microdevices surface has been made rougher and more hydrophilic so it's possible to start the procedures related to the electroless deposition of the Cu layer.

5.1.2.3 Electroless Copper layer

The first metallic layer to be deposited is the electroless Cu, this because it provides good adhesion and activation properties for the next magnetic CoNiP layer which, if applied directly on the resin's surface, would show low adhesion, activation problems for the electroless plating, and poor morphological quality of the magnetic alloy [54].

The electroless deposition doesn't need any external power supply but needs the presence of a catalyst on the substrate surface (as reported in chapter 1) so the resin activation step is required to make the polymeric substrate active to the Cu plating reactions.

The catalytic precursor species has to be adsorbed on the resin's surface to create, after the reduction by an appropriate reducing agent, the true catalytic species in the "starting sites" from which the Cu deposition starts.

The electroless technology is suitable whenever there's the need to deposit onto a non-conductive substrate a metallic thin layer because it's highly convenient from the cost and simplicity point of view and also provides more uniform layer thickness and homogeneous coating properties than the electrolytic technologies.

5.1.2.4 Experimental section, resin activation

In this work Neoganth 834 activator solution (by Atotech) has been used as catalyst source, its formulation is patented and unknown but it's the source of Pd ions which are the catalyst precursor needed for the electroless deposition of Cu. In order to avoid any problem related to the surface adsorption of Pd ions, in this work has been used longer immersion timings than the one stated by Atotech (5 min). The Neoganth 834 activator must be reduced to have metallic Pd on the microdevice's surface (the "starting sites" are composed by metallic Pd), and this is done with a reducing bath composed by a 20 mg/l $NaBH_4$ solution in which the microdevices are immersed. The resin activation procedure used is reported in table 5.4:

step	Procedure	Time
1	Immersion of the microdevices (after the washing step to remove the remaining KOH solution) into the Neoganth 834 activator solution	10 min
2	Removal of the Neoganth 834 activator solution excess from the microdevices	//
3	Reduction of the adsorbed Pd ions with the $NaBH_4$ solution	1 min
4	Washing of the devices with deionized water to remove the remained reducing agent traces from the surface	//

Table 5.4 - Activation procedure resume for DL260 resin

All the steps have to be repeated three times to have the appropriate deposition of activator [55], it is important not to wash the devices with water between the 1-3 steps, but only rinsing after the step 4.

At this point the microdevices exhibits the optimal surface properties (roughness) and has the metallic Pd sites adsorbed to allow the electroless deposition of the first metallic layer. All chemicals used were purchased from Sigma-Aldrich or Carlo Erba and used without further purification.

5.1.2.5 Experimental section, electroless Copper layer

In this part of the work, based on the Cuneo thesis [59] and Bernasconi paper [55], the bath formulation and operative conditions have been already optimized for the purposes and are reported in table 5.5 and 5.6. The devices, already freed from the printing support, are free to move in the solution thanks to the stirring.

Compound	**Concentration [g/l]**
$CuSO_4 \cdot 5H_2O$	20
EDTA	40
2,2'-bipyridine	0.01
$Fe(CN)_6$	0.01
Glyoxylic acid solution (50%wt)	10.50

Table 5.6 - Electroless Cu, bath composition

T	45°C
pH	12
Agitation	Vigorous
t	15 min

Table 5.6 - Electroless Cu, operative conditions

Where in particular:

- $CuSO_4 \cdot 5H_2O$ is the Cu ion source, which are deposited on the surface thanks to the metallic Pd sites present after the activation step.
- EDTA is the buffering and complexing agent.
- Glyoxylic acid is reducing agent.
- $Fe(CN)_6$ and 2,2'-bipyridine are additives used as brighteners and stabilizers that improve the quality of the deposit mainly due to the inhibition of product formation in the bath.

EDTA generally leads to a slowing of the deposition rate because of its capability to form strong complexes with Cu ions due to its carboxylate and amines

groups. Note that generally the complex formation leads to bath stability, which in turn typically decreases the deposition rate, but in this case it's possible to increase it by working at high pH values.

The typical reducing agent was formaldehyde, but due to the related health and safety problems it was substituted by the glyoxylic acid, which in turn presents an extra advantage of increasing the deposition rate because its oxidation rate tends to increase with the increase of pH. For these reasons in this work has been chosen to work with pH=12, using NaOH solution addition.

The temperature has been chosen mainly as result from the balance of two factors [54]:

- The DL260 resin exhibits a glassy transition temperature around 50°C [55] so there's the need to work below 50°C to avoid any possible related problem.
- The electroless Cu deposition rate on the DL260 resin surface increases with temperature following a typical Arrhenius exponential trend as shown in figure 5.9 [55], so temperature has to be as high as possible to allow high deposit rates.

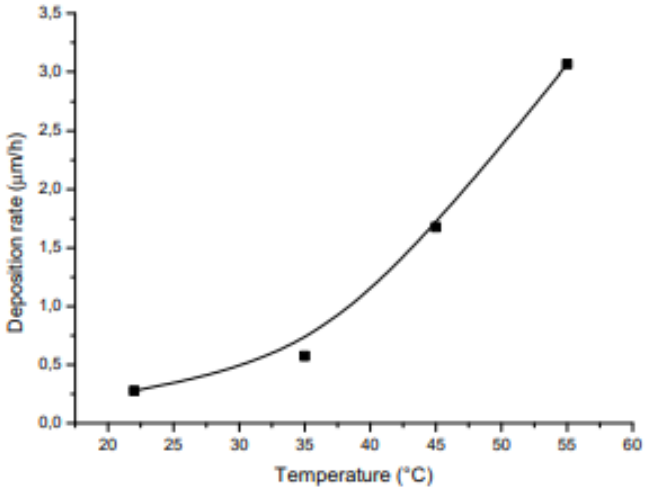

Figure 5.22 - Electroless Cu deposition rate versus temperature

So, at last, the temperature has been set to T=45°C and, in these working conditions, the deposit rate has been experimentally estimated [54, 58] to be around 1.678 µm/h. For a deposition time of 15 min, a good uniform base copper layer thickness of about 400 nm has been obtained [54, 55].

After the Cu layer deposition, the microdevices are recovered, washed with deionized water and dried with nitrogen flux. All chemicals used were purchased from Sigma-Aldrich or Carlo Erba and used without further purification.

5.1.2.6 Magnetic CoNiP alloy layer

As previously stated, the magnetic CoNiP alloy layer is deposited on the Cu layer to make the microdevices magnetically viable but has also the secondary effect of improving their mechanical properties and shape stability.

The most important properties of this layer are [54]:

- High magnetic coercivity and good remanence, as said before, because the microdevices need to be properly actuated with the Octomag technology (this will be discussed later on) and have to maintain their magnetization when exposed to the magnetic actuation field.
- Good mechanical properties, specially the mechanical resistance, in order to to be able to move within the body for drug delivery purposes; E_{CoNiP}=139 GPa while $E_{DL260resin}$=1.82 GPa. The final microdevice behaves mechanically as a composite.

At this point of the metallization procedure, the microdevices already have a conductive (Cu layer) surface, so in principle it's possible to exploit either the electrolytic or electroless deposition technologies to deposit the magnetic layer.

In this work has been chosen the electroless deposition of the CoNiP layer because the electroless technique allows to end up with a more uniform layer thickness on the microdevices and the related less anisotropic magnetic properties. There's always anisotropy in magnetic properties, basically due to the combination of two contributes: the geometry of the MEMS itself and the magnetic layer properties.

While the former contribution is fixed because the geometry doesn't change, we can work on the latter by paying attention to the uniformity in layer thickness

and composition during deposition process and bath formulation. This is due to the fact that the magnetic properties are mainly determined by the microstructure, composition and thickness, which are in turn determined by the chemical species present in the plating bath and the operating conditions of the deposition step itself.

Typically, the CoNiP electroless depositions are performed in alkaline conditions with high deposition rates, so both the metallic and the reducing agent species are rapidly consumed. This leads to a decrease in pH, and so the pH control is crucial in this step and it must be maintained as constant as possible, typically by adding ammonium hydroxide to the plating bath [57].

There is the need of another activation step before proceeding with the electroless deposition and it's performed with a simple $PdCl_2$ solution, instead of using the more expensive Neoganth 834 activator solution, because of the presence of the copper layer.

The main drawback in this case is that no CoNiP metallization occurs in the eventually present Cu-free areas of the devices, because the simple $PdCl_2$ solution is not able to activate the resin itself.

The most important plating bath operative parameters are:

- Co/Ni ratio and P content. They have high impact on the deposit composition and structure, which in turn impacts the magnetic properties of the microdevice.
- Temperature. This is important for the same reasons related to the deposition of the Cu layer, and because it affects also the layer composition.
- pH. pH strongly affects important properties such as layer composition and growing rate. In this case the growing rate exhibits a maximum trend with the highest growing rate at pH=9.5

5.1.2.7 Experimental section, CoNiP alloy layer

The activation step follows the same logic reported for the resin activation, with the exception for the use of the $PdCl_2$ solution instead of the Neoganth 834 activator solution.

The complete procedure is the following:

- The microdevices are activated by immersion in the $PdCl_2$ solution for 1 min, in this case a one-time activation is sufficient because of the Cu surface presence instead of the three-time activation required by the first metallization step of the resin.
- Then wash in deionized water to avoid the contact between the activator and the plating bath, because otherwise it will rapidly decompose.
- Immersion in the plating bath reported in table 5.7 with operative parameters of table 5.8.
- Recovery from the electroless bath by filtration.
- Carefully wash in deionized water and dry.

In this work pH control has been performed by a two-step logic instead of the typical ammonium hydroxide method:

- In the formulation step, the pH is set to 9.5 by adding NH_3 solution.
- In the further depositions of CoNiP it has been restored by addition of an NaOH solution.

This because of the complexing ability of NH_3 which, if not present, will lead to very low Co/Ni ratios and a sequential worsening of magnetic properties.

Compound	Concentration [g/l]
cobalt sulfate hexahydrate	39.3
nickel sulfate hexahydrate	7
trisodium citrate dihydrate	50
boric acid	30
Sodium hypophosphite monohydrate	25

Table 5.7 - Electroless CoNiP bath composition

Parameter	Value
pH	9.5
T	45°C
t	3h
Agitation	Vigorous

Table 5.8 - Electroless CoNiP layer deposition operative conditions

According to Bernasconi's work [54], the CoNiP layer has been found composed by 3 wt% P, 26 wt% Ni and71 wt% Co.

The experimental parameters and bath composition are taken from Cuneo's work [59] and are chosen to be optimal parameters in terms of layer magnetic properties, morphology and crystallographic structures, to satisfy the main properties requirements listed before, with the highest emphasis on the magnetic properties.

The bath composition is optimized particularly to obtain a magnetically harder alloy and exhibits the presence of the typical players of an electroless plating solution, as stated in chapter 2, where:

- Boric acid and sodium citrate acts as complexing agent.
- Cobalt sulphate hexahydrate and nickel sulphate hexahydrate are the source of metallic ions.
- Sodium hypophosphite monohydrate is the reducing agent and during its oxidation supplies the P, as side-product, to the layer to have the ternary alloy.

It is important to underline that the bath composition comes from a compromise between different parameters and trends, such as the need to minimize the deposition times, thus having high growing rates which are related to low Co/Ni ratios in the bath, and the need of appropriate magnetic properties, such as coercivity, which increases with Co content in the layer, that in turn increases with

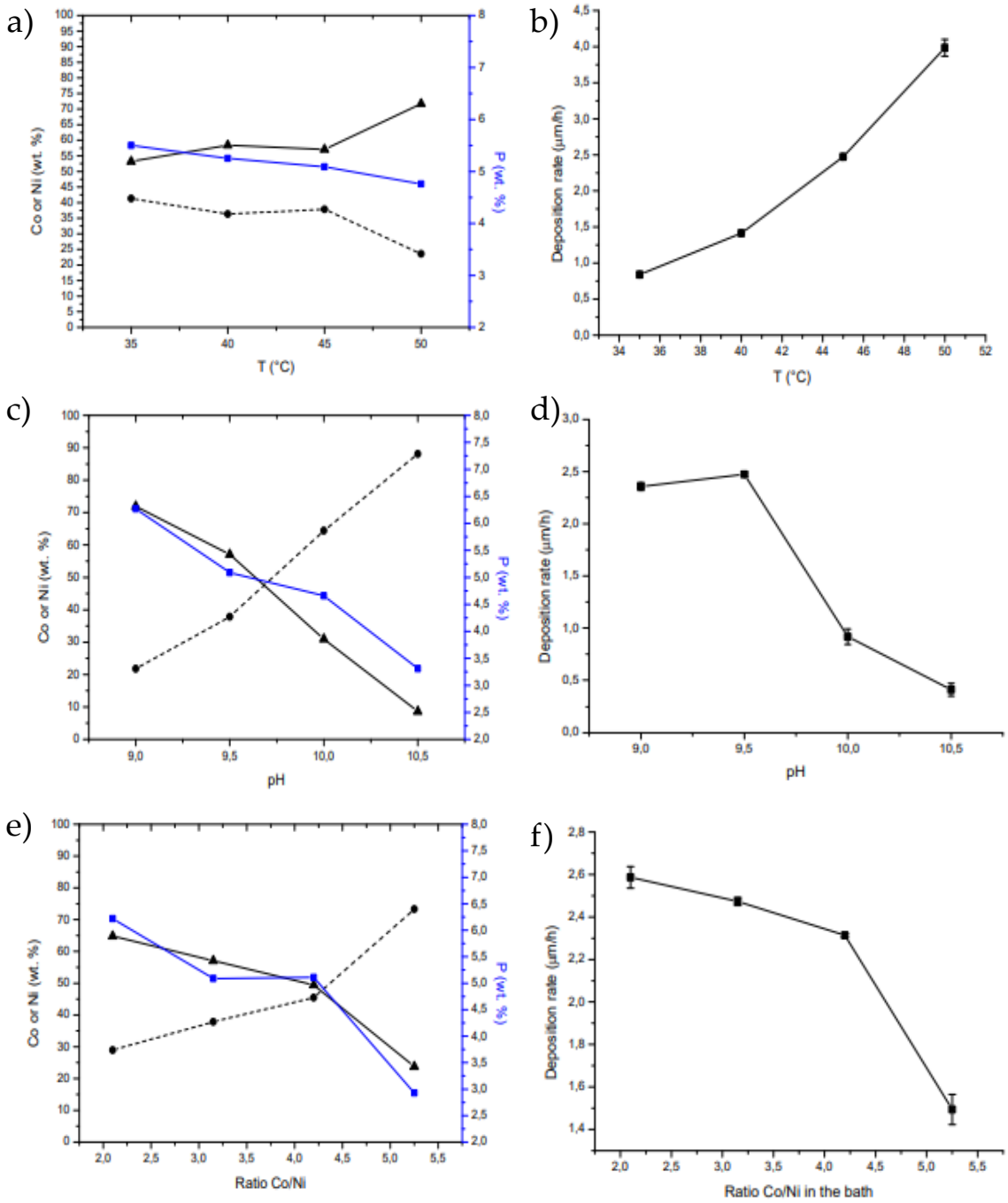

Figure 5.23 - a) Effect of temperature on deposit composition. b) Effect of temperature on CoNiP deposition rate. c) Effect of plating bath pH on deposit composition. d) Effect of plating bath pH on CoNiP deposition rate. e) Effect of bath's Co/Ni ratio on deposit composition. f) Effect of bath's Co/Ni ratio on CoNiP deposition rate.

the rising of Co/Ni ratio in the bath. Figure 5.10 provides a summary of some of these parameters and trends, and how the vary following the variations of other properties. In this case the need for proper magnetic properties of the microdevices was the more stringent parameter, so the plating time was adopted as 3 h.

5.1.2.8 Finishing Au layer, ENIG process

As said before, the finishing gold layer is adopted as solution to the biocompatibility problems of the inner layers, it's used to insulate the MEMS core materials (DL260 resin, Cu, Co, Ni and P) from the outside environment to avoid any cytotoxicity.

The complete ENIG plating technology used to golden plate the microdevices is constituted by a two-step process:

- Electroless Nickel (EN). Deposition of a NiP thin layer as a third metallic deposit to allow the displacement deposition of gold.
- Immersion Gold (IG). Plating the NiP layer with the gold one.

The gold layer is deposited following the complete ENIG process because the CoNiP surface is not optimal for gold direct deposition. If only the Immersion Gold step is applied without the Electroless Nickel, the microrobots surface results poorly bright and not sufficiently uniform. The NiP layer improves the final Au layer uniformity, homogeneity and brightness.

The two solutions behaviour is well known and the whole ENIG plating process has been applied directly on the CoNiP layer.

A key point for the proper insulating action of the Au layer is the complete surface covering, with minimal layer porosity, because the presence of nanopores causes a galvanic coupling corrosion between the NiP layer and the Au layer leading to an exposure of the cytotoxic inner layers. The higher the immersion gold plating times, the lower is the gold layer porosity, thus the better biocompatibility.

5.1.2.9 Experimental section, Electroless Nickel (EN) and Immersion gold (IG)

The first step of the ENIG plating process is the electroless plating of the microdevices with a NiP layer. Before starting there is the need of an activation of the surface to allow the starting of the NiP deposition. So, the microdevices are activated with $PdCl_2$ solution by displacement deposition.

A typical composition of a NiP electroless bath is:

- Nickel salts. They are the ion source. Commonly nickel sulphate is used due to its low cost and high plating performances.
- Sodium hypophosphite. Reducing agent for water-based bath, it's important to underline that the plating rate is linearly dependent from the hypophosphite content.
- Complexing agents. They are organic acids and their related salts or inorganic pyrophosphate anion and ammonium ion. They are used to control the bath pH.

The final deposit composition depends mainly on the reducing agent present in the bath (except in case of hydrazine, that allows a >99% Ni deposit), in this case sodium hypophosphite is source of P which will be found in the final alloy. There are a lot of reducing agent's types, such as the B-containing ones and in that case the alloy will be NiB.

The electroless nickel deposition is accompanied by hydrogen evolution due to reducing agent's oxidation. So, a typical signal that the solution is starting to decompose is the increase in hydrogen bubble formation. However, these kinds of plating bath can operate without any stabilizer addition.

The operative procedure is the classical one related to electroless deposition processes with the surface activation step. It can be summarized as follows:

- Activation in the Pd-based solution.
- Washing in deionized water.
- Immersion in the plating bath reported in table 5.9 according with the

parameters listed in table 5.10.

- Recovery from bath by filtration.
- Cleaning to eliminate any contaminant.
- Drying.

The pH was adjusted to 9.00 adding NH_3 solution to the bath.

Compound	Concentration [g/l]
Nickel sulphate hexahydrate	32
Trisodium citrate dihydrate	20
Ammonium chloride	25
Sodium hypophosphite monohydrate	28

Table 5.9 - EN bath composition

Parameter	Value
T	45°C
pH	9
t	15 min
Agitation	Vigorous

Table 5.10 - EN plating operative conditions

Low immersion timings have been used to obtain thin NiP layers.

In the "immersion gold" step, the Au layer is deposited directly on the NiP layer as it is, without any activation step of the surface, by a displacement deposition.

Usually it's performed at high temperature (of about 85°C) but in this case the temperature has to be set at maximum to 45°C because, as stated before, the DL260 resin exhibits a glassy transition temperature of about 50°C.

At these low temperatures the plating has an intrinsic low kinetics so, in order to obtain appropriate biocompatibility properties, the immersion gold step duration need to be prolonged for about 5 hours. This duration time has shown to provide a cell viability of 92% after 2 days [54].

The immersion gold solution formulation is secreted (Aurotech by Atotech)

and only the general components are known, which usually are $KAu(CN)_2$ as source of gold, citric acid, ammonia, ammonium sulphate and aminocarboxylic acid salt [59, 60].

The procedure used for the IG step is:

- Immersion of microdevices in the Aurotech® solution for plating
- Recovery of the finished MEMS, by filtration
- Final washing with deionized water
- Final drying

The working conditions, as reported from Bernasconi and Cuneo's work [54, 59], are reported in table 5.11.

Parameter	Value
T	45°C
pH	6
Agitation	Vigorous

Table 5.11 - Operative conditions of IG step

Typical Au thickness after the ENIG process ranges from 80 to 120 nm [54] but it can be increased by another electroless deposition step if necessary. After the Au layer deposition, the microdevices are finished and are ready to be coated with the proper hydrogel.

5.1.3 Biocompatibility considerations

Biocompatibility is the ability to perform with living tissue or system by not being toxic, injurious, or physiologically reactive and not causing any immunological rejection of the host. Typically, a bio-test is performed to see if the devices can have a certain cell viability. Gold is widely used in the biomedical field because it's known to be a biocompatible material [62, 63].

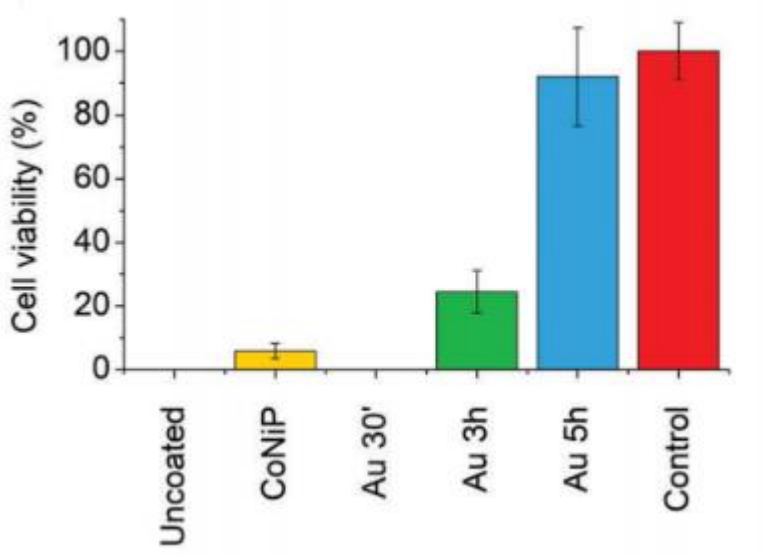

Figure 5.11 - cell viability after 2 days for microdevices with different coatings

Since the final purpose of these MEMS is the controlled and targeted drug delivery, they must be biocompatible and avoid any cytotoxicity problem. The solution adopted in this work, as previously said, is the external finishing gold layer which insulates the inner layers from the outside environment. The biocompatibility of Au deposit already been confirmed, but only on nanometric magnetically actuated devices [61].

Referring to the results of Bernasconi's work [54], the biocompatibility of these MEMS (L-type) has been proved by a cell viability measurement after 2 days, at different metallization stages (as-printed DL260 resin, after CoNiP layer deposition and after Au plating), and at different Au plating timings (30 min, 3h and 5h). As reported in figure 5.11, the uncoated DL260 resin shows a 0% cell viability after 2 days, both the CoNiP and the 30 minutes Gold plating are not

biocompatible as well. The problem of the 30 minutes gold plating is the slow plating kinetics of the finishing gold layer at 45°C, which leads to an incomplete coating of the surface with nanopores, which starts a strong galvanic coupling corrosion with then NiP layer below [60]. This phenomenon can be reduced by increasing the Au plating time. As shown in figure 5.11, after 3h of plating the cytotoxicity of the surface is decreased, while for 5h of Au plating the cell viability reaches 92%.

5.1.4 Magnetic actuation

The MEMS are designed to be able to move under the action of an applied external magnetic field, for this purpose the semi-hard magnetic CoNiP layer has been applied on the MEMS itself.

There are mainly three magnetic actuation typologies [66, 67]:

- Gradient field, in which the MEMS is directly entrained to the final position and stopped thanks to the magnetic gradient.
- Oscillating field, the oscillating motion of the MEMS is caused by the application of a resonant magnetic field, but these MEMS require complex shapes and geometries.
- Rotating field, the MEMS moves thanks to a magnetic torque caused by the rotating field, typically these MEMS rolls

The microdevices of this work can be classified in the latter category, they have a rolling motion. The application of the external rotating magnetic field generates a magnetic torque ($\overrightarrow{T_m}$) on the devices.

The torque can be expressed as:

$$\overrightarrow{T_m} = V_m \cdot \vec{M} \times \vec{B}$$

Where:

- V_m is the volume of magnetic material which in turn depends on the CoNiP

layer thickness.

- M is the magnetization of the material; the MEMS must show a permanent magnetization which is provided by the CoNiP layer and its semi-hard magnetic properties.
- B is the externally applied magnetic field used to control the motion of the MEMS in terms of both direction and speed.

The microdevices, metallized following the methods reported in the previous paragraphs, satisfy the magnetic properties values required to an appropriate magnetic actuation (coercivity and remanence levels reported before), in particular they show, as stated in Bernasconi's work [54]:

- Remanence of 140 and 96 emu/cm^3 in parallel and perpendicular direction (with respect to the cylindrical axis).
- Coercivity higher than 600 Oe in both parallel and perpendicular direction (with respect to the cylindrical axis), to avoid the loss of magnetization when exposed to the external magnetic field.

5.1.4.1 OctoMag

The OctoMag is an apparatus for the magnetic actuation of MEMS designed and built at the Multi-Scale Robotics Lab of ETH, Zurich. It's made by eight electromagnets, 4 of them are in-plane at 90°, and four are offset by 45° and tilted down by 45° as shown in figure 12. This configuration allows to have 5 degree of freedom, three DOF for the position and two for the pointing orientation, for a wireless control of a microrobot which can move on a large space and it's completely free in rotation.

In addition to that, it creates more isotropic magnetic fields and gradients which allow a better control of the MEMS motion respect to other systems [64, 65], and gives the possibility to position microdevices under a closed-loop control by a computer or also by visual feedback of the human operator during the operation.

Figure 5.12 - On the left the OctoMag apparatus in ETH Zurich, on the right OctoMag application conceptual layout.

The OctoMag was originally thought to be applied to ocular surgery, in order to have an optimal control of MEMS designed to operate in the small space of the eye (as shown in figure 5.12), but this machine can also be adapted to the geometry of other body parts.

5.1.4.2 Experimental section

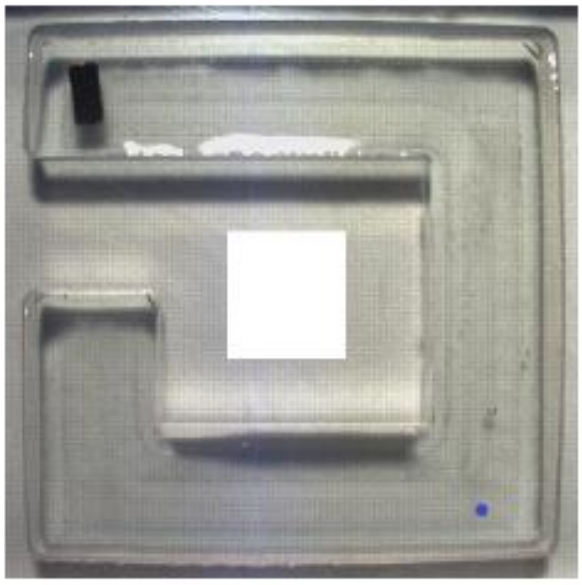

Figure 5.13 - Arena for the OctoMag actuation

Microdevices were pre-magnetized by contacting them with a cylindrical (radius 2 cm, thickness 1 cm) NdFeB permanent magnet for 1 minute. After the pre-magnetization step the MEMS were placed into appositely designed arenas (test basin) to test both velocities and trajectories with OctaMag, with particular care on

the relation speed-frequency and on the control of the trajectories followed by the MEMS. An example of an arena for MEMS test is shown in figure 5.13, in which it is present also the microdevice to be tested.

The arenas were custom-made and are filled with different fluids. Different route shapes to be followed by the device have been tested.

The rolling motion of the MEMS is provided by the rotation of the magnetic field. This is due to the fact that when immersed in a magnetic field the devices tend to align their magnetization vector M with the direction of the magnetic field B. If B continuously rotates around an axis, M will continuously align with B, creating the magnetic torque which allows the MEMS to have a wheel-like forward motion on its cylindrical axis when placed on a solid substrate according to the equation:

$$v = 2\pi r\omega$$

Where:

- ω is the rotation frequency of the magnetic field B
- r is the radius of the microdevice
- v is the linear velocity of the microdevice

Figure 5.14 shows the direction of the vectors mentioned before. The relationship between speed and frequency has been obtained by sampling at certain time-points the OctoMag video of the actuation at each frequency, using an arena with a proper dimension mesh on the background (figure 5.15). So, it is possible, knowing the frequency, to calculate the speed by just looking at the space travelled by the MEMS in the timespan between the selected photograms. It is important to

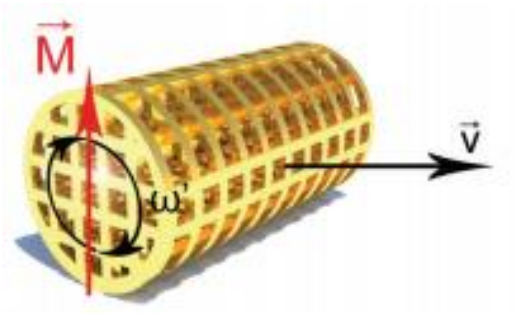

Figure 5.14 - schematization of the M, v and ω vectors

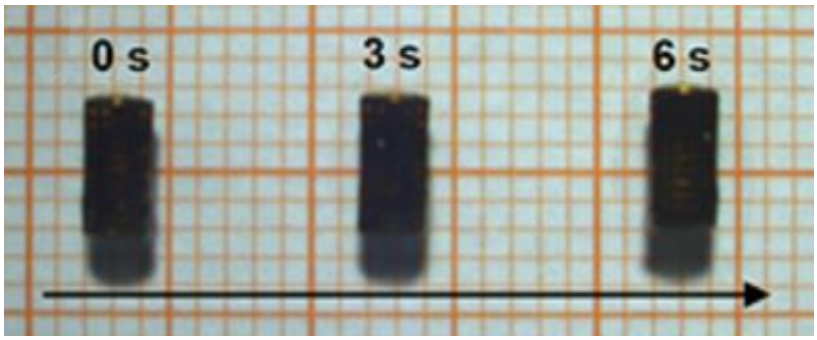

Figure 5.15 - example of photograms taken from the OctoMag actuation video

consider that this relationship is fulfilled only if M follows B in an ideal way, without any delay, for example in the case in which the MEMS was immersed in fluids like air or water.

In that case the correlation between velocity and frequency has founded to be linear, allowing an indirect calculation of the device's radius by inverting the formula. The radius was found to be 1156 μm, a value very close to the nominal one, 1200 μm, expected from 3D printing.

The delay can be introduced if the motion is performed in those condition which cause fluid dynamic drag such as viscous solutions, as shown if figure 5.16.

The speeds of the L-devices and S-devices follows the same trend but have different values because of the different radius of the MEMS, it's easy to note that the delay occurs when the devices are placed in a viscous environment such as oil

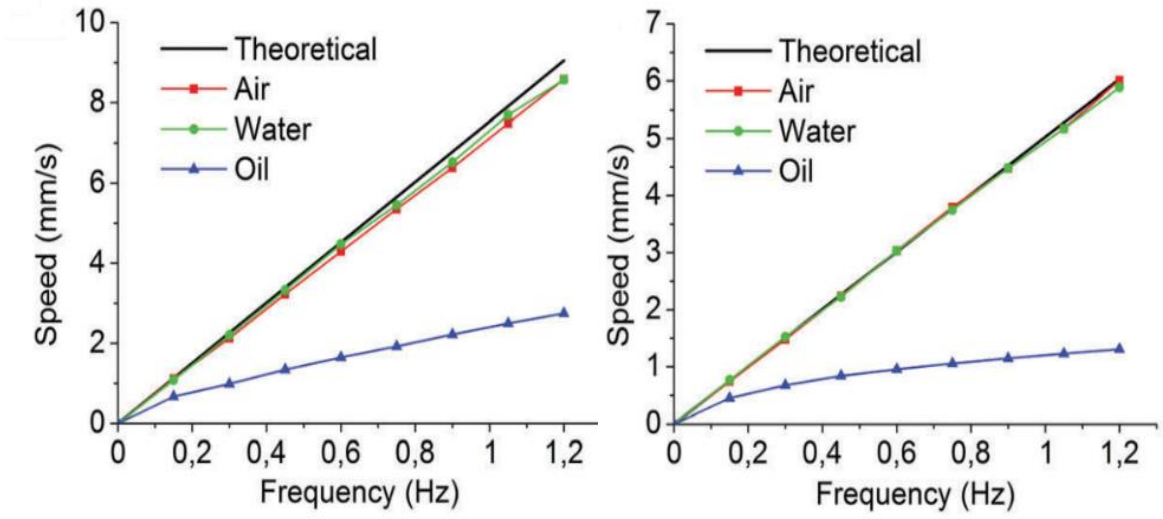

Figure 5.16 - correlation between MEMS speed and B rotational frequency of an L-type device (left) and an S-type device (right)

more than when placed in both air or water.

The microdevices, without the hydrogel coating, have been found to be easily guided and well controlled with the OctoMag technology, varying the orientation of external magnetic field it's possible to make the MEMS follow different trajectories in a very flexible way, as shown in figure 5.17.

It's important to notice that, as reported in Carrara's work [69], more than one microdevice can be guided at the same time in the same arena with the OctoMag technology and the microdevices are also able to climb a step of an height up to 50% the diameter of the microdevice itself.

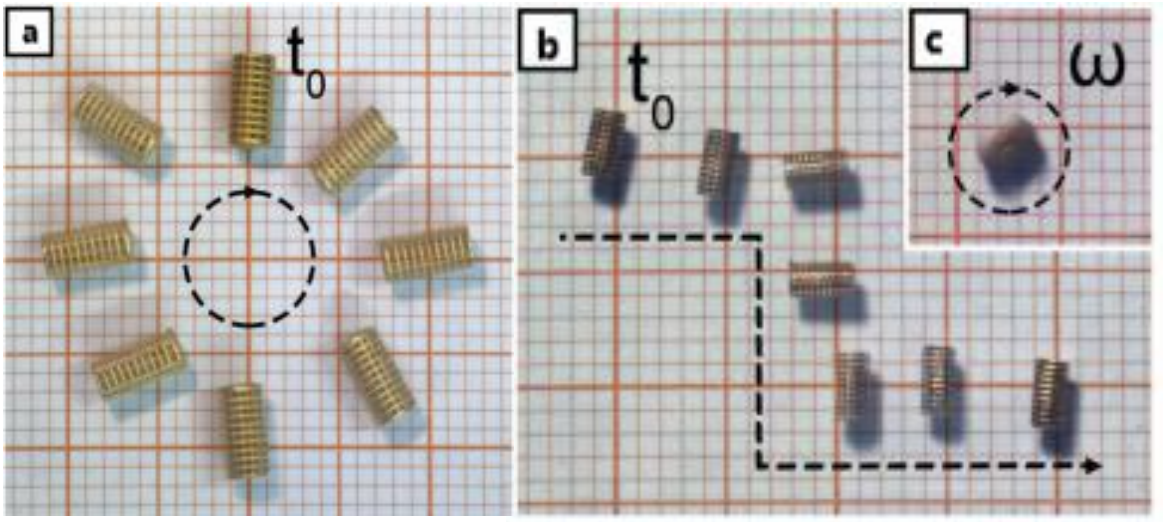

Figure 5.17 - Examples of different trajectories using the OctoMag technology

5.1.5 Metallization of planar samples for adhesion tests

In order to select the proper hydrogel type to be applied on the microdevices, planar adhesion tests have been made to investigate the interaction between the metallic support and the polymeric matrix of hydrogels (further discussion in the next paragraphs).

The planar samples were metallized in order to mimic the surface of the microdevices, but since the samples were constituted by stainless steel and they were not supposed to be magnetically actuated, there was no need of the intermediate metallic layers (Cu and CoNiP).

The only properties of interest in this part of the work are the surface properties of the samples and, being the microdevices surface properties determined by the final metallic layers, it's been chosen to metallize the samples with a first Nickel layer followed by a finishing Platinum layer. This Pt layer is able to mimic the microdevices surface and to reduce the metallization costs related to the Aurotech solution for the external gold layer.

5.1.5.1 Experimental section

The planar samples (figure 5.18) were made by rectangular stainless-steel slabs (L_1 2.5 cm, L_2 6 cm, thickness 1 mm).

In the metallization steps the only area which has been metallized is an area

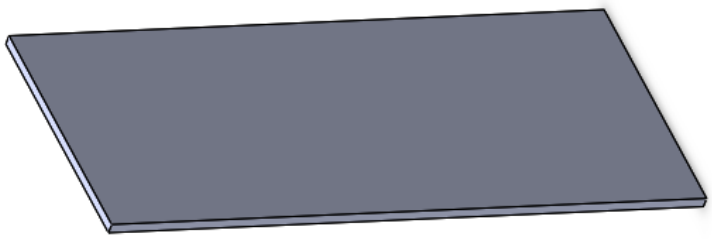

Figure 5.18 - 3D representation of the planar samples used for the experimental work

of 1.5x1.5 cm, while the remaining part of the planar samples were used to perform the electrical junction for the electrodeposition steps.

First of all, the sample was cleaned and prepared for the metallic layer deposition by:

- Cleaning and degreasing by immersing the samples in acetone under sonication.
- Surface preparation by immersing the samples in HCl solution (37%).

After that, the stainless-steel samples have been electrolytically metallized with the first Ni layer and then with the finishing Pt layer.

Electrolytic Ni aqueous bath formulation, for a final volume of 200ml:

- 50 g Ni chloride
- 50 ml HCl solution (30%)

Deposited for 1 min with a current of 300 mA (133 mA/cm^2), using a soluble Ni anode.

The Pt layer was electrolytically deposited above the Ni one, using a patented commercial solution and an insoluble Ti anode.

The plating was performed with a current of 47 mA (21 mA/cm^2) at 50°C for 20 min.

It's important to underline that the current has to be applied as soon as possible to the samples because of the spontaneity of the substitution reaction, which immediately starts.

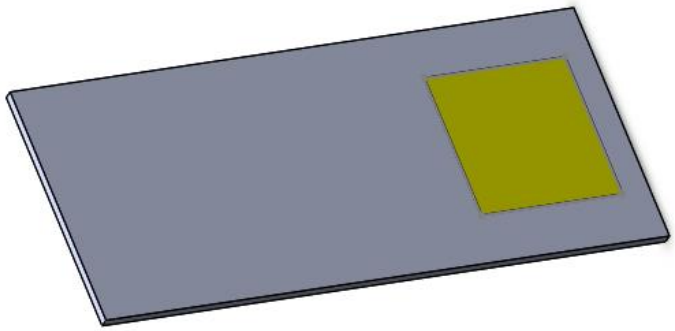

Figure 5.19 - Conceptual representation of the sample after metallization

The conceptual result after the metallization steps is shown in figure 5.19, in which the yellow area is the only one covered in Platinum and, only on that area, will be performed the adhesion tests. After the final Pt layer deposit, the samples were cleaned with deionized water and then dried.

5.2 Hydrogel coating

5.2.1 Hydrogel choice

After the preparation of the scaffolds, the problem was the hydrogel choice. during this work different kind of hydrogel were tested. In particular the parameter most taken into consideration was the hydrogel adhesion to a metal substrate. Planar metallic samples covered with platinum were prepared in order to test adhesion. In particular two families of hydrogel were tested: AC hydrogels and alginate hydrogels. These polymers were chosen because of their known biocompatibility.

Alginate hydrogels have been thoroughly described in the previous chapters, while AC hydrogels were prepared through chemical cross-linking of two polymers, agarose and Carbomer 974P (the name AC comes from these two components). The various AC gels differ slightly in mesh size and toughness. Gelation occurs via microwave-assisted free radical polymerization. Heating to 80 °C leads to a higher macromer mobility, and thus enhances short-range interconnections among functional groups of the polymers. Esterification, the main reaction, between Carbomer carboxylic groups and the agarose hydroxyl groups. Gelation becomes preponderant when the temperature drops below a certain degree, increasing rapidly the viscosity [70].

All the adhesion tests were performed also with the mimic drug (Rhodamine B from Sigma-Aldrich) inside, in order to rule out the possibility that the gel will

behave in a different manner when applied on the scaffolds together with the mimic drug.

In order to economically research the effectiveness of drug release matrices, a model drug is commonly used [71 - 73]. Rhodamine B was selected as the model drug for this investigation. This small molecule is assumed to accurately mimic the release of actual small molecule medications. Rhodamine B is fluorescent magenta, which allows for easy absorbance readings. With rhodamine B at low concentrations, the Beer-Lambert law can be used to model the absorbance as a function of concentration. Due to this fact, it is possible to create a connection between the amount of drug released and the time spent, as will be further discussed later on.

5.2.1.1 Experimental section

The following table describe the composition of the various AC gel tested and their synthesis method:

Gel	Composition	Quantity
AC 1	PBS	9.95 ml
	Carbomer 974P	50 mg
	pH	7.9
AC 6	PBS	6.85 ml
	Carbomer 974P	50 mg
	Propylene glycol	3 ml
	Glycerol	0.1 ml
	pH	7.4
AC PEG	PBS	5 ml
	Carbomer 974P	35 mg
	PEG (2000)	300 mg
	pH	7.4

Table 5.12 - AC gels composition

Where:

- PBS (Phosphate Buffer Saline). It is a water-based salt solution containing sodium phosphate, sodium chloride, potassium phosphate and minor amounts of carbonates and other sodium salts. PBS is used because it helps maintaining a constant pH in hydrogel synthesis thanks to its buffer nature.
- Carbomer 974P. This compound is a cross-linked poly-acrylic acid characterized by the presence of several carboxylic groups (65%), that make it an ionisable molecule. It has a molecular weight of about 1 million Da and it has a structure that underlines the presence of a carboxylic group in each monomer.

- Agarose ultra-pure. It is a purified linear galactan hydrocolloid isolated from agar or agar-bearing marine algae. Structurally, it is essentially a linear polymer constituted of alternating D-galactose and 3,6-anhydro-L-galactose units.
- PEG (2000). It is Polyethylene glycol with average molecular weight of the chains equal to 2000 g/mol.

Hydrogel preparation is divided into two parts: the first differ for the three hydrogels while the second part is the same for every one.

Part 1

- AC 1. Mix PBS and Carbomer, stir for 30 minutes. Let it settle for 1 hour, then change the pH to 7.9 with NaOH 1 mol/l.
- AC 6. Mix PBS and Carbomer, stir for 30 minutes. Add Propylene glycol and glycerol, stir for 45 minutes. Let it settle for 1 hour, then change the pH to 7.4 with NaOH 1 mol/l.
- AC PEG. Mix PBS and Carbomer, stir for 30 minutes. Add PEG and stir for 45 minutes. Let it settle for 1 hour, then change the pH to 7.4 with NaOH 1 mol/l.

Part 2

Put 25 mg of agarose in 5 ml of one of the three previous formulations. After complete mixing the whole system is put into a microwave at 500 W for 30 seconds to 1 minute until the solution reaches 80 °C. After this passage it is imperative to keep the solution heated above at least 50 °C otherwise it will solidify.

The coating method on the planar sample is performed by dipping the object in the solution, which once activated, is kept over 50 °C. After dipping the object is removed and a thin film of liquid gel will be present on the surface due to its viscosity. The film solidifies after cooling and then the adhesion can be evaluated. In this part of the work, our only aim was to choose the most promising hydrogel to be used on metallic devices, therefore the adhesion analysis was just qualitative.

Other than the Agarose-Carbomer based hydrogels also the alginate

hydrogel was tested. It was prepared in the following way.

- Prepare a solution of ultrapure sodium alginate in distilled water (2% w/w).
- Stir for at least 30 minutes, then add 1 mg of Rhodamine B every ml of distilled water in the water/alginate solution.
- In another container prepare a solution of CaCl2 1% (w/w) in distilled water. The coating method on the planar sample is performed in the following way:
- Dipping the object in the Rhodamine B/alginate/water solution.
- The object is removed, and a thin film of liquid gel will be present on the surface due to its viscosity. Figure 5.20 shows an example of the kind of result we obtained with AC 6 hydrogel.
- Then the object is dipped in the CaCl2 solution to trigger gelation. At this point the adhesion is qualitatively evaluated.

The film of gel is considered both just following gelation and after 30 minutes, the planar devices have been put for several minutes in water to test adhesion also in that condition. The interaction between the AC hydrogels and the metallic surface was in general really poor, while the alginate hydrogel showed more interaction. The most promising hydrogel was therefore estimated to be the alginate hydrogel, so we choose to proceed using this compound.

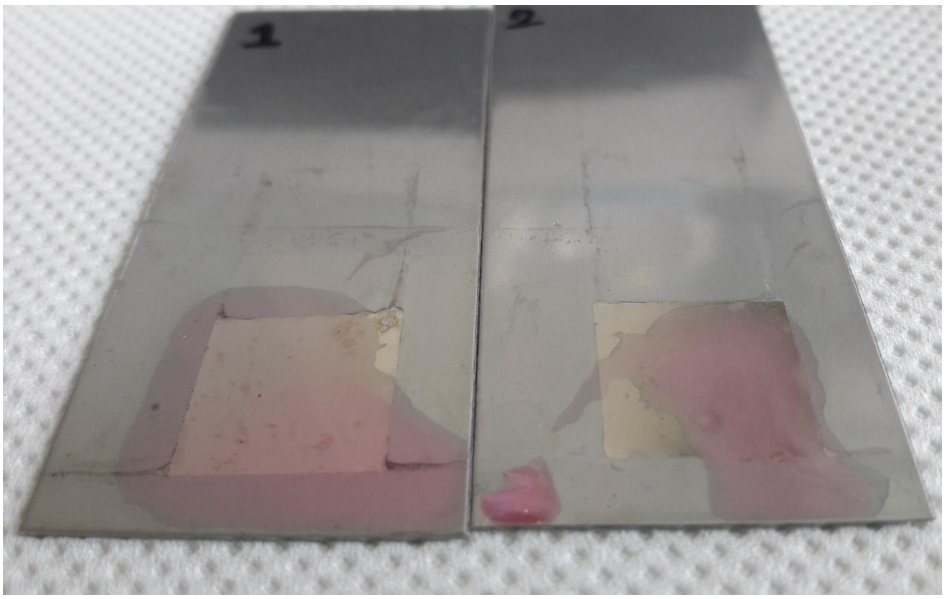

Figure 5.20 - AC 6 hydrogel and its adhesion on planar metallic device

5.2.2 Coating method – part 1

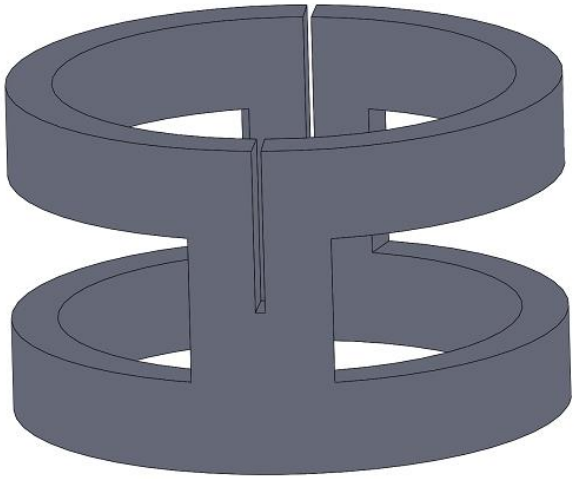

Figure 5.21 - Structure used to hang the device

The coating method of the scaffolds is hereby described. The robots are coated by dipping them in the solution of sodium alginate and Rhodamine B and then in the solution of CaCl2, as previously described. The first problem was to obtain a homogeneous coating on the device, so a small plastic structure was utilized together with a very thin thread in order to hang the device, preventing it from touching any part of the container. The plastic structure shape is represented in figure 5.21.

5.2.2.1 Experimental section

Figure 3 shows the steps followed in order to obtain the final coating.

- The device is immersed with the plastic structure in the alginate/Rhodamine B aqueous solution for 20 minutes (figure 5.22a). This step is performed inside an ultrasonic bath sonicator in order to favour the penetration of the alginate chains inside the scaffold matrix.
- Then the structure is immersed in the CaCl2 aqueous solution for 1 minute to obtain the first hydrogel layer (figure 5.22b).

- At this point steps a and b are repeated in order to obtain the second hydrogel layer (figure 5.22c and 5.22d).

  Figure 5.23 shows the final result.

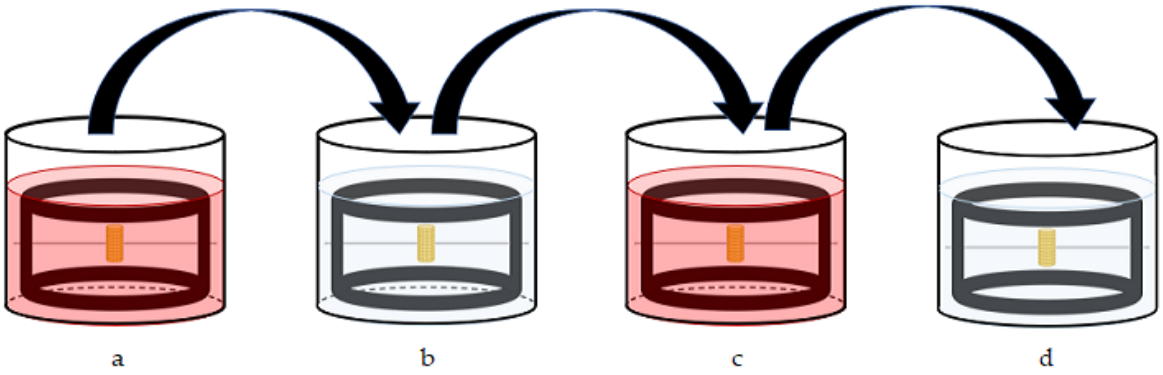

Figure 5.22 - Coating method

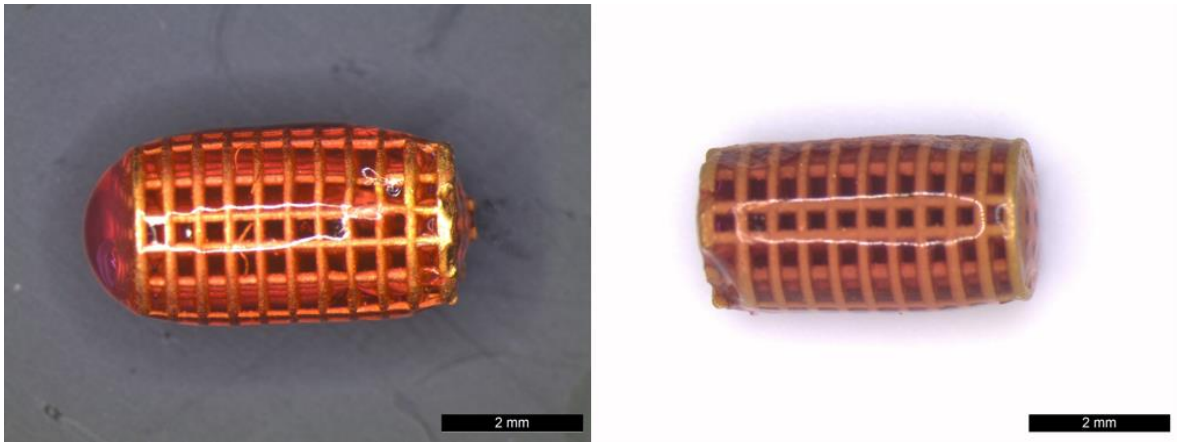

Figure 5.23 - Coated scaffold

5.2.3 Miscellaneous – part 1

5.2.3.1 About the number of cycles

Determining the number of cycles means defining the mass quantity of hydrogel present on the device. This is important for a number of reasons. Mainly, if a large quantity of matter covers the magnetic device, the electromagnetic interaction is severely hindered. On the other hand, too little hydrogel means that the quantity of drug the device will carry will be really low. So, an optimum had to be found. A statistic test has been performed in order to define the average quantity of gel deposited every cycle. Here the results will be presented.

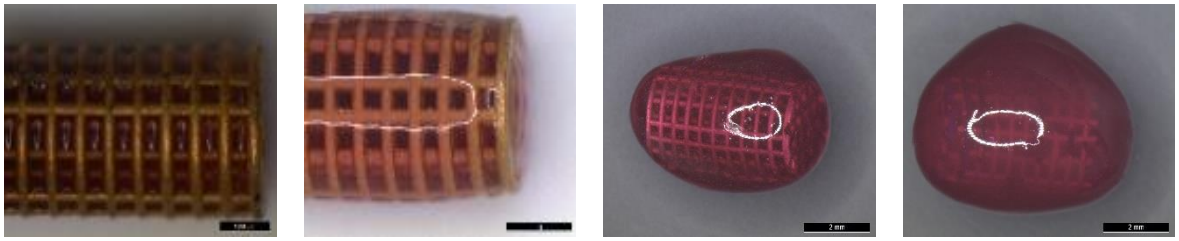

Figure 5.24 - Metallic scaffold coated with alginate hydrogel. From left to right 1, 2, 3 and 4 layers of gel.

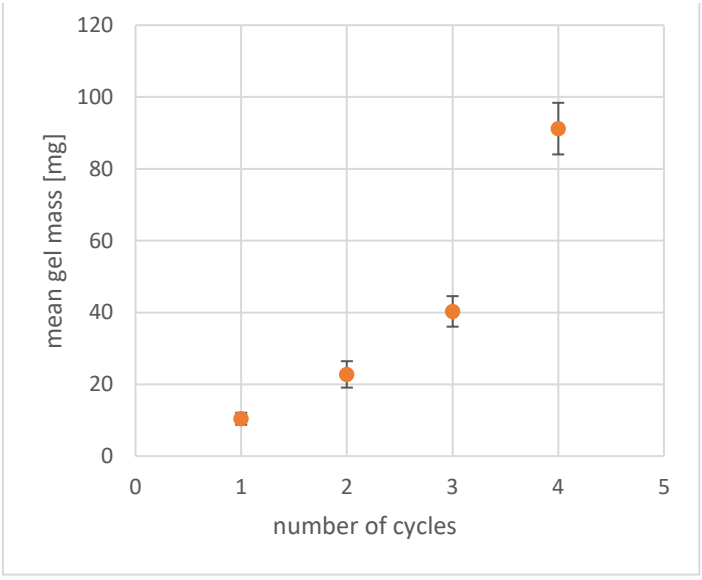

Figure 5.25 - Hydrogel mass on the device versus the number of cycles

Figure 5.24 shows the results we obtained for each number of cycles, and the plot in figure 5.25 shows the average increase in mass of the hydrogel with every

cycle. Just from the image it can be seen that after the third hydrogel layer the device was barely visible. The magnetic tests also confirmed that after the second cycle the scaffold was not very responsive when subjected to a magnetic field. At last the optimum number of cycles was fixed at two.

5.2.3.2 About time and bath concentration

The data on gelation time, alginate solution concentration and CaCl2 solution concentration was found in literature [74]. We took several tests and conclude that for a CaCl2 solution concentration higher than 1% (w/v) the thickness of the layer was too big. The concentration of Rhodamine B in the alginate solution was chosen due to its solubility in water, which according to Sigma-Aldrich is 1 mg/ml.

5.2.3.3 About Hydrogel dissolution

After consulting literature [75], we decided to use a solution 0.3 M of Sodium Citrate in distilled water. Indeed, alginate forms stable gels in the presence of certain cations; gelling conditions are mild, and the gelation process can be reversed by extracting calcium ions. This can be done, for instance, by adding citrate.

The coated scaffolds were put in this solution for at least 3 hours in order to obtain complete dissolution of the hydrogel. Figure 5.26 shows the reduction of

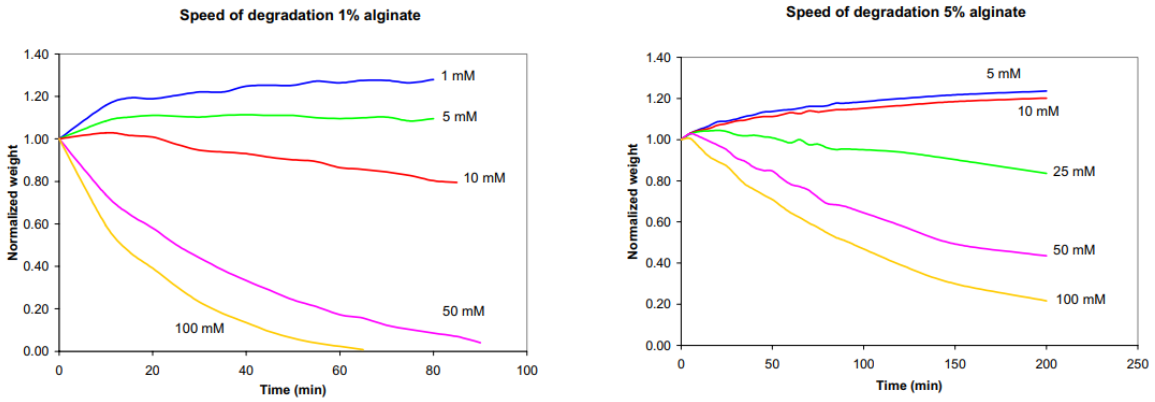

Figure 5.26 - Degradation of alginate hydrogel under the influence of several citrate solutions

weight of alginate gel when put inside a citrate solution. Both graphs demonstrate that the speed of degradation increases for higher citrate concentrations. For lower concentrations there was a slight increase of weight due to swelling of the samples.

5.2.3.4 About scaffold reutilization

By using the Sodium citrate method, we were able to utilize several times the scaffolds in our tests. However, at every cycle, some of the metallic coating went missing and the scaffold were found to be less magnetic. Also, by looking at the scaffolds, it was evident that after some reutilizations a part of the final gold layer went missing, exposing the black CoNiP layer below. So, in the end the scaffold has to be replaced after some coating/degradation cycles. We performed some experiment in order to plot the average weight loss as a function of the number of citrate washing (figure 5.27). It is important to consider that while our concern was just the Rhodamine B drug release from the scaffolds, we could accept some imperfection in the final gold layer.

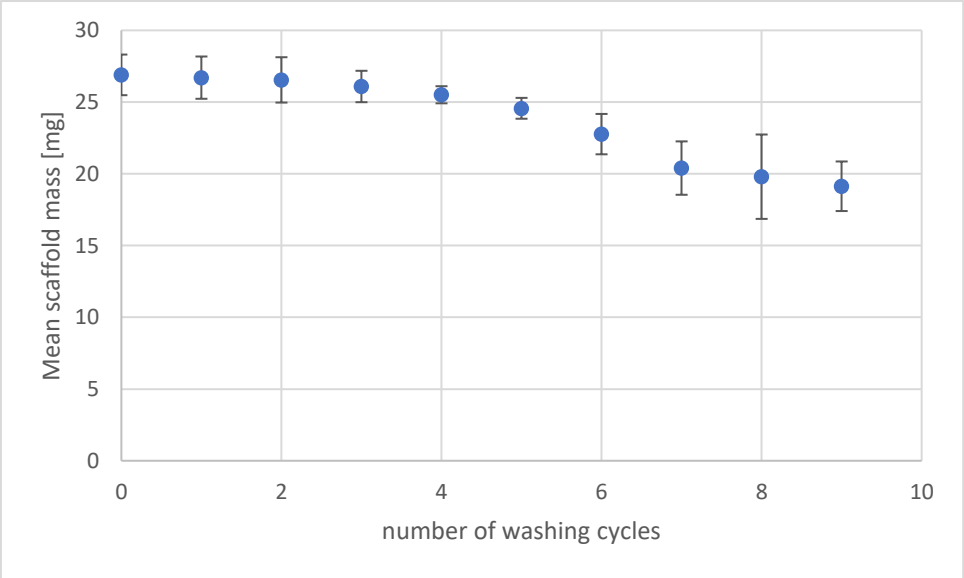

Figure 5.27 - Average scaffold mass versus the number of washing cycles. The weight loss can be seen

5.2.3.5 About Rhodamine B concentration

The quantity of Rhodamine B per gram of total gel mass (table 5.13) is an important parameter, used to draw the release plots.

Species	Normal Sodium Alginate	Water	Rhodamine B	Total
Quantity (g)	2	100	0.1	102.1
Quantity approximated (%)	1.96	97.94	0.1	100

Table 5.13 - Quantity of Rhodamine B in the Alginate hydrogel

5.2.4 Magnetic tests

Magnetic tests were performed with OctaMag exactly like the ones for the uncoated scaffolds. The correlation velocity-frequency was evaluated, and some considerations were made concerning the difference with respect to the uncoated case. These aspects will be addressed in results and discussion.

5.3 Drug delivery – part 1

5.3.1 UV spectrophotometer

The instrument used in order to study drug delivery is called UV spectrophotometer. The spectrophotometry is a technique that exploits the absorption of light from a sample, by passing a light beam through it. Thus, it is possible to measure the light intensity and eventually to find the chemical concentration of our target in the samples.

It's basically constituted by two instruments:

- Spectrometer, to produce light at any wavelength
- Photometer, to measure the light intensity

The sample at unknown concentration is placed between the two parts so that the light is able to pass through it and thus be weakened. The photometer is able to sense the attenuation and based on that the spectrophotometer, being set the parameter related to the specific chemical analysed, returns the absorbance values, from which it's possible to calculate the concentration.

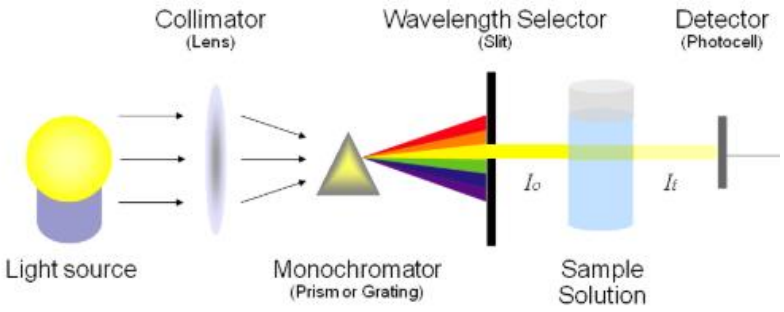

Figure 5.28 - Conceptual sketch of a spectrophotometer

The basic spectrophotometer instrument is shown in figure 5.28. It is composed of a light source, a monochromator, a wavelength selector to pass only the selected wavelength, a collimator to direct the light beam and the photoelectric detector.

Important parameters are:

- I_0 light intensity before passing through the sample.
- I_t light intensity before passing through the sample.
- Transmittance (T) defined as $T=I_t/I_0$
- Absorbance (Abs), that is the output of the instrument, $Abs=-\log(T)=-\log(I_t/I_0)$

I_t and I_0 are known since the former is measured by the photometer while the latter is generated by the spectrometer (figure 5.29), thus both Abs and T are straightforward calculated and reported by the instrument itself.

The concentration calculation is then based on the Lambert-Beer law which is the following:

$$Abs = k * l * C$$

where:

- Abs is the dimensionless absorbance calculated before.
- k is the molar extinction coefficient or molar absorptivity (or absorption coefficient), given as a constant and varies for each molecule.
- l is the path length, known from the sample (standard) dimensions.
- C is the chemical concentration.

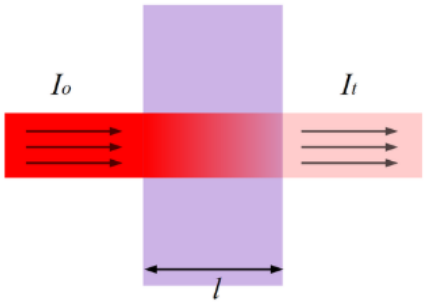

Figure 5.29 - Graphical model of LB

The samples are multiwell plates used for UV spectrophotometry through which, thanks to their matrix-like configuration, it's possible to perform multiple simultaneous concentration measurements of the desired chemical.

5.3.2 Rhodamine B

Drug release experiments were done in order to describe the kinetic of release of the mimic drug Rhodamine B, which was loaded into the matrix of the hydrogel attached to the metallic scaffold.

- For each drug release test at least 3 different metallic scaffolds were coated in the exact same conditions, this is due to ensure statistic relevance of the results.
- The samples were prepared in the way described before. The scaffolds were weighted before and after the application of the gel, in order to know exactly the mass of hydrogel present on each scaffold. This data is essential to know the initial quantity of drug loaded and as a consequence it is essential to draw the release curve.
- Each different scaffold is put in a different well and exactly 1 ml of distilled water is added. The wells were then put in a heater at exactly 37 °C, which is the temperature of the human body. So, the release was performed in these conditions.
- At different time points, 0.5 ml of solution is taken from each well and put in different vials. The vials are conserved in the fridge at around 4 °C.
- Consecutively, 0.5 ml of distilled water is added to each well in order to restore the initial 1 ml of solution.
- These withdrawals are done at 30 minutes, 1 hour, 2 hours, 3 hours and so on, until complete release.
- After the test is ended, the withdrawals have to be put in multiwell plates in order to be read by the UV spectrophotometer.
- In order to in interpret the data acquired the calibration curve have to be built. The construction of the calibration curve is reported in the next chapter.

5.3.3 Dextran 70k

The behaviour of small drugs can be accurately characterized by using the Rhodamine B. However, other drug molecules are way bigger than the molecule of Rhodamine B. In order to analyse the release rate of big drugs in the same conditions from the alginate hydrogel we then substitute Rhodamine B with another fluorescent mimic drug: Fluorescein isothiocyanate–dextran average molecular weight 70,000 g/mol from Sigma-Aldrich. Like Rhodamine B it is fluorescent, and its concentration can be calculated with the aid of the UV spectrophotometer. However, a different calibration curve has to be done. Being the Dextran molecule almost 150 times bigger than the Rhodamine B molecule (molecular weight 479.02 g/mol), a different release rate is expected. The difference can be due to the steric hindrance of the Dextran, which might diffuse slower through the matrix of the alginate hydrogel.

5.4 Functionalization of alginate hydrogel

The controlled drug release from polymeric systems, and specifically from hydrogels, is a key point in this work.

The classic drug delivery systems are essentially driven by diffusion, which is very quick because of the high concentration gradient during the release process within the organism.

In the past years, new concepts and ideas were generated to better control the drug release's key features such as pharmacokinetics, bioavailability and drug effectiveness, they're called smart drug delivery systems.

Among all the smart drug delivery systems a lot of interest has been given to the so called "smart polymers" which are basically particular polymers with peculiar properties given by their functionalization, as already said in the previous

chapters.

The set of smart polymers is constituted by a wide class of polymers, but surely hydrogels are one of the most promising polymer-based drug delivery systems because of their soft and elastic behaviour and the thermodynamic compatibility with water. In addition to that, it's possible to tune their behaviour

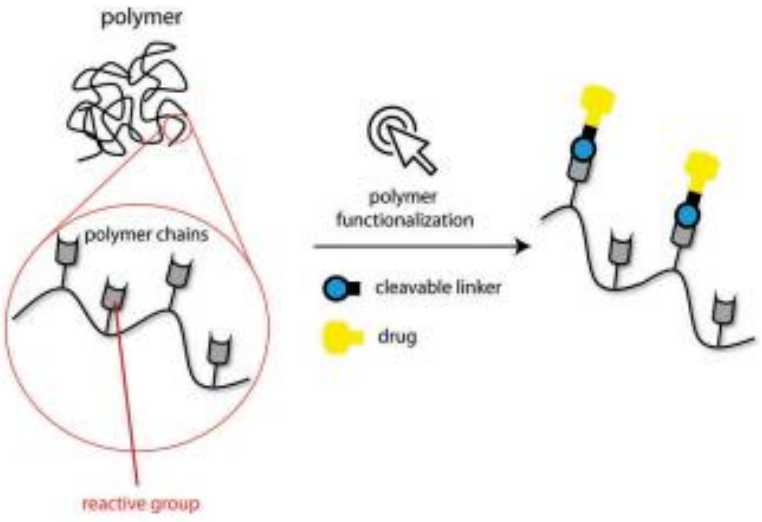

Figure 5.30 - Post-polymerization conceptual representation. Polymer functionalization with drugs

based on the surrounding environment's properties such as temperature, pH and so on [78 - 80, 86]. The most used hydrogels are chitosan and alginate hydrogels [76, 77].

Typically, the functionalization is carried out in a post-polymerization way [81, 82] as schematized in figure 5.30. This method is based on the direct polymerization of monomers to obtain the polymeric chain avoiding the attack of their chemoselective sites, which are inert respect to the polymerization conditions but can be converted in a quantitative and controlled way, with a subsequent modification step, into other functional groups able to be linked with the drug, or otherwise directly linked with the drug itself. It has been demonstrated that it is possible to obtain excellent conversions under mild conditions [84].

In this work we choose to functionalize the polysaccharide Sodium Alginate polymer with click-chemistry [83, 85, 69] and amidation [87] methods in order to

allow the related hydrogel to have an enviro-stimuli responsive behaviour and, in particular, to release the chemically loaded mimic drug only in response to a change in the environment's pH.

The drug bounded to the polymeric chain of the hydrogel is able to be released due to the breakage of the cleavable chemical bond that links the drug to the polymer's backbone.

The two different bonds we obtained through the two different functionalizations have a dissimilar strength and stability behaviour in response to a change in pH conditions. So, we investigated the release profile of both.

It's possible to tune the degree of functionalization by carrying out the Alginate functionalization reaction with an appropriate molar ratio between the polymer and the opportunely modified mimic drug molecule.

In the first functionalization strategy, the ester-functionalization, the propargylamine modifies the carboxyl (-COOH) group of the alginate monomer according to the desired molar ratio. Then, only the only the modified Alginate monomers (the ones which exhibits the propargyl functional group) are able to be attached with the modified Rhodamine azide. We can define the degree of functionalization DF like this:

$$DF = \frac{m}{n + m}$$

Where m (modified) is the number of modified alginate monomers and n (normal) is the number of unmodified ones.

The same concept has been exploited also for the second functionalization strategy, the amidic-functionalized Alginate, with the only difference that in this case the Alginate reacts directly with the aminoethyl Rhodamine to form the amidic bond through which the polymer is functionalized.

It's nevertheless important to underline the fact that the Alginate gelling behaviour and the final hydrogel's mechanical properties are given by the interaction between the carboxyl group of the polymer and the Ca^{2+} ions provided

during the gelation by the $CaCl_2$ solution.

So, due to the functionalization of a percentage of the carboxyl groups present in the polymer chain, there will be less carboxyl groups able to interact with the Ca^{2+} ions to build the hydrogel 3D matrix with the consequent worsening in mechanical properties and gelling behaviour of hydrogel itself.

We will address this fact in detail later on.

5.4.1 Ester functionalization, ester link functionalized Alginate

The Alginate functionalization based on the creation of a cleavable ester link with the related Rhodamine B derivate is constituted by the sum of different chemical steps, involving also a copper-catalysed Azide-Alkyne Cycloaddition click chemistry reaction (CuAAC) and the formation of an amidic bond on the alginate carboxyl groups in order to insert the $-N_3$ group on the polymer chain itself through which the click reaction can be carried out.

To exploit the CuAAC click chemistry reaction, both the starting Sodium Alginate and the Rhodamine B need to be chemically modified in order to obtain the appropriate functional groups (the azide group on the polymer chain and the alkyne group on the drug molecule), which reactivity will be further exploited.

The click reaction is a typical triazole formation in presence of Cu (catalyst) starting from the azide group (present in the modified Rhodamine) and the propargyl group of the modified alginate (alkyne).

The most difficult steps in this case are the chemical modification of the alginate to create the propargyl-derivate of the polymer itself and the azide modification of the starting Rhodamine B.

The conceptual reactive steps for the functionalization of Sodium Alginate with Rhodamine B, with the ester bond, are:

- Synthesis of a molecular spacer that will provide the azide group ($-N_3$) to the Rhodamine B molecule to make it able to undergo click reaction and form

the triazole (R1 in figure 5.31).

- Chemical modification of Rhodamine B [88], by reaction with the previously synthetized spacer to form the RhB-N_3 ester (Rhodamine B azide, R2 in figure 5.31) that, thanks to the presence of the azide group, is able to undergo to the click reaction that will follow.
- Chemical modification of the starting Sodium Alginate, by reacting with propargylamine via amidation reaction (R3 in figure 5.31) [87], in order to provide to the Alginate, the propargyl group for the click CuAAC reaction with the Rhodamine B azide.
- Click reaction, to finally obtain the Rhodamine-functionalized Alginate through the formation of a triazole link between the Rhodamine B and the Alginate derivate (R4 in figure 5.31).

The involved reactions are the following:

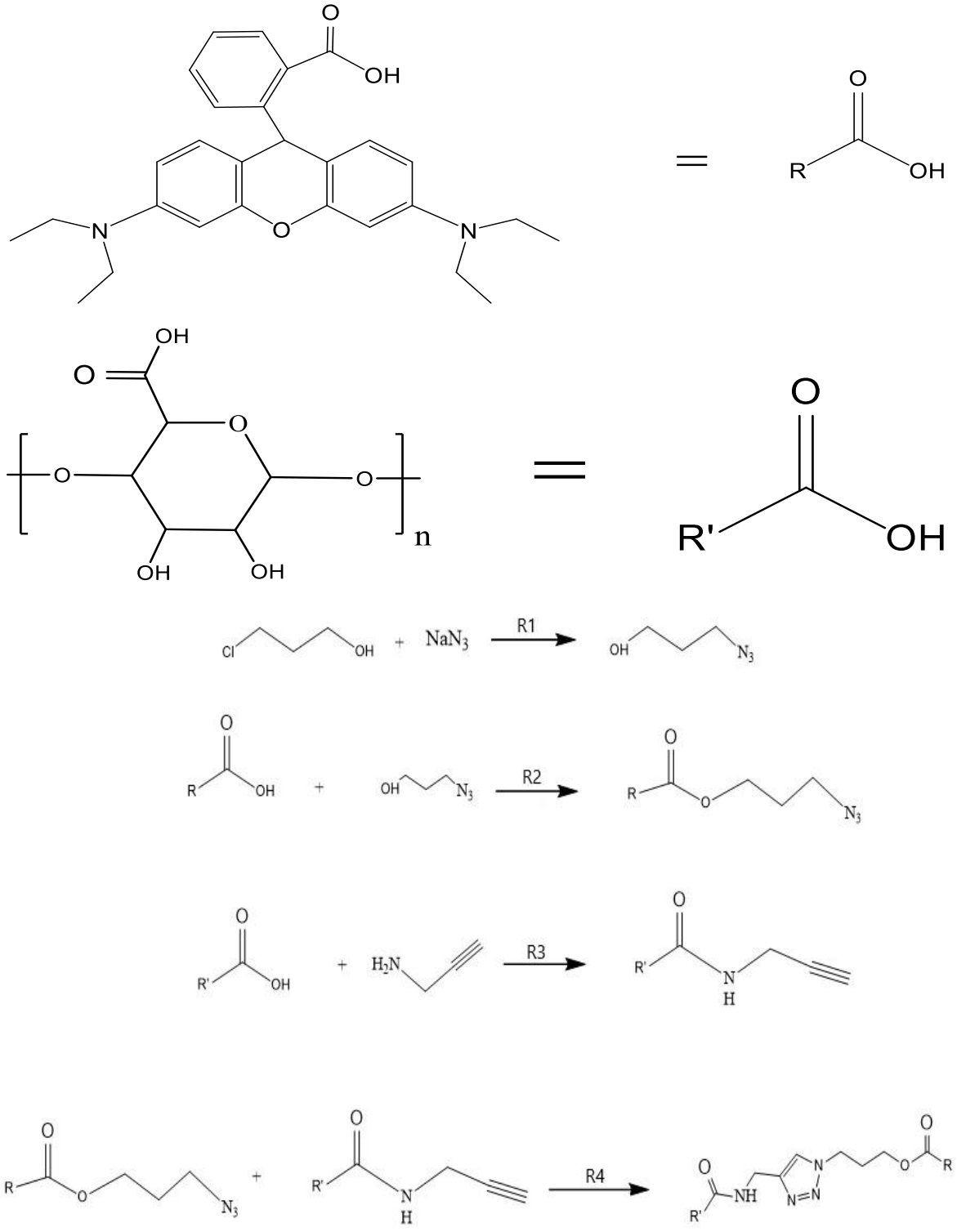

Figure 5.31 - Compendium of reactions to obtain the ester-functionalized Alginate

The obtained ester bond functionalized Alginate structure is reported in figure 5.32. It is possible to identify the drug-polymer link constituted by a sequence of ester, triazole and amidic links.

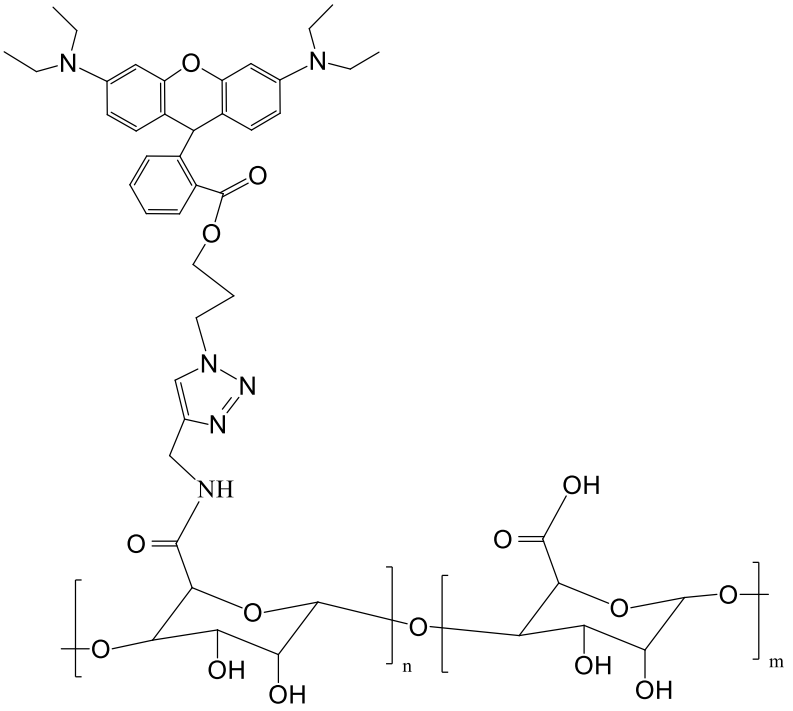

Figure 5.32 - Ester-functionalized Sodium Alginate structure

5.4.2 Experimental section

All the chemicals were purchased by Sigma-Aldrich and used as they are without further purifications.

5.4.2.1 synthesis of the molecular spacer

The molecular spacer was synthetized according to the reaction R1 of figure 5.31, here reported in figure 5.33.

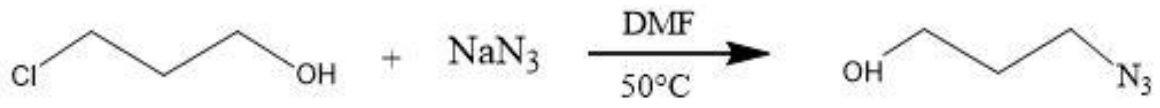

Figure 5.33 - Synthesis of the molecular spacer for ester bond creation

The chemicals and their related quantities are reported in table 5.14.

Compound	Quantity	MW [g/mol]	n [mol]	Ratio [-]
$Cl(CH_2)_3OH$	1 g (0.877ml)	94.54	0.010578	1
NaN_3	0,79 g	65.0099	0.012164	1.15
DMF	20 ml			

Table 5.14 - compounds and quantities for reaction R1

The DMF (Dimethylformamide) was used as solvent for the reaction.

The molar ratio between the Sodium azide (NaN_3) and the 3-Chloro-1-propanol was set to 1.15 in order to have a 15% excess of NaN_3 in order to be sure to have a 100% of conversion of the $Cl(CH_2)_3OH$.

The 3-Chloro-1-propanol was in liquid form so to have 1g of reactant, 0.877 ml of liquid solution were taken with an appropriate pipette.

The reaction procedure is simply mixing, in a reactor with magnetic stirrer, the 3-Chloro-1-propanol in the DMF, then adding the Sodium azide, the reaction is carried on at a Temperature of 50°C for a period 24 h under stirring.

The purification sequence is the following:

- Solvent extraction, with diethyl ether and brine, in order to obtain an organic phase at the top of the separating funnel and one aqueous phase at the bottom. The product remains in the top organic phase and the extraction of the remaining product from the aqueous phase need to be performed another time to be completed, always with diethyl ether.
- The two organic phases are mixed and then washed with brine for five times to remove all the traces of the lipophobic compounds.
- Removing the remaining aqueous phase from the organic one (there are traces of aqueous phase in the extraction step) using $NaSO_4$, particular care to this step because Sodium azide is dangerous in the rotavapor drying step that will follow.
- Filtering to remove the Sodium sulphate.
- Drying in rotavapor at 45°C.

At this point the spacer has been obtained and it's ready to react with the

Rhodamine B.

5.4.2.2 modification of Rhodamine, bonding of the spacer

Typically, the modification of Rhodamine B is a complicated and expensive process that often requires highly reactive reagents (e.g. trimethylaluminum, for the dyes and pigments industrial sector) as well as tedious purification steps.

In literature are reported a lot of possible chemical modifications that allows to obtain an ester link on the carboxyl functional group of Rhodamine B, but the smartest approach possible is the one that allows to easily obtain the desired product minimizing both costs and procedures complexity.

To match those requirements, the X. Chen et al. work [88] has been analysed and, among all the possible functional groups modifications, the selected one was the modification of Rhodamine B with the ester link to obtain the triazole group.

The procedure is simple, and the product can be obtained directly from the reaction mixture following a simple and straight forward workup procedure, with trivial purification steps.

Based on the previously mentioned work, the Rhodamine B modification reaction has a yield of about 60% with a product purity greater than 97%, and it's possible to separate the product of interest by a simply solvent extraction because the starting Rhodamine B is polar and very hydrophile while the product is less polar thanks to its substituent, thus it tends to stay in the organic phase while the reactant tends to remain in the aqueous one allowing to have the high purity level in the product.

The one-step general process through which the spacer attachment reaction of this work has been based, is reported in figure 5.34.

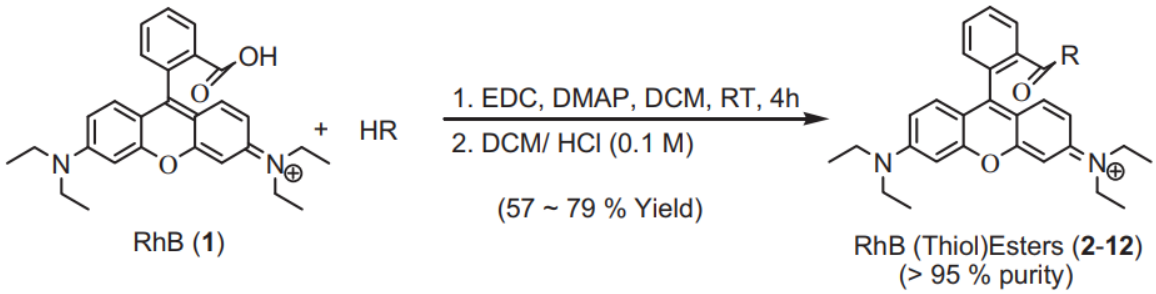

Figure 24.34 - Generalised reaction for Rhodamine B esterification

In this work has been adopted the Chen et al. pathway, as reported in the reaction of figure 5.35 [88], that allows an approach for the preparation of Rhodamine modifications featuring the required ester bond linkage, without having Spirolactam by-product, thus simplifying the purification procedure, the reaction (R2 of figure 5.31) is reported in figure 5.35.

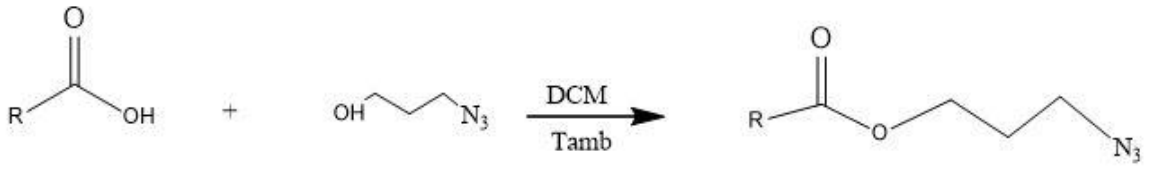

Figure 5.35 - Bonding of molecular spacer on Rhodamine B, ester bond creation

The chemical species, the related quantities and molecular ratios are reported in table 5.15:

Compound	Quantity [mg]	MW [g/mol]	n [mol]	Ratio [-]
Rhodamine B (open configuration)	300	444	0.6756757	1
Spacer N3(CH2)3OH	88,8	101.11	0.8783784	1.3
EDC*HCl	142.5	191.7	0.7432432	1.1
DMAP	16.6	122.7	0.1351351	0.2
DCM	10+5 ml			

Table 5.15 - Compounds and quantities for reaction R2

The DCM (dichloromethane) was used as solvent for the reaction and the molar ratio between Rhodamine B and the previously synthetized molecular spacer was set to 1.3 in order to have a 30% excess of spacer and to be sure to have 100% conversion of Rhodamine B during reaction.

DMAP (4-Dimethylaminopyridine) is a typical esterification reaction catalyst while EDC*HCl is a coupling agent, as will be further discussed.

The synthesis procedure is the following:

- Mix the reactants in the following order: Rhodamine B, molecular spacer, EDC*HCl and DMAP, in a reactor already filled with the first 10 ml of DCM, under magnetic stirring.
- Stirring for 4 h at T_{amb} having care of insulating the reaction environment from the light with an aluminium foil.
- Add the remaining 5 ml of DCM to make easier the subsequent solvent extraction.

The purification procedure is the following:

- Solvent extraction. In a separating funnel, a three-step extraction procedure is required with three different solvents that are, in order: distilled water, HCl solution (0.1M) and brine. Each step has to be performed twice with particular care to the organic phase (in which there's the product) that remains at the bottom of the separating funnel because of the higher density of DCM with respect to the aqueous one.
- Removing the remaining aqueous phase from the organic one (there are traces of aqueous phase in the extraction step) using $NaSO_4$.
- Filtering, to remove $NaSO_4$.
- Drying in rotavapor at 45°C.

The product has to be stored in fridge with particular care to insulate it from the light to avoid degradation.

5.4.2.3 Modification of alginate, synthesis of propargyl alginate

The reaction is formally an amidation, according to the example reaction shown in figure 5.36 [86, 91]. Sodium Alginate was modified by the use of the coupling agent 1-ethyl-3-(3-dimethylaminopropyl) carbodiimide hydrochloride (EDC-HCl) to form the amide link between the amine-containing molecule

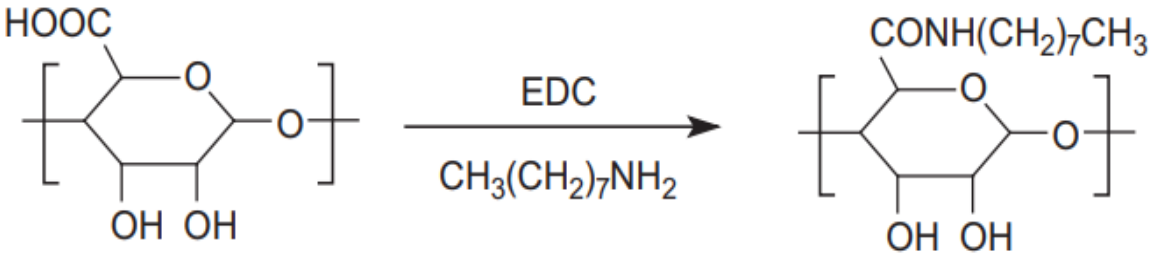

Figure 5.36 - General example of amidation reaction on Sodium Alginate

(propargylamine) and the carboxyl groups of the polymer itself.

The starting alginate was chemically modified to obtain propargyl alginate according to the reaction (R3 in figure 5.31) reported in figure 5.37.

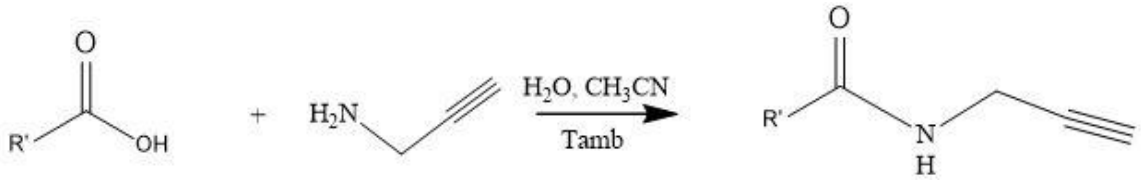

Figure 5.37 - Amidation reaction of Alginate with Propargylamine, insertion of the azide group on the polymer chain

The chemical species, the related quantities and molecular ratios reported in table 5.16 are adaptations based on the E. Mauri's work [90]:

Compound	Quantity [g]	MW [g/mol]	n [mol]	Ratio [-]
Alginate	1	216	0.00462963	1
Propargylamine	0.127 (0.107 ml)	55.08	0.002314815	0.5
HOBt	0.313	135.12	0.002314815	0.5
EDC*HCl	0.444	191.703	0.002314815	0.5
CH3CN	7.5 ml			
H2O	7.5 ml			

Table 5.16 - Compounds and quantities for reaction R3

As previously said, the degree of functionalization of the final hydrogel depends on the percentage of carboxyl groups attacked by the amidation reaction.

The molar ratios reported in table 5.16 have been chosen in order to obtain 50% of functionalization, which was expected to allow good gelation and hydrogel mechanical properties and at the same time allow a good drug loading for ensuring a quantitative delivery and an effective release.

The operating procedure is the following:

- Alginate is dissolved in distilled water under stirring.
- Propargylamine is added to the alginate solution using an appropriate pipette.
- HOBt is dissolved in a solution composed by water and CH3CN at about 50°C because of its insolubility at room temperature and is added dropwise to the mixture.
- EDC*HCl powder is added.
- Stirring for 24 h at room temperature.

The purification steps are:

- Dialysis, with a membrane cut-off of 3.5 kDa, and a dialysis bath made by 2 l of deionized water to which are added 11.2 g of Sodium Chloride and 4 drops of HCl (37%). The dialysis has to be maintained for at least 4 days, changing the water daily, in order to ensure a good product purity.
- Once dialyzed, the product is lyophilized.

The product is then ready to undergo the click reaction with the modified Rhodamine azide.

5.4.2.4 Click reaction

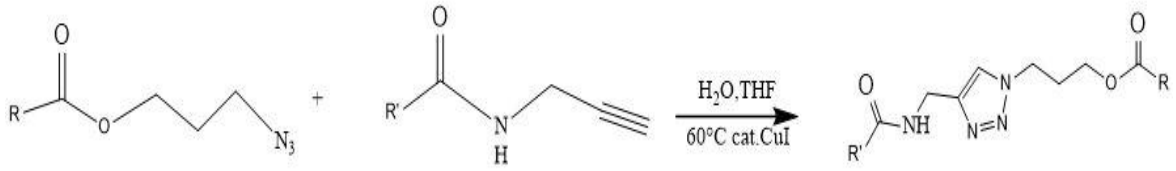

Figure 5.38 - CuAAC click reaction, functionalization of the polymer chain

The final click reaction is a Cu-Catalyzed Azide-Alkyne Cycloaddition (CuAAC) in which thiazide (-N_3) group of the Rhodamine B azide reacts with the alkyne group of the propargyl alginate, giving the triazole configuration of the final functionalized Sodium Alginate, as shown in figure 5.38.

The CuAAC reactions are characterized by the presence of [92]:

- The catalytic copper ions, coming from a Cu source (typically CuI, CuSO4 or CuBr). In literature there are also reported cases in which there's the metallic catalytic Cu.
- The reducing agent, which can typically be Sodium ascorbate, PPh3 or TCEP which acts as buffer, avoiding the oxidation of the catalytic Cu from 1+ to 2+. Most frequently, these reactions are performed with CuI in THF, CH3CN, or DMSO or with CuSO4/ascorbate in water/alcohol mixtures.

In this work, the catalytic Cu^+ ion source is CuI, while the reducing agent was Sodium ascorbate and the solvent was a mixture of water and THF (Tetrahydrofuran).

The required chemical species, the related quantities and molecular ratios are reported in table 5.17:

Compound	Quantity	MW [g/mol]	n [mmol]	Ratio [-]
Propargyl alginate	125 mg	252	0.496032	1
Rhodamine azide	100 mg	527	0.189753	0.6
Water	15 +4 ml			
THF	4 ml			
CuI	Catalytic amount			
Na ascorbate	Catalytic quantity			

Table 5.17 - Compounds and quantities for reaction R4

The Rhodamine azide molar ratio was set to 0.6 in order to have a 10% excess respect to the 50% of functionalized carboxyl groups present in the propargyl alginate, to be sure to attack all the propargyl groups present in the polymer chains.

The operative procedure is:

- Dissolving, in a reactor, the propargyl alginate in water (15 ml) under stirring.
- Into a 4 ml vial, dissolving the Rhodamine azide using water (4 ml).
- Adding the Rhodamine azide solution to the propargyl alginate one in the reactor.
- Recovery of the Rhodamine azide remaining traces present in the vial with THF and then add them to the reactor.
- Adding the Copper iodide and the Sodium ascorbate to the reaction environment.
- The reaction needs to proceed for 24 h at 60°C under stirring.

The purification procedure is the following:

- Dialysis, with a membrane cut-off of 3.5 kDa, and a dialysis bath made by 2 l of deionized water to which are added 11.2 g of Sodium Chloride and 4 drops of HCl (37%).

- After the dialysis, the product is lyophilized.

The product is the functionalized Sodium Alginate polymer with degree of functionalization of 50%.

5.5 Amidic functionalization

This Alginate functionalization type is based on the creation of an amidic bond to link to the Alginate backbone the relative Rhodamine B derivate (amino ethyl Rhodamine). It is constituted by the sum of two chemical steps in series:

- The first related to the Rhodamine B base chemical modification.
- The second related to the proper Sodium Alginate polymer functionalization with the aminoethyl Rhodamine produced in the first step.

The involved reactions are listed in figure 5.39:

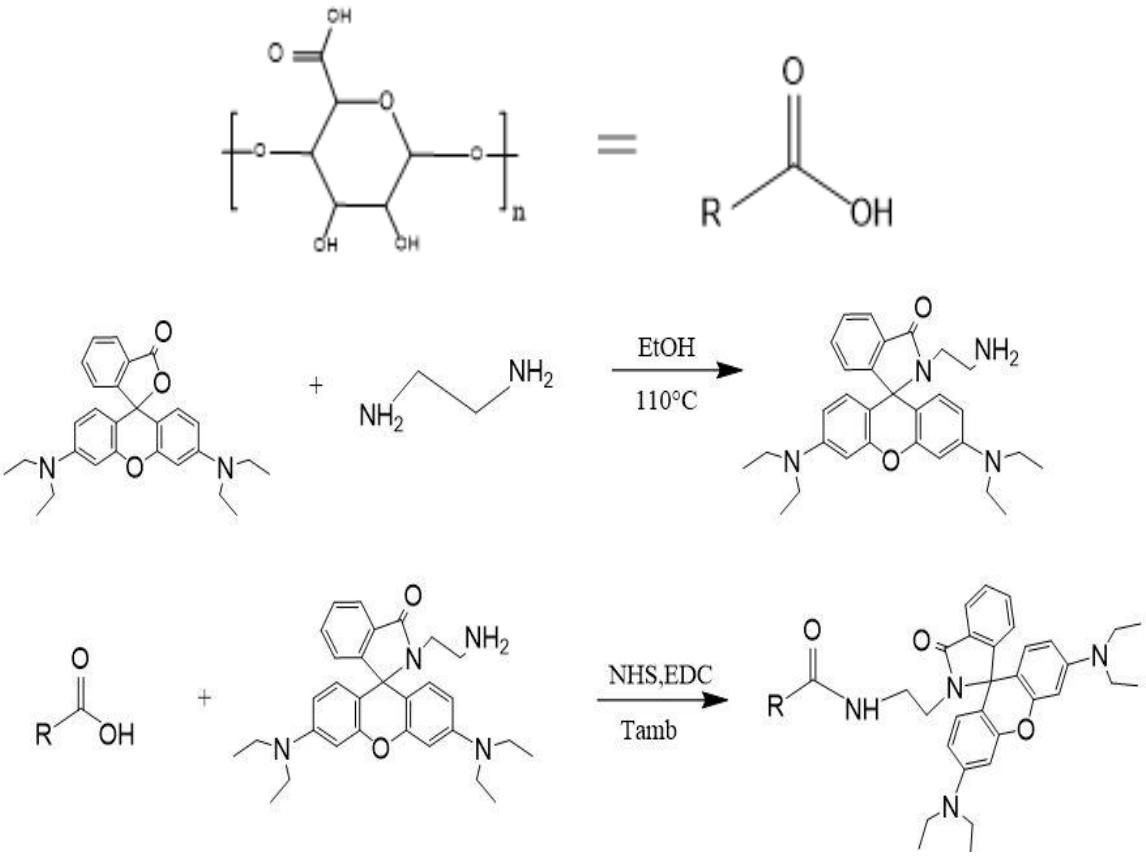

Figure 5.39 - List of the required reactions to obtain the amidic-functionalized Sodium Alginate

From the chemical structures of the species involved it's easy to notice that the starting Rhodamine B structure used for this functionalization is different with respect to the starting Rhodamine B used for the previous functionalization. While for the preparation of the Rhodamine B azide was adopted as reactant a Rhodamine B in its "open" configuration, in the preparation of the aminoethyl Rhodamine is adopted the Rhodamine B in its "closed" configuration (Rhodamine B base, the "lactone" one in figure 5.40).

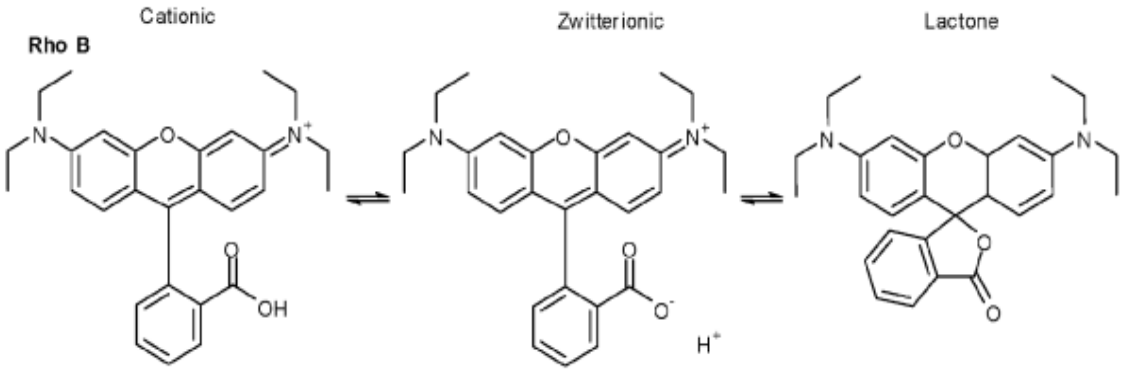

Figure 5.40 - Different configurations of Rhodamine B

The differences in Rhodamine B configurations are mainly due to pH and solvent polarity:

- In acidic solutions, the carboxyl group is protonated, and the Rhodamine B is in its cation form.
- In basic solutions, dissociation occurs, and the Rhodamine is converted in its zwitterionic form.
- In less polar organic solvents, the zwitterionic form of Rhodamine B is reversibly converted to the lactone form.

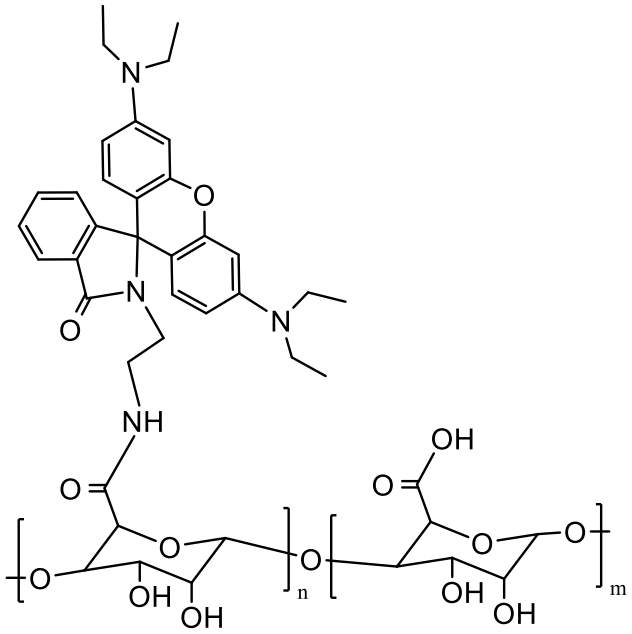

Figure 5.41 - Structure of the functionalized polymer, with the 50% of functionalized carboxyl group

Like for the ester bond functionalized polymer, also with the amidic bond functionalization has been chosen to functionalize the 50% of the polymer's carboxyl groups, for the same reasons said in the previous paragraphs, thus in the structure of the functionalized Alginate, as shown in figure 5.41, only 1 carboxyl group over 2 exhibits the polymer-drug linkage and the degree of functionalization is 50%.

5.5.1 Experimental section

All the chemicals were purchased by Sigma-Aldrich and used as they are without further purifications.

5.5.1.1 Synthesis of Aminoethyl Rhodamine

Since in this part of the work we were interested in obtaining an amidic linkage between Rhodamine B and the Sodium Alginate chain, the choice of Rhodamine B modification has been done in order to obtain a primary amidic group on the product of the modification reaction, in order to make possible the amidation reaction with Alginate's carboxyl groups.

In literature are reported a wide varieties of Rhodamine B modifications that exhibits the amidic group, the most widely used is the Rhodamine B hydrazide [94, 95], mainly for chemosensor fabrication purposes.

In this work the Rhodamine has been modified to obtain Aminoethyl Rhodamine, according to the reaction of figure 5.42, the attack of the Rhodamine B is basically analogous to the one reported in literature for the synthesis of the Rhodamine B azide [95, 96], with the same "entering group" (-NH_2) in the same molecule.

The required chemical species, the related quantities and molecular ratios are reported in table 5.18:

Compound	quantity	MW [g/mol]	n [mmol]
RhB_base	600 mg	442	1.357466063
EDA	3 ml (from an 85% solution)		
EtOH	15 ml		

Table 5.18 - Compounds and quantities for Rhodamine B base modification reaction

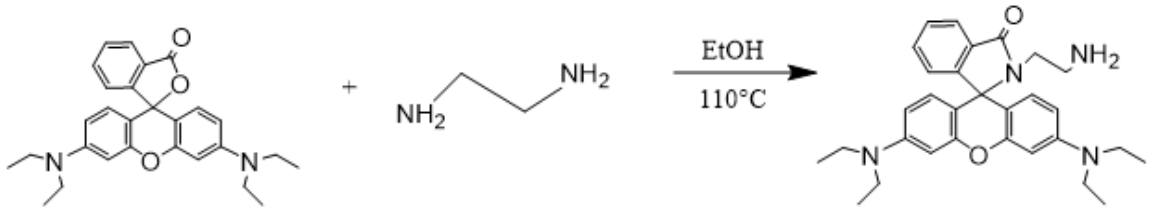

Figure 5.42 - Rhodamine B base modification reaction

The ethylenediamine (EDA) is in excess, to ensure a 100% conversion of the Rhodamine B base into product.

The solvent used is ethanol, in order to have the reactant Rhodamine B in its "closed" form.

The operating procedure is:

- In a reactor, with 15 ml of ethanol as solvent and under stirring, add 600 mg of Rhodamine B.
- Add to the mixture the 3 ml of ethylenediamine, taken with an appropriate pipette from an 85% solution.
- The temperature must be set to 110°C with an external diathermal oil bath and a thermostat coupled with a reflux condenser.
- The reaction must proceed for 24 h.
- After that, the reacted mixture needs to be left cooling until reaching room temperature.

Once the reacted solution is at room temperature, the product must be purified according to the following operations:

- On a rotavapor the mixture has to be dried. The rotavapor bath temperature is 45°C.
- Once dried, add 15 ml of HCl 1M to the solid residue remained in the reactor, and let it be dissolved in the HCl solution.
- Then add 23 ml of an NaOH solution (1M). A solid should start to precipitate.
- After the complete precipitation of the solid, filter to have the separation of the product (solid) from the mother liquor.
- Wash the filtered solid product with deionized water for three times in order

to obtain high purity aminoethyl Rhodamine solid product.

The starting Rhodamine B base solution has the typical Rhodamine B colour, while reaction proceeds after the EDA addition, the colour starts changing to light pink. The final product is a pink solid.

5.5.1.2 Functionalization of Alginate, amidation

The functionalization of Sodium Alginate polymer with the synthetized aminoethyl Rhodamine is an amidation reaction, that exploits the coupling agent EDC*HCl to form the amide link between the amine-containing molecule (aminoethyl Rhodamine B) and the carboxyl groups of the polymer itself.

The amidation reactions proceeds via the attack of the carboxyl groups present on the alginate backbone, creating the amide bond, through the insertion of the -NH_2 group of the aminoethyl Rhodamine B (that connects in form of -NH to the polymer's active site).

In literature [97 - 99] there's a discrete number of example of amidation reactions, made to functionalize Sodium Alginate with molecules of various complexity and dimensions through amidic bonds, such reactions typically work via carbodiimide-mediated activation chemistry or need a lot of reactive and operating steps leading to poor yields and difficult purification procedures.

In this work, to form the amide link between the aminoethyl Rhodamine and the alginate carboxyl groups, a one-reactive-step method has been used, with a simpler purification methodology, following the reaction shown in figure 5.43.

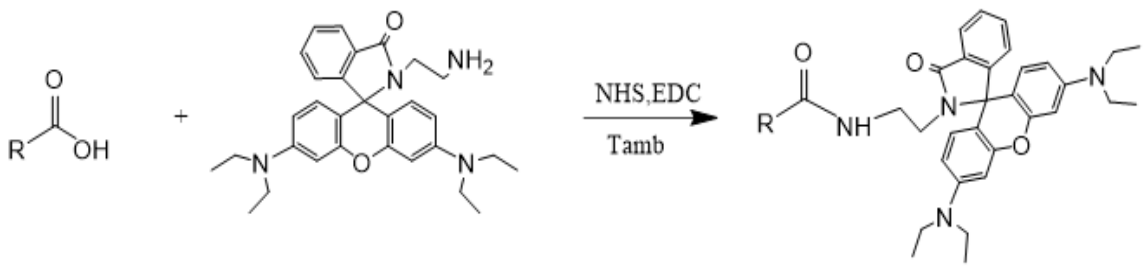

Table 5.43 - Amidation reaction to create the drug-polymer link

This reaction works according to the previously cited carbodiimide-based chemistry as reported in figure 5.44, in which there is the exploiting of the catalytic properties of carbodiimide.

The EDC attacks the carboxyl group of the Alginate forming the unstable intermediate o-acylurea that, if no nucleophiles are present, rearranges by a cyclic electronic displacement to N-acylurea which is more stable than the o-configuration. The N-acylurea is not very stable in aqueous solutions and quickly undergoes hydrolysis.

The reaction proceeds successfully only if the activated Sodium Alginate carboxyl is more stable than the o-acylurea derivates. NHS (N-Hydroxysuccinimide), in this reaction mechanism, works as an activating agent and the NHS-ester intermediate reacts with the aminoethyl Rhodamine molecule to form the amide bond and functionalize the alginate.

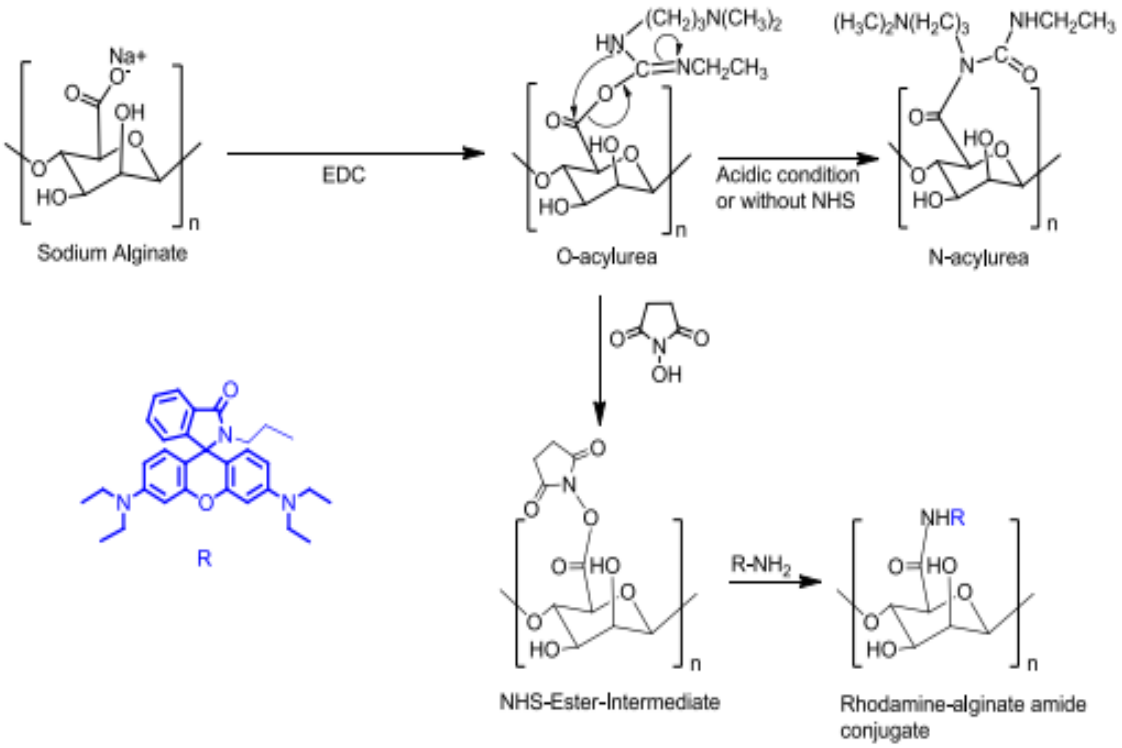

Figure 5.44 - Reaction mechanism of the amidation reaction with EDC and NHS to attack the Alginate's carboxyl groups

The required chemical species, the related quantities and molecular ratios are reported in table 5.19:

Compound	Quantity [mg]	MW [g/mol]	n [mmol]	Ratio
Alginate	200	216	0.925925926	1
Aminoethyl RhB	224	484	0.462962963	0.5
NHS	26.6412037	115.09	0.231481481	0.25
EDC*HCl	44.375	191.7	0.231481481	0.25
H2O	025 ml			

Table 5.19 - Compounds and quantities for the amidation reaction

As previously said, the required degree of functionalization of the final alginate polymer was 50% so the molar ratio between the starting Sodium Alginate and the aminoethyl Rhodamine was set to be 1:0.5 and deionized water was used as solvent.

The operating procedure for the reaction is:

- In a reactor under stirring, add the 200 mg of alginate to the 25 ml of water. Let it stir until complete dissolution.
- Add to the solution the aminoethyl Rhodamine
- Mix at room temperature for 10 min to allow the complete dissolution of the aminoethyl rhodamine, particular care needs to be taken to this step because the aminoethyl Rhodamine is difficultly dissolved by water and, if not appropriately solubilized, at the end of the procedure there will be a non-reacted amount of aminoethyl Rhodamine, leading to a wrong degree of functionalization of the polymer.
- Add the NHS
- Add EDC*HCl

The reaction has to proceed at room temperature for 12 h and, after that time, the purification sequence is:

- Dialysis with a membrane cut-off of 3.5kDa in a dialysis bath of 2 l to which has been added 11.2 g of NaCl, this dialysis step typically needs 2 days to obtain an appropriate product purity.
- Lyophilization, to end up with the dry functionalized polymer.

The product is a 50% functionalized amidic bond Alginate-Rhodamine, ready to undergo gelation.

5.5.2 Coating method – part 2

Hereafter we use the term "modified sodium alginate" referring to both the two different kind of functionalization indiscriminately. However, if we are referring to one of the two modifications in particular, we use the term "Alginate ester bond Rhodamine B" for one and "Alginate amide bond Rhodamine B" for the other.

The coating method of the scaffolds with the modified hydrogel is very similar to the standard one. The robots are coated by dipping them in the solution of modified sodium alginate and then in the solution of CaCl2, as previously described. The important difference we found is that, since approximately 50% of the total -COOH alginate groups are now occupied by the Rhodamine B, the gelation was slower and more difficult. Indeed, these groups are also responsible of the gelation because the calcium ions bind with the carboxylate groups of the polymer chains, as described before in the chapter Hydrogels. Al last, we resolved this problem by mixing the modified sodium alginate with pure sodium alginate in a ratio of 50/50. This way the total occupied carboxylate groups were 25%, and gelation proceed more smoothly. Another expedient we employed to produce a hydrogel as similar as possible to the one composed only of unmodified alginate was to increase the concentration of the CaCl2 solution from 1% w/w to 2% w/w.

5.5.2.1 Experimental section

- Prepare a solution of 1% (w/w) ultrapure sodium alginate in distilled water.
- Add modified sodium alginate 1% (w/w).
- Stir for at least 30 minutes.
- In another container prepare a solution of CaCl2 2% (w/w) in distilled water. The consecutive steps are the same described before for the unmodified Sodum Alginate:
- The device is immersed with the plastic structure in the alginate aqueous solution for 20 minutes (figure 5.22a). This step is performed inside an ultrasonic bath sonicator in order to favour the penetration of the alginate chains inside the scaffold matrix.
- Then the structure is immersed in the CaCl2 aqueous solution for 1 minute to obtain the first hydrogel layer (figure 5.22b).
- At this point steps a and b are repeated in order to obtain the second hydrogel layer (figure 5.22c and 5.22d).

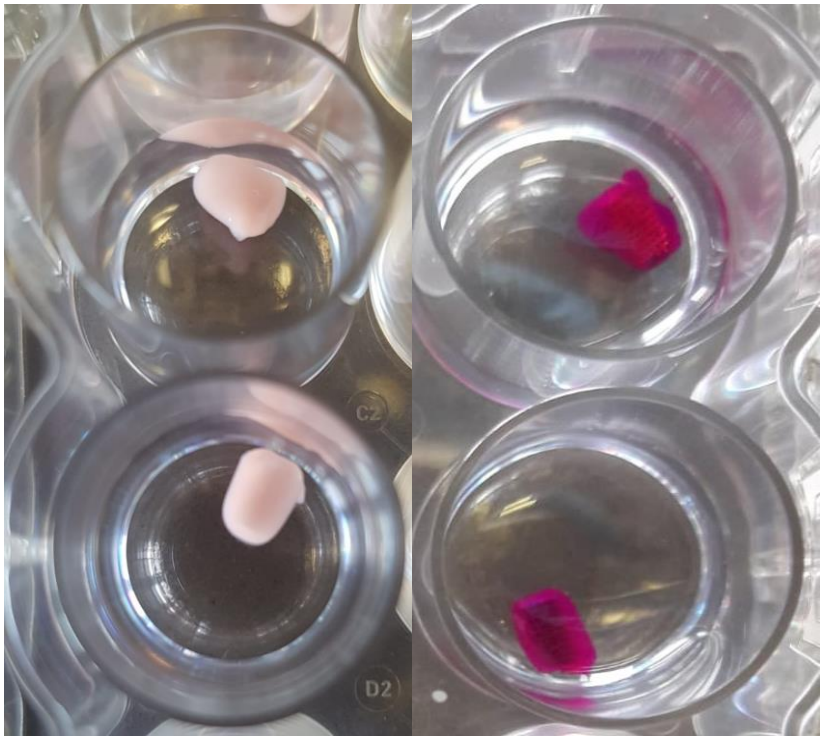

Figure 5.45 – On the left the amide bond Rhodamine B. On the right the ester bond Rhodamine B.

Figure 5.45 shows the final results. The change in colour with respect to the Rhodamine nonbonded alginate is evident to the eye (figure 5.23).

5.5.3 Miscellaneous – part 2

5.5.3.1 About operative conditions

As stated before, we had to change a little the operative conditions for the coating in order to obtain a gel as similar as possible to the one composed only of normal sodium alginate. In this case we performed several gelation tests and we gave a score to every gel obtained. The score goes from 1 to 5, where 1 means that the gel coating is far from uniform and 5 is the gel exactly like the one obtained before for the normal sodium alginate coating.

Test	**Alginate Bath Composition (w/w)**	**CaCl2 in solution (w/w)**	**Score**
Normal Sodium Alginate	2%	1%	5
Modified Sodium Alginate	2%	1%	2
Modified Sodium Alginate + Normal Sodium Alginate	1% normal + 1% modified	1%	3
Modified Sodium Alginate + Normal Sodium Alginate	1% normal + 1% modified	2%	5

Table 5.20 - Variation of operative conditions tested for the coating of the scaffolds.

At last we used the operative conditions written in the last line of the table for the coating used for the drug release tests.

5.5.3.2 About Rhodamine B concentration

The quantity of Rhodamine B per gram of total gel mass is an important parameter, used to draw the release plots. In this case the calculation is a bit tricky. We assumed that the ratio normal sodium alginate / modified sodium alginate was in the final gel different from the ratio of the solution, which was 50/50. This is due to the fact that in theory the normal alginate has twice the -COOH groups free, so twice the groups available for the gelation.

Species	Normal Sodium Alginate	Modified Sodium Alginate	Rhodamine B	Total
Ratio	2	1	0	3
Molecular weight	216	455.51	479.02	
Mass	432	455.51	0	887.51
Mass %	48.68	51.32	0	100

Table 5.21 - Quantity of the two alginates on the scaffold

- The molecular weight is intended of the monomers in the alginate chains
- The molecular weight of the monomer of the modified alginate written in the table is the average molecular weight of its monomers, knowing that half of its monomers will weight as the normal alginate monomers one (216), and the other half will weight as a monomer modified with the Rhodamine B attached.

  So now we can calculate the quantity in mass of Rhodamine B on the scaffold.

Species	Total Sodium Alginate	Normal Sodium Alginate	Modified Sodium Alginate	Water	Total
Quantity	2 %			100 ml	
Quantity (g)		0.97	1.03	100	102
Quantity (%)		0.95	1.01	98.04	1000
Number of moles		0.0045	0.0023		

Table 7.22 - Moles of Modified monomers on the scaffolds

Half of the moles of modified sodium alginate have actually a Rhodamine molecule attached, so 0.00115 moles of Rhodamine B every 100 grams of gel. This brings the Rhodamine B count at 0.54 grams every 100 grams of gel. More or less 5 times the Rhodamine B carried unbonded by the normal alginate hydrogel.

5.6 Drug delivery – part 2

Drug release experiments were done in order to describe the kinetic of release of the mimic drug Rhodamine B, which was in this case bonded to the alginate chains. The bond was hopefully designed to break in the spot for which exactly the Rhodamine B molecule is released.

- For each drug release test at least 3 different metallic scaffolds were coated in the exact same conditions, this is due to ensure statistic relevance of the results.
- The samples were prepared in the way described before. The scaffolds were weighted before and after the application of the gel, in order to know exactly the mass of hydrogel present on each scaffold. This data is essential to know

the initial quantity of drug loaded and as a consequence it is essential to draw the release curve.

- Each different scaffold is put in a different well and exactly 1 ml of distilled water is added. The wells were then put in a heater at exactly 37 °C, which is the temperature of the human body. So, the release was performed in these conditions.
- At different time points, 0.5 ml of solution is taken from each well and put in different vials. The vials are conserved in the fridge at around 4 °C.
- Consecutively, 0.5 ml of distilled water is added to each well in order to restore the initial 1 ml of solution.
- These withdrawals are done at 30 minutes, 1 hour, 2 hours, 3 hours and so on, until complete release.
- After the test is ended, the withdrawals have to be put in multiwell plates in order to be read by the UV spectrophotometer.
- In order to in interpret the data acquired the calibration curve have to be built. The construction of the calibration curve is reported in the next chapter.
- For the two modified alginate release tests, the release was performed both in distilled water and in water at pH of 3, lowered with some drop of HCl.

6 Results and discussions

The results of the product characterizations, the drug release tests and the magnetic tests, performed on the hydrogel-coated scaffolds are collected and commented in this chapter. In particular, it is underlined the difference in behaviour between alginate hydrogels with the mimic drug bounded and non-bounded to the polymer chains. All the drug release analysis were repeated several times in the same conditions, in order to increase the reliability of the results obtained.

6.1 Infrared spectroscopy of the products

The Fourier Transform – InfraRed (FT-IR) analysis of the products were performed in order to detect the success of the Alginate's functionalizations carried out with the reactions described in the previous chapters.

In particular, being interested in analysing the two different functionalizations, we have performed an FT-IR spectra comparison both between the starting Sodium Alginate polymer, purchased by Sigma Aldrich, and the two undergone to functionalization reactions and between the Rhodamine B and its modifications used for the functionalization of the polymer.

6.1.1 Ester bond functionalization

The FTIR spectra of the staring alginate, in figure 6.1 A, shows the presence of the two peaks at 1420 and 1620 cm^{-1} which are representative of the symmetric and asymmetric stretching of the carboxyl (-COOH) group present in the polymer chain while the peak underlined at 2920 cm^{-1} indicates the aliphatic C-H stretching and the one underlined at 3430 cm^{-1} represents the hydroxyl groups stretching.

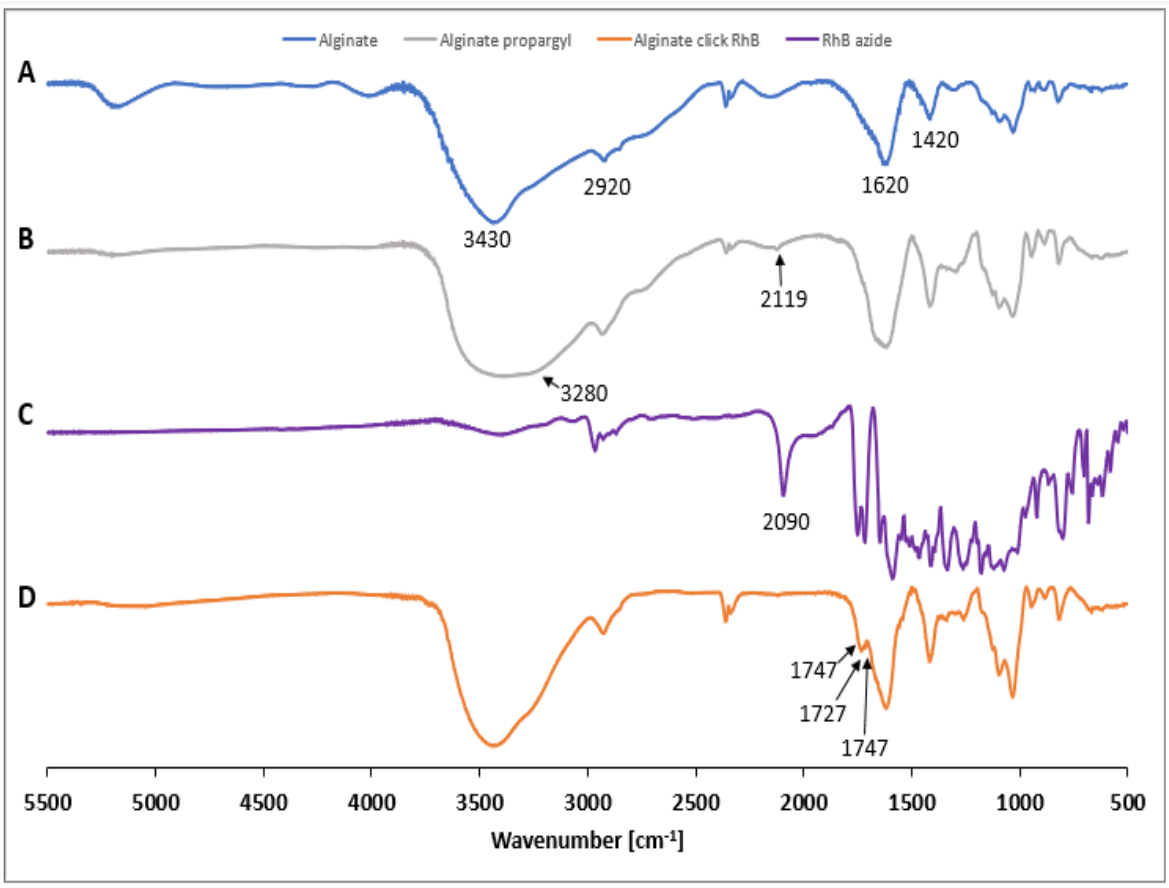

Figure 6.25 - FT-IR spectra comparison of the products involved in the ester bond functionalization, with the important peaks underlined

Regarding the propargyl Alginate (figure 5.37) in figure 6.1 B it is possible to notice, that both the 1420 and 1620 cm^{-1} are still present, this is related to the fact that in the ester-bond functionalization of the polymer and, precisely, in the reaction between the starting alginate and the propargylamine, only involved 50% of the monomers and thus, in the propargyl alginate polymer there are still free carboxyl groups.

The difference between 6.1 A and 6.1 B spectra underlined at 2119 cm^{-1}, is due to the alkyne C≡C group of the propargyl alginate, so the reaction between alginate and propargylamine was successful and there is the presence of the propargylic group in the product.

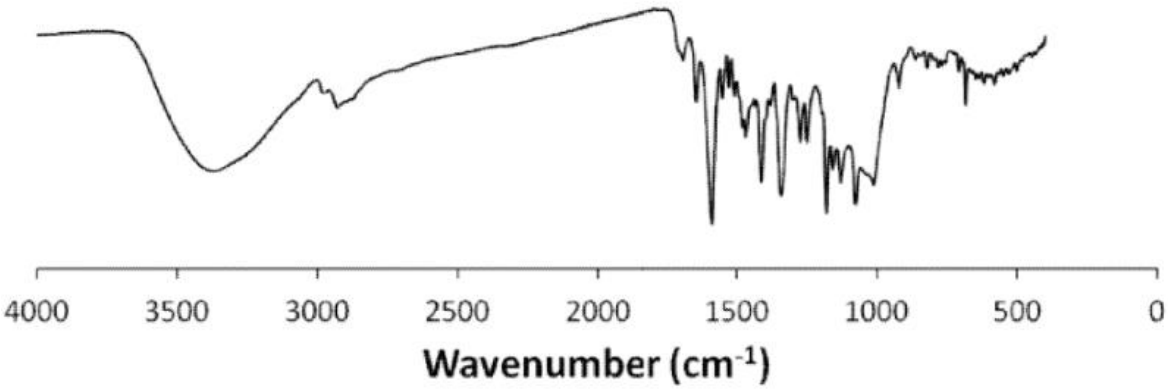

Figure 6.2 - FT-IR spectra of the staring Rhodamine B

The amidation reaction for the propargyl alginate synthesis has altered the shape related to the stretching hydroxyl vibrations in the band 3600-3300 cm^{-1}. The accentuation of the spectra going from the hydroxyl-related band to the lower wavenumbers, and particularly near the 3280 cm^{-1} (as pointed out in figure 6.1 B) is related to the stretching of the N-H bond present in the functionalized polymer, so that is another proof that the starting alginate has been attacked by the propargylamine with the amide bond.

Regarding the Rhodamine B azide (figure 5.35), it is possible to notice from the related spectra, named 6.1 C, the peak at 2090 cm^{-1} that indicates the azide ($-N_3$) group present in the molecule. This is proof that the starting Rhodamine B has been successfully modified to Rhodamine azide because, as reported in literature [100], the FT-IR spectra of Rhodamine B doesn't exhibit any characteristic peak in that region, as shown in figure 6.2, due to the fact that in the Rhodamine B molecule there aren't any azide groups.

Another proof that the synthetized molecular spacer has been successfully attached to the Rhodamine molecule is given by the presence of the characteristic

ester peaks in the region of 1750-1730 cm^{-1} as it is possible to see by making a comparison in that region between figure 6.1 C and figure 6.2.

The 2090 cm^{-1} peak disappears in the spectra of the final functionalized alginate (6.1 D) because in the click reaction the azide group present in the Rhodamine B azide has been successfully reacted according to the CuAAC click reaction forming the triazole link.

In the spectra of the final ester-bond functionalized alginate (figure 5.38) is possible to see that the 2119 cm^{-1} peak has disappeared, that's another proof that the click reaction was successfully carried out leading to a quantitative consumption of the alkyne group via click chemistry.

The 1420 and 1620 cm^{-1} characteristic peaks are present in all the spectra related to alginates, because in alginate and its modifications there are always free carboxyl groups. However, it is possible to notice that only in the ester-bond functionalized polymer spectra are present the characteristic peaks related to the ester link, which comes from the Rhodamine B azide, in the band around 1730-1750 cm^{-1}, pointed out in 6.1 D. These are the same exhibited in the Rhodamine B azide spectrum, with the only difference that if in the Rhodamine azide the ester link is present in equimolar quantity with respect to the analysed molecule, in the ester-bond functionalized alginate those links are present in only a 50% of monomers thus the peaks result attenuated.

6.1.2 Amide bond functionalization

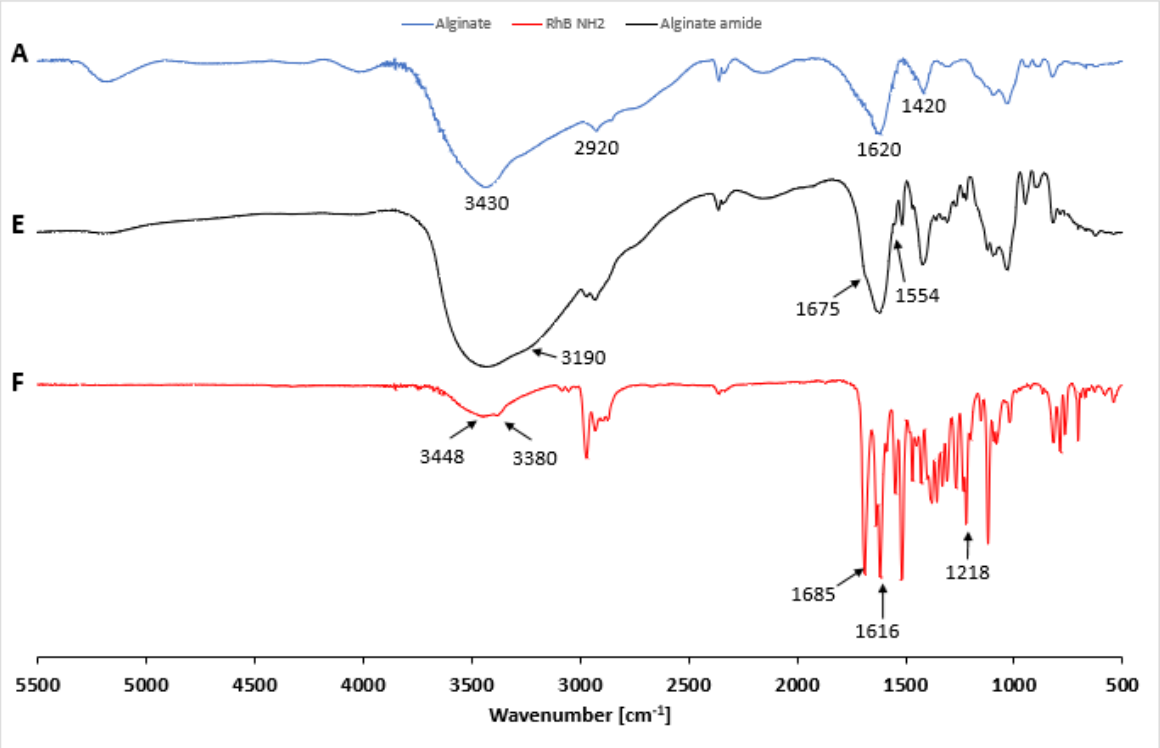

Figure 6.3 - FT-IR spectra of the species involved in the amide-bond functionalization, with the important peaks underlined

The same starting alginate was analysed, and the underlined FT-IR peaks are the same as previously discussed.

In the amide-bond functionalization the polymer was successfully functionalized with the Rhodamine B derivate, Aminoethyl Rhodamine, through an amidic bond.

By comparing the FT-IR spectra of the starting Rhodamine B (figure 6.2) and the Aminoethyl Rhodamine (figure 5.42) spectra in figure 6.3 F, it is possible to see that the modification of the starting Rhodamine has been successfully fulfilled, as confirmed by:

- The new peaks exhibited in the 1610-1690 cm^{-1} (figure 6.3 F) which are attributed to the amide bond, the characteristic peaks of the N-H bond of secondary amines (R_1-NH-R_2).
- The peaks at 3448 and 3380 cm^{-1} that are characteristic of the N-H stretching.
- The peak present at 1218 cm^{-1} that is representative of the C-N stretching

In the Amide-bond functionalized alginate (figure 5.43) spectra in figure 6.3 E, it is possible to see that while the 3430 cm^{-1} peak of the hydroxyl group stretching is maintained, there is the appearance of the characteristic amidic bond peak near 3190 cm^{-1} given by the N-H bond stretching.

In the amide-bond functionalized polymer's spectra are underlined the characteristic peaks shown around 1675 and 1554 cm^{-1} that are the same shown in the aminoethyl Rhodamine and are due to the amide bond stretching vibration of C=O peak. In spectra 6.3 E they appear shifted in wavenumber, this can be due to the different environment in which the bond stays, more specifically, in one case there is only the part related to the aminoethyl Rhodamine while in the other there is the influence of the polymer.

It is possible to notice from 6.3 E that also the carboxyl group characteristic peaks are still present in the final functionalized polymer's spectra.

From the discussion above it is proved that both the Rhodamine B modification to aminoethyl Rhodamine and the alginate functionalization with aminoethyl Rhodamine have been successfully carried out while preserving the carboxyl group of the polymer for the further gelation thus having a 50% of functionalization.

6.2 Drug release

6.2.1 Calibration curves

Calibration curves were built in order to determine the concentration on the mimic drug in a certain solution. The measures were done with the UV spectrophotometer starting from a solution of known concentration and then diluting this solution with distilled water until reaching very low concentrations. The curves obtained are reported in figure 6.4 to 6.6.

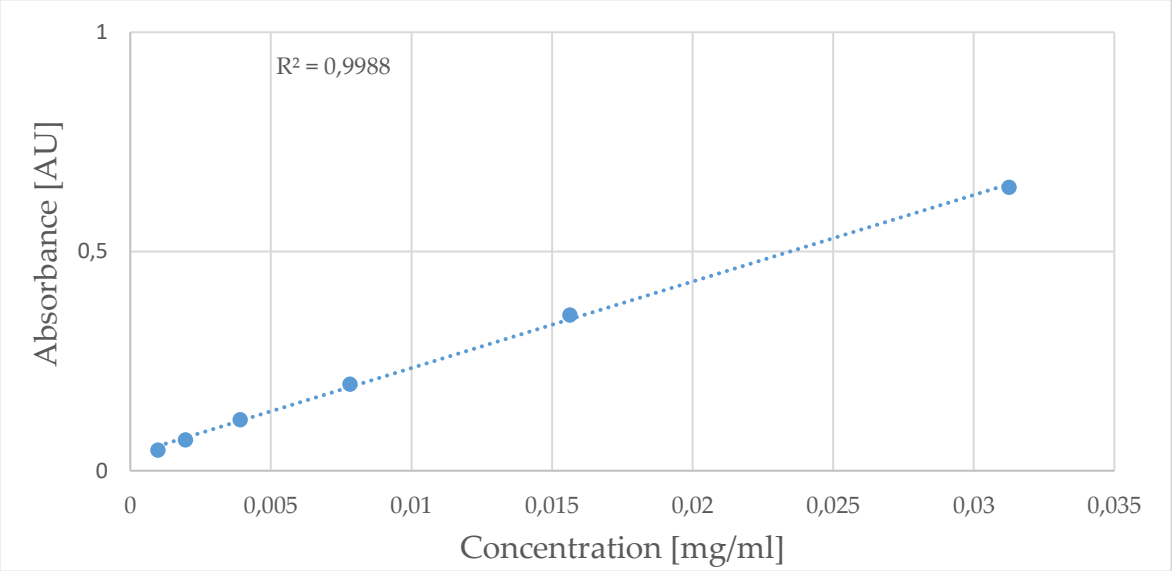

Figure 6.4 - Calibration curve of Rhodamine B

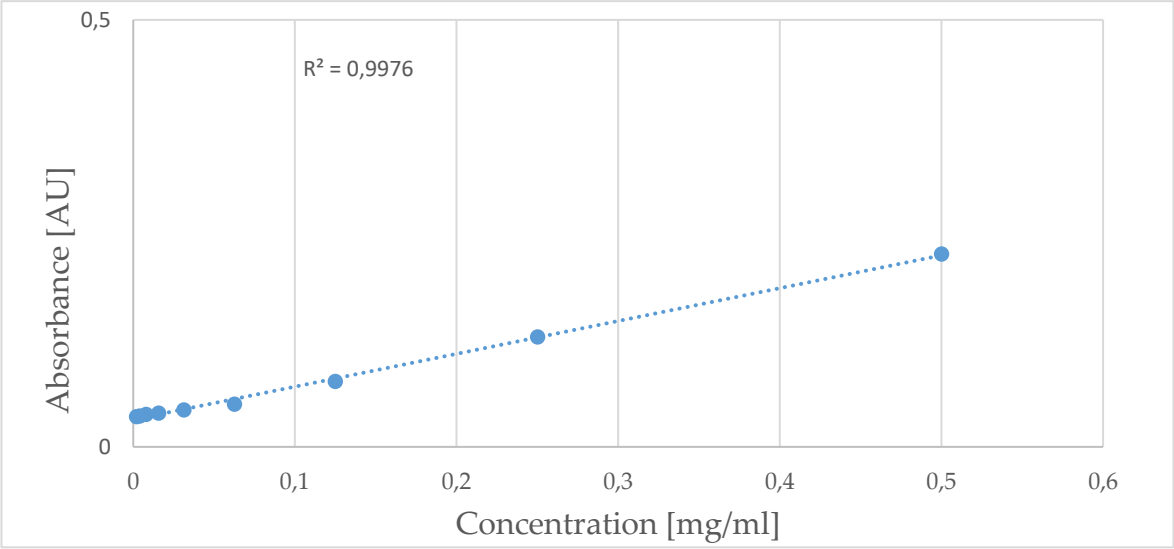

Figure 6.5 - Calibration curve of Aminoethyl Rhodamine B

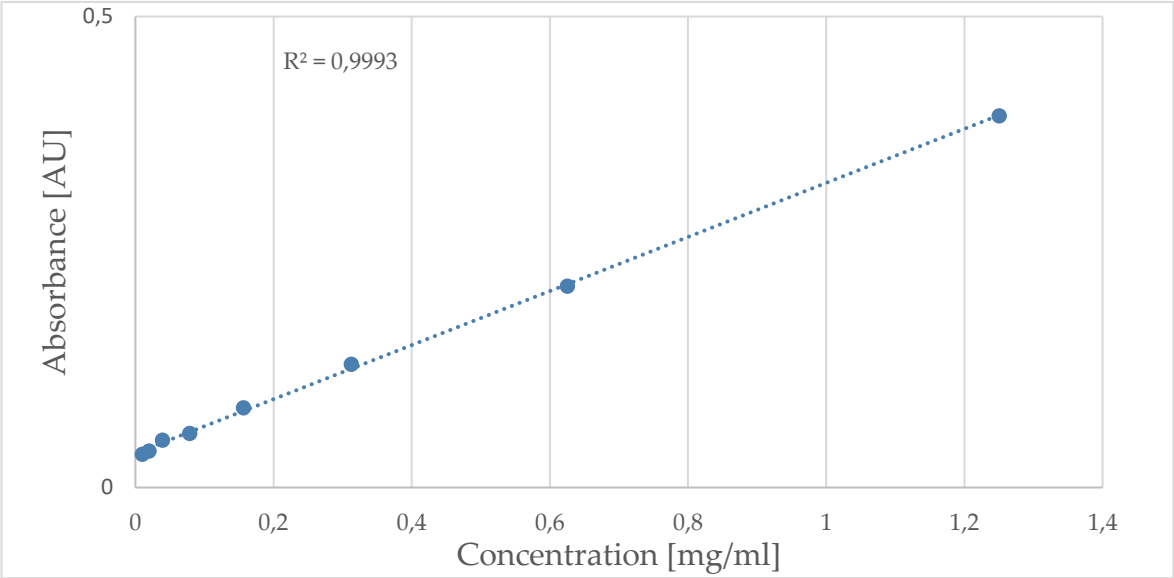

Figure 6.6 - Calibration curve of Dextran 70K

6.2.2 Drug release of unbonded Rhodamine B

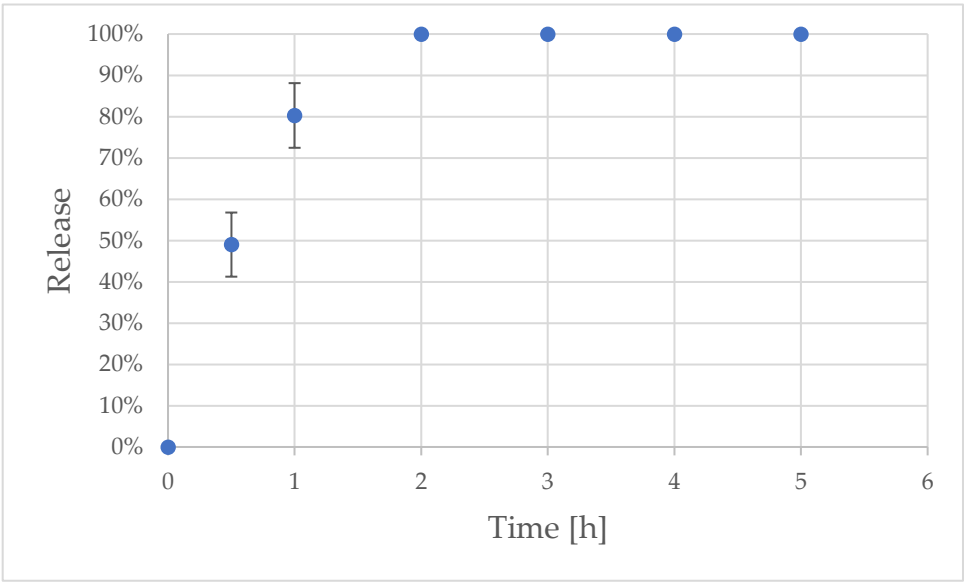

Figure 6.7 - Unbonded Rhodamine B release from the scaffolds

Figure 6.7 shows what we obtained for the drug release of unbonded Rhodamine B from the scaffolds. As shown, the alginate matrix does not seem to slow significantly the release of the drug, which goes to completion in a couple of hours. This might be because the alginate mesh size is, in this case, way bigger than the volume of the Rhodamine B molecule, and therefore it does not particularly hinder its release.

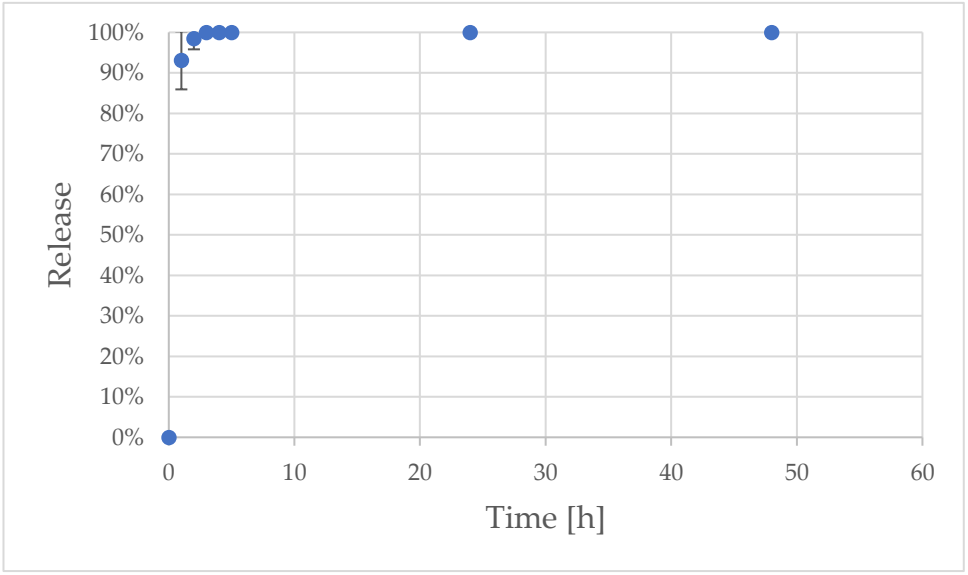

Figure 6.8 - Unbonded Dextran 70K release from the scaffolds

6.2.3 Drug release of unbonded Dextran 70000

In this second case (figure 6.8) we investigated the unbonded Dextran 70K release from the gel matrix. Being the molecular weight of this molecule like 100 times the one of molecule Rhodamine B, we expected the release to be delayed significantly. Truth be told, it does not seem to show a significant delay, with release going to completion in about 3 hours average. Figure 6.9 is a comparison between these two releases. The release path is almost superimposable.

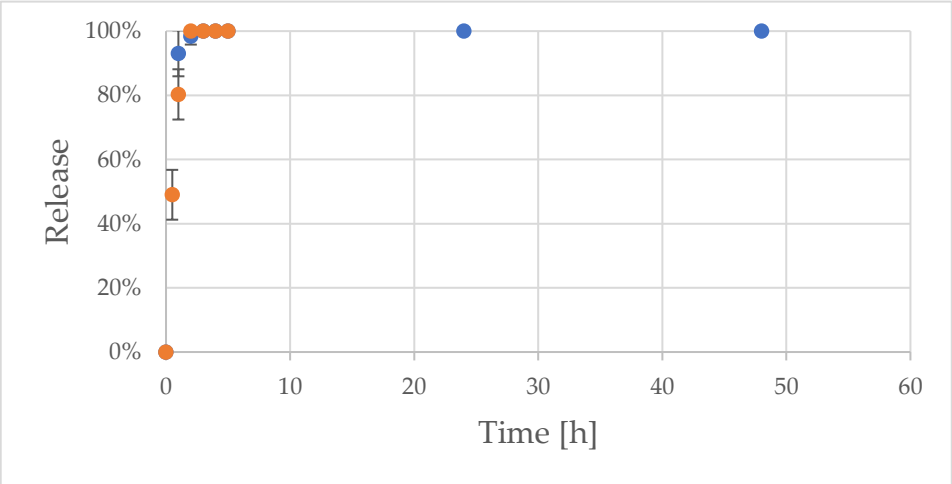

Figure 6.9 - Unbonded Rhodamine B release (orange) versus Unbonded Dextran 70K release (blue)

6.2.4 Drug release of amide bond Rhodamine B

6.2.4.1 In neutral environment

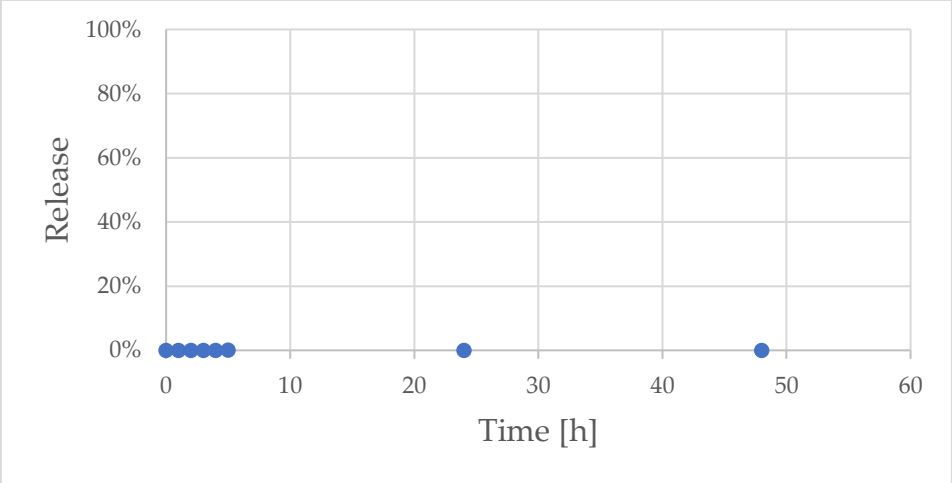

Figure 6.10 - Amide bond Rhodamine B release from the scaffolds at pH 7

In this case (figure 6.10) we were not able to detect any release from the scaffolds at pH 7. The water remained completely transparent also after several hours and no release was detected by the UV-spectroscopy.

6.2.4.2 In acid environment

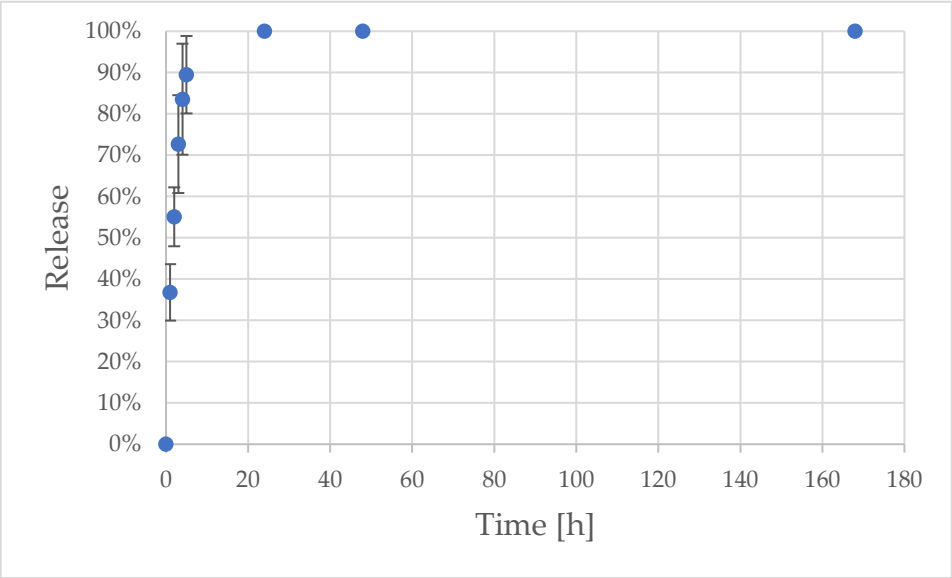

Figure 6.11 - Amide bond Rhodamine B release from the scaffolds at pH 3

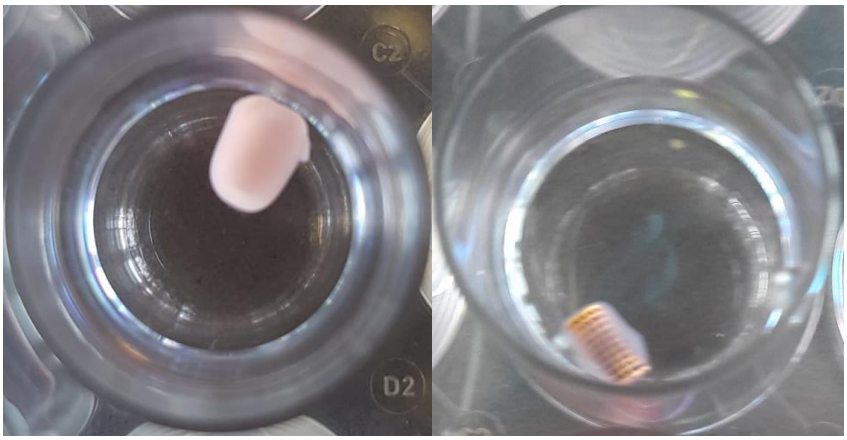

Figure 6.12 - Comparison between Amide bond Rhodamine B Hydrogel before the release (left) and after 24 h (right) at pH 3

The release at pH 3 of the amide bond Rhodamine B (figure 6.11) seems to be really different from the same release at pH 7. Just by visually looking at the release environment, the water solution was tinted red after some hours. The UV machine detected a complete release after 24 hours average. This result was coherent with what we could see with our own eyes: the gel was initially pink, like the colour of the modified Rhodamine described and shown in materials and methods for this particular alginate functionalization, after 24 hours the gel turned almost completely transparent. As shown in figure 6.12, the gel is so transparent the scaffold below is completely visible. Figure 6.13 shows the difference in release obtained with the UV spectroscopy for the amide bond alginate at pH 7 and pH 3.

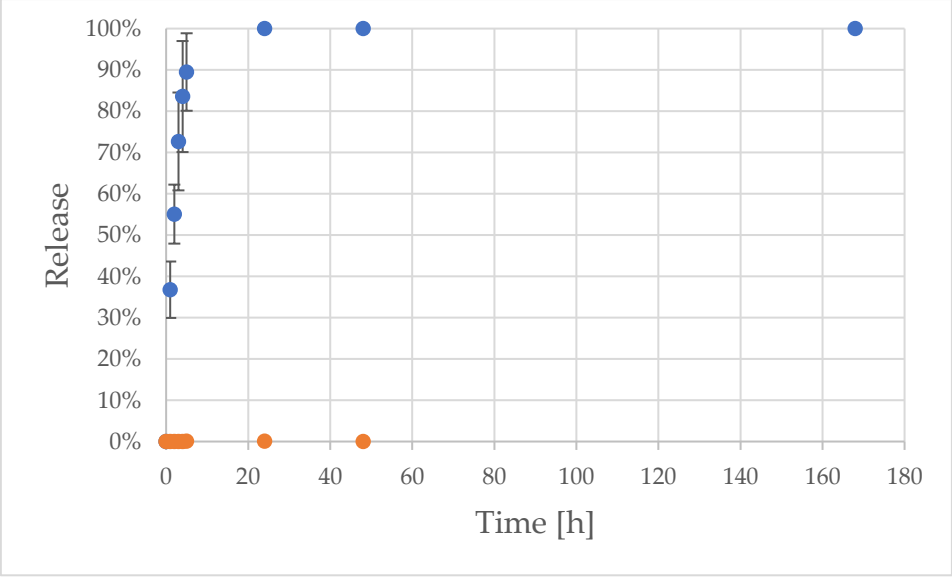

Figure 6.13 - Amide bond Rhodamine B release at pH 7 (orange) versus Amide bond Rhodamine B release at pH 3 (blue)

6.2.5 Drug release of ester bond Rhodamine B

6.2.5.1 In neutral environment

In this case (figure 6.14) we find an average release of about 3% after 2 to 3 days. The water was transparent to the eye. About that 3% release there are several explanations we can think of:

- It might just be Rhodamine B remained unreacted inside the alginate. It should diffuse out of the scaffold like in the previously mentioned case of the unbonded Rhodamine B release.
- It might be due to an experimental error, an instrumental error, or an error in the calibration curve.
- It might be some ester bond Rhodamine B that slowly severs its bonds with the alginate and then diffuses out of the scaffold.

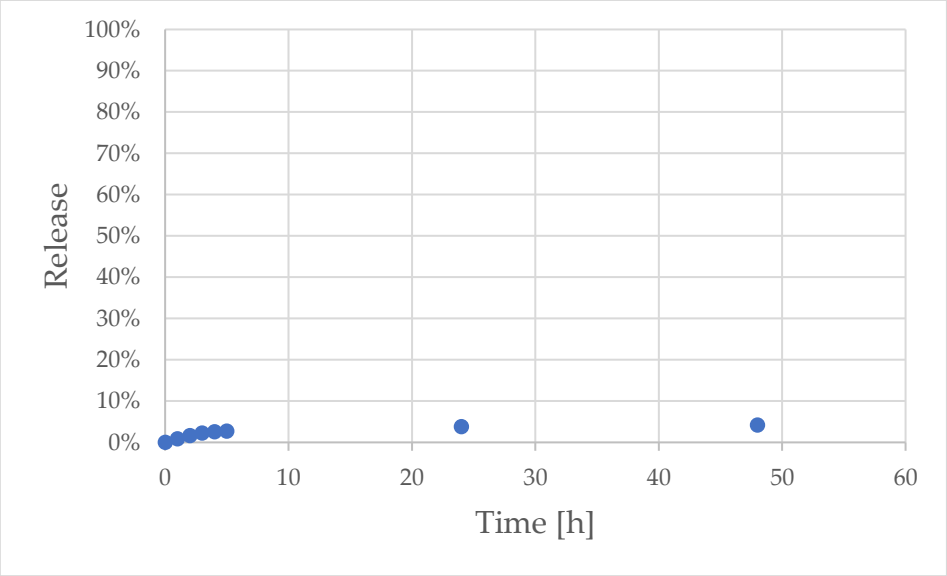

Figure 6.14 - Ester bond Rhodamine B release from the scaffolds at pH 7

6.2.5.2 In acid environment

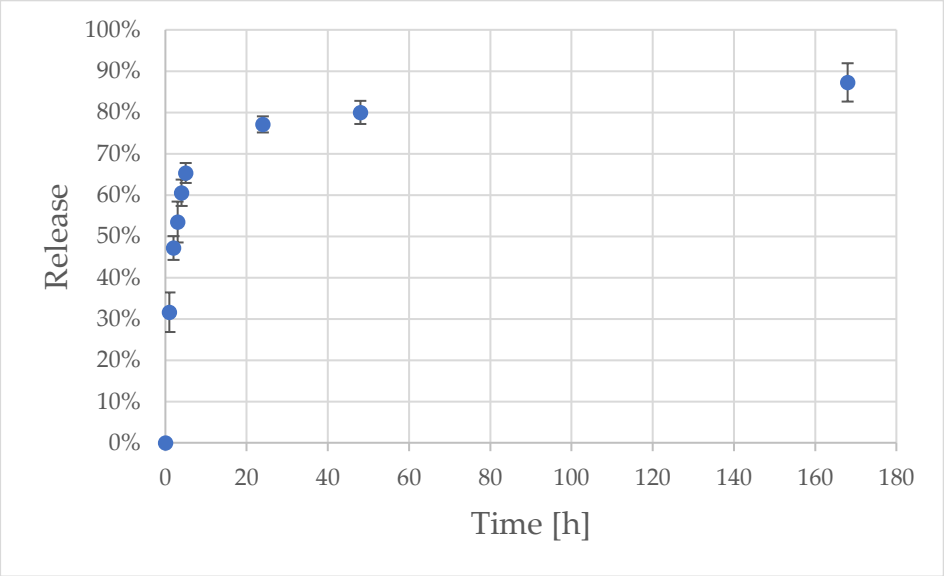

Figure 6.15 - Ester bond Rhodamine B release from the scaffolds at pH 3

Like for the amide bond Rhodamine B, the release seems to be pH triggered. We could visually ascertain that in this case the water at pH 3 turned red after some hour during the release test. Figure 6.15 shows the release we obtained with the UV-spectroscopy machine. As shown in the plot, the release seems to not go to 100% but it tends to form a plateau around 80%. It seems that some Rhodamine B remains bonded to the alginate chain. The reason is not clear, but this fact is also confirmed by our visual observation. In fact, as opposite to the amide bond Rhodamine B, whose gel turned completely transparent, in this case the alginate remained the same colour as before the release, as shown in figure 6.16.

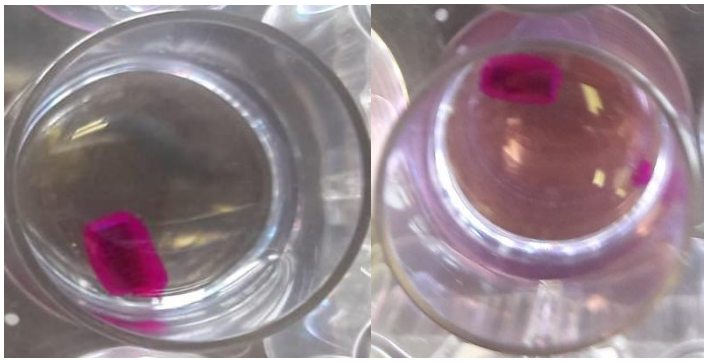

Figure 6.16 - Comparison between Ester bond Rhodamine B Hydrogel before the release (left) and after 1 week (right) at pH 3

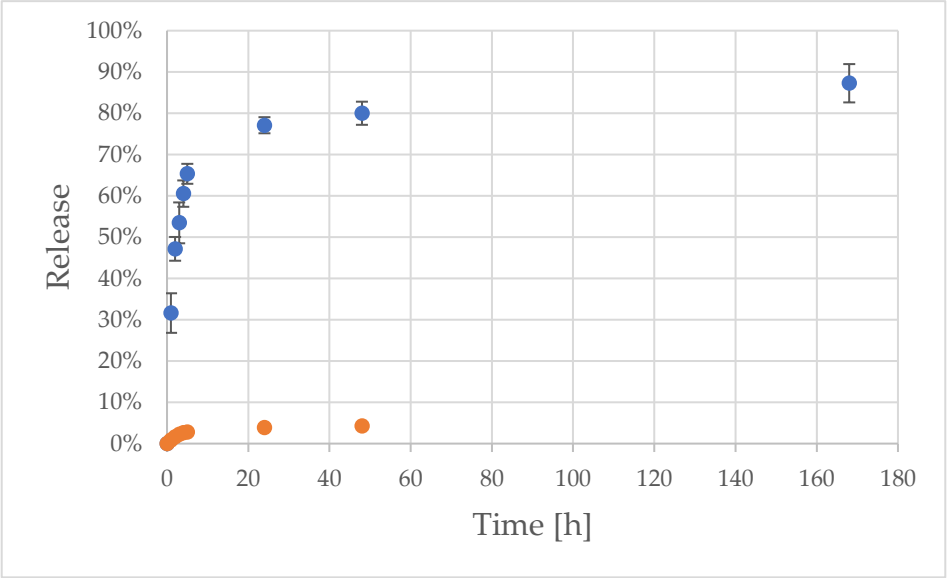

Figure 6.17 - Ester bond Rhodamine B release from the scaffolds at pH 7 (orange) versus Ester bond Rhodamine B release from the scaffolds at pH 3 (blue)

Figure 6.17 shows the difference in release obtained at the two different pH.

6.3 Magnetic tests

6.3.1 Movement of a hydrogel coated device

The magnetic tests performed on the hydrogel coated scaffolds were very similar to the ones reported for the uncoated scaffolds, described in the chapter "Microdevices fabrication" of Materials and Methods.

Basically, the MEMS were placed into appositely designed arenas to test both velocities and trajectories with OctaMag. Particular care was placed on the relationship speed-frequency and on the control of the trajectories followed by the MEMS also in this case. It was important to discover if the gel coating was causing some anomaly in the scaffold movement. The arenas were custom-made and are filled with distilled water. Different route shapes to be followed by the device have been tested.

The most important effect of hydrogel addition was discovered to be an

introduction of a non-linear behaviour at high actuation frequencies. This anomaly starts when rotation frequency exceeded 0.8 Hz, causing deviation from the behaviour described before for the non-coated scaffolds. Indeed, speed values were found to be lower than expected ones.

The two main reasons for this change might be:

- The change in weight of the device, which increased by 80% with the addition of the hydrogel layer.
- Hydrogel coated microrobots might mechanically interact with the substrate in a different way with respect to uncoated devices. In particular, friction coefficient might be significantly lower.

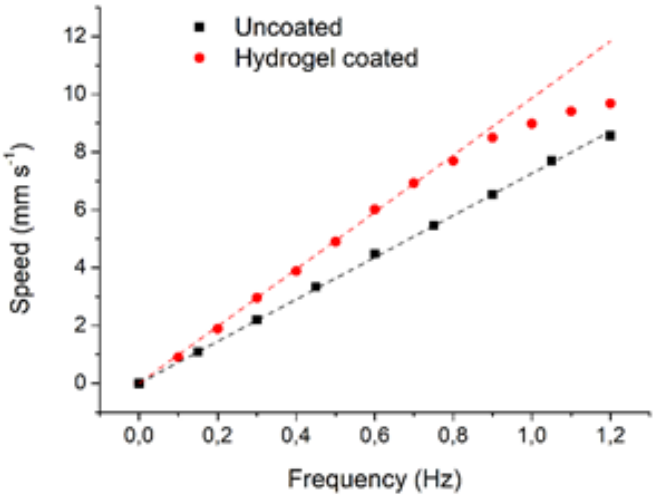

Figure 6.18 - Relation speed-frequency for coated and uncoated scaffold

The linear part of the red curve in Figure 6.18 was linearly fitted to evaluate the radius of the devices, by inversion of the following formula:

$$v = 2\pi r\omega$$

A radius of 1570 μm was calculated, with a 414 μm difference with respect to the uncoated sample. Such difference corresponds to the mean thickness of the hydrogel on the outer zone of the microrobot. Obviously, the distribution of the hydrogel is not perfectly uniform. For this reason, the value obtained must be considered and indirectly measured mediated value.

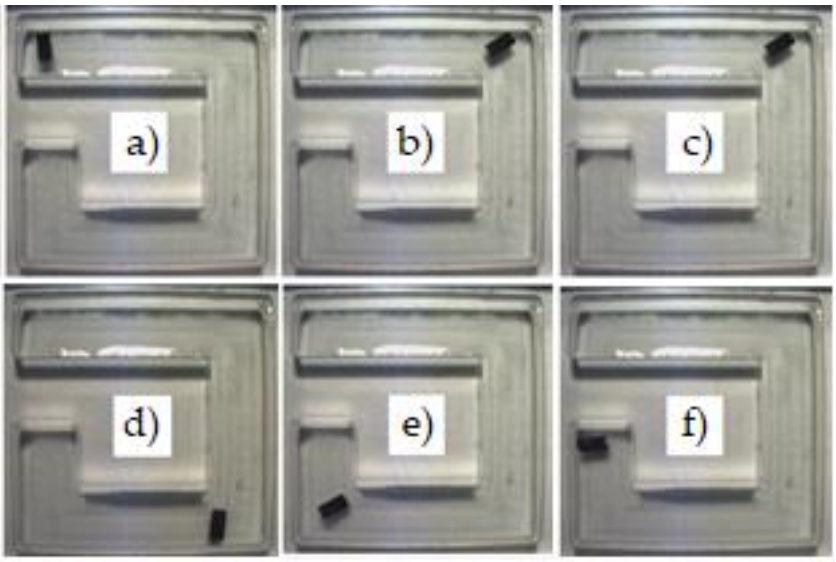

Figure 6.19 - Actuation of the gel coated scaffold in the arena

As discussed in detail previously, devices can be put in movement by varying the inclination of the rotation axis of the applied field B. By doing this, the devices can be efficiently guided towards the target inside complex shaped environments, while immersed in distilled water, as evidenced in figure 6.19.

6.3.2 Targeted drug delivery

To test the possibility of pH triggered drug delivery from hydrogel coated microrobots, we employed the same test arena depicted in figure 6.19, with the same actuation pattern. In this case, the end of the circuit represents the target organ for drug release. Consequently, it would be good if drug delivery would preferentially take place exclusively in correspondence of the target zone. This result is in theory possible by looking at the drug release obtained and described before. Indeed, as discussed before, the release of Rhodamine B from scaffolds coated with alginate modified by linking the mimic drug to the hydrogel chains is almost null at pH around 7, while it is important for low pH (around 3).

In the first tests performed, a sample was guided towards the target zone. This sample was the scaffold coated with the alginate hydrogel with the unbonded Rhodamine B immersed in distilled water. Figure 6.20 from a to f depict the result

obtained in a time order. As expected, the device immediately started releasing the mimic drug from the moment it came in contact with the water. During motion it left a clearly visible trace of Rhodamine B stained water. When it reached the target zone, it continued to release the mimic drug (several minutes passed from e to f).

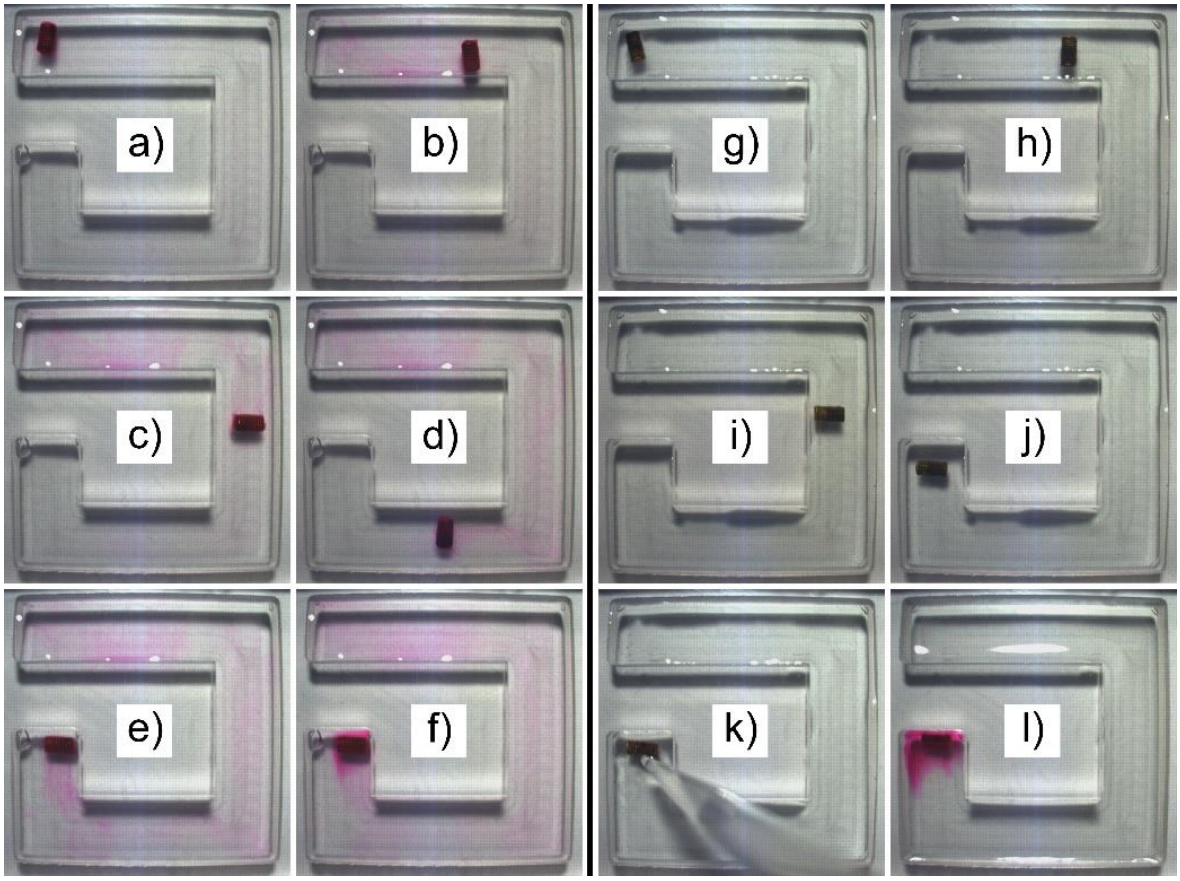

Figure 6.20 - from a) to f): Scaffold coated with the alginate hydrogel with the unbonded Rhodamine B immersed in distilled water. From g) to l) Scaffold coated with the alginate hydrogel with the bonded Rhodamine B immersed in distilled water.

From this we concluded that by using unbonded Rhodamine B a non-negligible amount of the chemical was released in zones of the arena far from the target zone. This implies a considerable waste of drug, which would be released in unwanted zones of the organism in the case of a real application.

In the second test, a different sample was employed. Scaffold coated with the alginate hydrogel with the bonded Rhodamine B immersed in distilled water. As clearly evidenced in figure 6.20 from g to j, no unwanted release was observed when the device was placed in the water nor when it was guided towards the target zone.

Upon reaching the end of the arena, pH was lowered in order to start the

Rhodamine B release. At least this was what was expected to happen based on the analysis of the release tests discussed before. To change the pH, 200 μl of a 1 M sulfuric acid solution were pipetted in correspondence of the device at the end of the arena (figure 6.20k). The pH variation induced by the presence of the acid immediately triggered Rhodamine B to do cleavage of the corresponding bond. As a consequence, the target zone was readily coloured by the released mimic drug. Photos in 6.20l is taken 15 minutes after the acid addition.

So, unlike the first experiment, the important result is that in the second case it was possible to:

- Avoid drug release in places where it was not wanted.
- Trigger drug release by changing the pH.

7 Conclusions

This thesis work intends to address two important aspects that have to be considered when searching for an efficient drug delivery system: the on-target drug delivery and the controlled release of a drug. By on-target delivery is intended the possibility to release the drug exactly where its action is needed and nowhere else. By controlled release is intended the slowdown of the release in order to keep an adequate and steady concentration of the drug, thing that gives many advantages, which have been discussed thoroughly before in this work. The investigation lead us through several pathways, so in this final chapter we present a summary of the considerations we were able to make.

The first point was to obtain 3D printed magnetic biocompatible microscaffolds. The technology had already been studied in detail by Bernasconi's group, so we took it and used it as a steppingstone for the start of our work. The scaffolds have been tested for biocompatibility and are also able to be magnetically actuated by a particular machine called OctoMag by exploiting a rotation of the magnetic field described in detail previously in this work.

We had now to define the method to load a drug onto these scaffolds, so that the property of the scaffolds of being magnetically actuable could be used to carry the drug to the place where it has to be released.

For this objective, we decided to use a common hydrogel, Sodium Alginate, because it showed a good adhesion to the metallic scaffold. There are basically two methods to load a drug in a hydrogel: steric loading and chemical loading.

By steric loading we mean to mix the drug directly in the liquid part of the hydrogel. In this case the drug is free to move in the aqueous solution, but somewhat hindered by the mesh size of the gel matrix. In this case the driving force for the release is the difference in concentration of the drug between inside and outside of the hydrogel. This release should in theory be delayed by the presence of

the gel matrix. To investigate this aspect, we made release tests with two drugs with very different size: Rhodamine B and Dextran 70kDa. We discovered that the release of both molecules in water seems to go to completion in about 2 to 3 hours average, so no significant delay was introduced by the second bigger molecule.

By chemical loading we mean to link the drug directly to the chains of the hydrogel with a cleavable bond. In this case we went through with two different set of reactions to obtain two different kind of bonds: ester bond and amide bond. In both cases the release at neutral pH was almost zero, while in acid pH we obtained complete release in about 24 hours. This means that the cleavable links obtained seems to be more labile at low pH. This result is confirmed by the theory since, as previously stated, both the amidic and the ester bond are subjected to hydrolysis in acid solutions. This means that in the event of an application in the human body we can obtain the release of the drug only in the stomach, where pH is about 3, no drug is wasted in other areas of the gastrointestinal tract (chapter 4 “Drug delivery”).

At last we tested the hydrogel coated microscaffolds with the OctoMag technology and found out that they were able to retain their magnetic properties, as long as the hydrogel coating was not too thick.

Combining these information, we were able to conclude that 3D printed magnetic and biocompatible microscaffolds show the potential to be applied in the drug delivery field. They have the important quality of being able to be moved inside the body by applying an external magnetic field, which is harmless for the human body, up to the precise location where there is the need of a treatment. Moreover, they can host and carry a drug in various ways. Among these ways, if they are covered with Sodium Alginate which has been modified by attaching a drug with a pH sensitive bond, they can release this drug in the stomach minimizing drug waste and side effects.

This thesis work is just the starting point for these types of application, since if we consider all the hydrogels present on the market, and all the different drug-hydrogel bonds we can obtain, the research possibilities are very large.

References

[1] John D. Robert and Marjorie C. Caserio *Basic principle of organic chemistry*. 1997

[2] Xin Wanga, Man Jiangb, Zuowan Zhoub, Jihua Goua, and David Hui. *3D printing of polymer matrix composites: A review and prospective.* Composites, 2016

[3] I Gibson, DW Rosen, and B Stucker. *Additive manufacturing technologies: rapid prototyping to direct digital manufacturing*. Springer, 2010

[4] R Bernasconi, F Cuneo, E Carrara, G Chatzipirpiridis, M Hoop, X Chen, B J Nelson, S Pane´, C Credi, M Levic, and L Magagnin. *Hard-magnetic cell microscaffolds from electroless coated 3D printed architectures.* Materials Horizons, 2018

[5] V. S. Bagotsky. *Fundamentals of electrochemistry, second edition*. John Wiley Sons, Inc, 2006

[6] B. Kavitha, P. Santhosh, M. Renukadevi, A. Kalpana, P. Shakkthivel, and T.Vasudevan *Role of organic additives on zinc plating.* Surface and Coating Technology, 2006

[7] A. Abdel Aal, A. Shaaban, and Z. Abdel Hamid *Nanocrystalline soft ferromagnetic Ni–Co–P thin film on Al alloy by low temperature electroless deposition.* Applied Surface Science, 2008

[8] Famin Qiu, Bradley J. Nelson *Magnetic Helical Micro- and Nanorobots: Toward Their Biomedical Applications.* Engineering, 2015

[9] Olgac Ergeneman, George Chatzipirpiridis, Juho Pokki, Marta Marìn-Suàrez, Georgios A. Sotiriou, Santiago Medina-Rodrìguez, Jorge F. Fernàndez Sànchez, Alberto Fernàndez-Gutìerrez, Salvador Pané and Bradley J. Nelson *In Vitro Oxygen Sensing Using Intraocular Microrobots.* IEEE Transactions on Biomedical Engineering, 2000

[10] Enas M. Ahmed *Hydrogel Preparation, characterization, and applications: A review*. Journal of Advanced Research, 2015

[11] Muhammad Faheem Akhtar, Muhammad Hanif, and Nazar Muhammad

Ranjha *Methods of synthesis of hydrogels … A review*. Saudi Pharmaceutical Journal, 2015

[12] Naziha Chirani, L'Hocine Yahia, Lukas Gritsch, Federico Leonardo Motta1, SoumiaChirani, and Silvia Fare *History and Applications of Hydrogels.* Journal of Biomedical Sciences, 2015

[13] Manjeet Deshmukh, Yashveer Singh, Simi Gunaseelan, Dayuan Gao, Stanley Stein, and Patrick J. Sinko *Biodegradable Poly(Ethylene Glycol) Hydrogels Based on a Self-Elimination Degradation Mechanism.* Biomaterials, 2010

[14] Nasim Annabi, Jason W. Nichol, Xia Zhong, Chengdong Ji, Sandeep Koshy, Ali Khademhosseini, and Fariba Dehghani *Controlling the Porosity and Microarchitecture of Hydrogels for Tissue Engineering.* Tissue Engineering. Part B, Reviews, 2010

[15] Leda Klouda, and Antonios G. Mikos *Thermoresponsive hydrogels in biomedical applications.* European Journal of Pharmaceutics and Biopharmaceutics, 2008

[16] Moreno-Garrido I. *Microalgae immobilization: current techniques and uses.* Bioresource Technology, 2008

[17] Maryam Irani, Hanafi Ismail, Zulkifli Ahmad, and Maohong Fan *Synthesis of linear low-density polyethylene-g-poly (acrylic acid)-co-starch/organo-montmorillonite hydrogel composite as an adsorbent for removal of Pb(II) from aqueous solutions.* Journal of Environmental Sciences, 2015

[18] Yuqiao Fang, Yi Zhang, and Zunan Qiu *Removal of oil from concentrated wastewater by attapulgite and coagulant.* Water Quality Research Journal of Canada, 1995

[19] Xin Bai, Mingzhu Gao, Sahla Syed, Jerry Zhuang, Xiaoyang Xu, and Xue-Qing Zhang *Bioactive hydrogels for bone regeneration.* Bioactive Materials, 2018

[20] Kuen Yong Lee, and David J. Mooney *Alginate: properties and biomedical applications.* Progress in Polymer Science, 2012

[21] G. Orive, S. Ponce, R. M. Hernández, A. R. Gascón, M. Igartua, and J. L. Pedraz *Biocompatibility of microcapsules for cell immobilization elaborated with different type of alginates.* Biomaterials, 2002

[22] Siddhesh N. Pawar *Chemical Modification of Alginate.* Seaweed Polysaccharides: isolation, Biological and Biomedical Applications, 2017

[23] Aymen Al-Shamkhani, and Ruth Duncan *Radioiodination of Alginate via Covalently-Bound Tyrosinamide Allows Monitoring of its Fate In Vivo*. Journal of Bioactive and Compatible Polymers, 1995

[24] Ji-Sheng Yang, Ying-Jian Xie, Wen He *Research progress on chemical modification of alginate: A review*. Carbohydrate Polymers, 2010

[25] Klein E. *The role of extended-release benzodiazepines in the treatment of anxiety: a risk–benefit evaluation with a focus on extended-release alprazolam.* Journal of Clinical Psychiatry, 2002

[26] Wagstaff AJ, and Goa KL *Once-weekly fluoxetine.* Drugs, 2001

[27] Michelson EL *Calcium antagonists in cardiology: update on sustained-release drug delivery systems.* Clinical Cardiology, 1991

[28] Nishan S. Gunasekara, and Stuart Noble *Isosorbide 5-Mononitrate A Review of a Sustained-Release Formulation (Imdur) in Stable Angina Pectoris.* Drugs, 1999

[29] Michel MC. *A benefit–risk assessment of extended-release oxybutynin.* Drug safety, 2002

[30] Zhoupeng Zhang, and Wei Tang *Drug metabolism in drug discovery and development.* Acta Pharmaceutica Sinica B, 2018

[31] Naiem T. Issa, Henri Wathieu, Abiola Ojo, Stephen W. Byers, and Sivanesan Dakshanamurthy *Drug Metabolism in Preclinical Drug Development: A Survey of the Discovery Process, Toxicology, and Computational Tools.* Current Drug Metabolism, 2018

[32] *Drug Delivery Systems Market (Delivery System - Intrauterine Implants, Prodrug Implants, Polymeric Drug Delivery, Targeted Drug Delivery; Application - Infectious Diseases, Oncology, Urology, Diabetes, CNS; Route of Administration - Oral, Injectable, Inhalation, Transdermal, Ocular, Nasal, and Topical) - Global Industry Analysis, Size, Share, Growth, Trends, and Forecast 2017 – 2025.* Market research report, 2018

[33] Park K. *Controlled drug delivery systems: past forward and future back*. Journal of

Controlled Release, 2014

[34] Ronald A. Siegel, Mahmood Falamarzian, Bruce A. Firestone, and Bret C. Moxley *pH-Controlled release from hydrophobic/polyelectrolyte copolymer hydrogels.* Journal of Controlled Release, 1988

[35] Schmaljohann D. *Thermo- and pH-responsive polymers in drug delivery.* Advanced Drug Delivery Reviews, 2006

[36] Patel A, Cholkar K, Agrahari V, and Mitra AK *Ocular drug delivery systems: An overview.* World journal of Pharmacology, 2013

[37] Stefano Fusco, George Chatzipirpiridis, Kartik M. Sivaraman, Olgaç Ergeneman, Bradley J. Nelson, and Salvador Pané *Chitosan Electrodeposition for Microrobotic Drug Delivery.* Advanced Healthcare Materials, 2013

[38] George Chatzipirpiridis, Olgaç Ergeneman, Juho Pokki, Franziska Ullrich, Stefano Fusco, José A. Ortega, Kartik M. Sivaraman, Bradley J. Nelson, and Salvador Pané *Electroforming of Implantable Tubular Magnetic Microrobots for Wireless Ophthalmologic Applications.* Advanced Healthcare Materials, 2015

[39] Gorkem Dogangil, Olgac Ergeneman, Jake J. Abbott, Salvador Pane, Heike Hall, Simon Muntwyler, and Bradley J. Nelson *Toward Targeted Retinal Drug Delivery with Wireless Magnetic Microrobots.* IEEE/RSJ International Conference on Intelligent Robots and Systems, 2008

[40] T. V. Thulasiramaraju, B. Tejeswar Kumar, M. Nikilesh Babu *Pulmonary drug delivery system: an overview.* Asian Journal of Research in Pharmaceutical Sciences and Biotechnology, 2013

[41] Per Gisle Djupesland *Nasal drug delivery devices: characteristics and performance in a clinical perspective—a review.* Drug Delivery and Translational Research, 2013

[42] Marc B. Brown, Gary P. Martin, Stuart A. Jones & Franklin K. Akomeah *Dermal and Transdermal Drug Delivery Systems: Current and Future Prospects.* Drug Delivery, 2008

[43] Yi Shi, William Porter, Thomas Merdan, and Luk Chiu Li *Recent advances in intravenous delivery of poorly water-soluble compounds*. Expert Opinion on Drug

Delivery, 2009

[44] Prakash Khadka, Jieun Ro, Hyeongmin Kim, Iksoo Kim, Jeong Tae Kim, Hyunil Kim, Jae Min Cho, Gyiae Yun, and Jaehwi Lee *Pharmaceutical particle technologies: An approach to improve drug solubility, dissolution and bioavailability*. Asian Journal of Pharmaceutical Sciences, 2014

[45] Xiaodi Guo, Rong-Kun Chang, and Munir A. Hussain *Ion-Exchange Resins as Drug Delivery Carriers.* Journal of Pharmaceutical Sciences, 2009

[46] Inderbir Singh, Ashish K. Rehni, Rohit Kalra, Gaurav Joshi, Manoj Kumar, Hassan Y. Aboul-Enein *Ion Exchange Resins: Drug Delivery and Therapeutic Applications.* Journal of Pharmaceutical Sciences, 2007

[47] Mongkol Sriwongjanya, and Roland Bodmeier *Effect of ion exchange resins on the drug release from matrix tablets European.* Journal of Pharmaceutics and Biopharmaceutics, 1998

[48] Seong Hoon Jeong, Kinam Park *Development of sustained release fast-disintegrating tablets using various polymer-coated ion-exchange resin complexes.* International Journal of Pharmaceutics, 2007

[49] Joana Mota *Matrix -and reservoir- type oral multiparticulate drug delivery systems.* Dissertation zur Erlangung des akademischen Grades des Doktors der Naturwissenschaften (Dr. rer. nat.) eingereicht im Fachbereich Biologie, Chemie, Pharmazie der Freien Universität Berlin, 2010

[50] Luciana Lisa Laoa, Nicholas A. Peppas, Freddy Yin Chiang Boeya, Subbu S. Venkatramana M*odeling of drug release from bulk-degrading polymers*. International Journal of Pharmaceutics, 2010

[51] Paolo Arosio, Valentina Busini, Giuseppe Perale, Davide Moscatelli and Maurizio Masi *A new model of resorbable device degradation and drug release - part I: zero order model.* Polymer International, 2008

[52] Emanuele Mauri, Simonetta Papa, Maurizio Masi, Pietro Veglianese, and Filippo Rossi *Novel functionalization strategies to improve drug delivery from polymers.* Expert Opinion on Drug Delivery, 2017

[53] David Rosen and Brent Stucker *Additive Manufacturing Technologies: 3D Printing, Rapid Prototyping, and Direct Digital Manufacturing*. Springer Science+Business Media, 2015

[54] R. Bernasconi, F. Cuneo, E. Carrara, G. Chatzipirpiridis, M. Hoop, X. Chen, B. J. Nelson, S. Pane′, C. Credi, M. Levi and L. Magagnin *Hard-magnetic cell microscaffolds from electroless coated 3D printed architectures.* Materials Horizons, 2018

[55] R. Bernasconi, C. Credi, M. Tironi, M. Levi and L. Magagnin *Electroless Metallization of Stereolithographic Photocurable Resins for 3D Printing of Functional Microdevices.* Journal of The Electrochemical Society, 2017

[56] R. Bernasconi, G. Natale, M. Levi, and L. Magagnin *Electroless Plating of NiP and Cu on Polylactic Acid and Polyethylene Terephthalate Glycol-Modified for 3D Printed Flexible Substrates*. Journal of The Electrochemical Society, 2016

[57] A. Abdel Aal, A. Shaaban, Z. Abdel Hamid *Nanocrystalline soft ferromagnetic Ni–Co–P thin film on Al alloy by low temperature electroless deposition.* Applied Surface Science, 2008

[58] M. Tironi *Metallization of stereolithography 3d printed microdevices*. Master's thesis Politecnico di Milano Department of Chemistry, Materials and Chemical Engineering «Giulio Natta» Master of Science in Materials Engineering and Nanotechnology, 2016

[59] F. Cuneo *Metallization of 3D printed μscaffolds for magnetic actuation.* Master's thesis, Politecnico di Milano Department of Chemistry, Materials and Chemical Engineering «Giulio Natta» Master of Science in Materials Engineering and Nanotechnology, 2016

[60] Y. S. Won, S. S. Park, J. Lee, Kim, and S. Lee *The pH effect on black spots in surface finish: Electroless nickel immersion gold.* Applied Surface Science, 2010

[61] C. Hsu, C. Li and G. Wang *Fabrication of biocompatible high aspect ratio Au–Ni coaxial nanorod arrays using the electroless galvanic displacement reaction method*. RSC Advances, 2014

[62] C. Bellmann, N. Beshchasna, J. Uhlemann, and K.J. Wolter *Parylene C and silicone*

as biocompatible protection encapsulants for PCB. 32nd Int. Spring Seminar Electronics Technology, Brno, Czech Republic, 2009 (ISSE)

[63] A. Bozkurt, and A. Lal *Low-cost flexible printed circuit technology based microelectrode array for extracellular stimulation of the invertebrate locomotory system*. Sensors and actuators, 2011

[64] S. Erni, S. Schurle, A. Fakhraee, B. E. Kratochvil, and B. J. Nelson *Comparison, optimization, and limitations of magnetic manipulation systems.* Journal of Micro-Bio Robotics, 2013

[65] M. P. Kummer, J. J. Abbott, B. E. Kratochvil, R. Borer, A. Sengul, and B.y J. Nelson *OctoMag: An Electromagnetic System for 5-DOF Wireless Micromanipulation.* IEEE transactions on robotics, 2010

[66] B. Jang, E. Gutman, N. Stucki, B. F. Seitz, P.D. Wendel-García, T. Newton, J. Pokki, O. Ergeneman, S. Pane, Y. Or and B. J. Nelson *Undulatory Locomotion of Magnetic Multilink Nanoswimmers.* NanoLetters, 2015

[67] C. Peters, M. Hoop , S. Pané , B. J. Nelson ,and C. Hierold *Degradable Magnetic Composites for Minimally Invasive Interventions: Device Fabrication, Targeted Drug Delivery, and Cytotoxicity Tests.* Advanced Materials, 2016

[68] K. Berk Yesin, K. Vollmers and B. J. Nelson *Modeling and Control of Untethered Biomicrorobots in a Fluidic Environment Using Electromagnetic fields*. The International Journal of Robotics Research, 2006

[69] E. Carrara *Magnetically actuated microdevices combining pollutants photodegradation with bacteria killing functionalities for water quality control*. Master's thesis, Politecnico di Milano Department of Chemistry, Materials and Chemical Engineering "Giulio Natta" Master of Science in Materials Engineering and Nanotechnology, 2017

[70] Giuseppe Perale, Filippo Rossi, Marco Santoro, Marco Peviani, Simonetta Papa, Dorina Llupi, Paola Torriani, Edoardo Micotti, Sara Previdi, Luigi Cervo, Erik Sundström, Aldo R. Boccaccini, Maurizio Masi, Gianluigi Forloni, and Pietro Veglianese *Multiple drug delivery hydrogel system for spinal cord injury repair strategies.*

Journal of Controlled Release, 2012

[71] Samantha Forster, Alfred E. Thumser, Steve R. Hood, and Nick Plant *Characterization of Rhodamine-123 as a Tracer Dye for Use In In vitro Drug Transport Assays.* PLoS ONE, 2012

[72] Antranik Jonderian and Rita Maalouf *Formulation and In vitro Interaction of Rhodamine-B Loaded PLGA Nanoparticles with Cardiac Myocytes.* Frontiers in pharmacology, 2016

[73] William Clarke *Drug Monitoring and Clinical Chemistry* in Handbook of Analytical Separations, 2004

[74] Ana Blandino, Manuel Macìas, and Dominigo Cantero *Formation of Calcium Alginate Gel Capsules: Influence of Sodium Alginate and CaCl2 Concentration on Gelation Kinetics.* Journal of Bioscience and Bioengineering, 1999

[75] Thijs Grünhagen *Characterisation of the degrading properties of alginate under influence of citrate*. Section Materials Technology Department of Tissue-engineering and Biomechanics Eindhoven University of Technology, 2002

[76] Giri, T. K., Thakur, A., Alexander, A., Badwaik, H. & Tripathi, D. K. *Modified chitosan hydrogels as drug delivery and tissue engineering systems: present status and applications*. Acta Pharm., 2012

[77] Agüero, Zaldivar-Silva, Pena and Dias *Alginate microparticles as oral colon drug delivery device: A review*. Carbohydrates Polymers, 2017.

[78] N. K. Sing, D.S. Lee *In situ gelling pH- and temperature-sensitive biodegradable block 3 copolymer hydrogels for drug delivery.* Journal of Controlled Release, 2014

[79] Mohd Cairul Iqbal Mohd Amin, Naveed Ahmad, Manisha Pandey, Muhammad Mustafa Abeer & Najwa Mohamad *Recent advances in the role of supramolecular hydrogels in drug delivery.* Expert opinion on drug delivery, 2015

[80] Rashmi Boppana, Raghavendra V. Kulkarni, G. Krishna Mohan, Srinivas Mutalikc and Tejraj M. Aminabhavi *In vitro and in vivo assessment of novel pHsensitive interpenetrating polymer networks of a graft copolymer for gastro-protective delivery of ketoprofen.* RSC Adv., 2016

[81] Frank Biedermann, Eric A. Appel, Jesus del Barrio, Till Gruendling, Christopher Barner-Kowollik, and Oren A. Scherman *Postpolymerization Modification of Hydroxyl-Functionalized Polymers with Isocyanates.* Macromolecules, 2011

[82] Bin Wei,a Liangqi Ouyang,a Jinglin Liua and David C. Martin *Post-polymerization functionalization of poly(3,4-propylenedioxythiophene) (PProDOT) via thiol–ene ''click'' chemistry.* Journal of Materials Chemistry B, 2015

83] García-Astrain, C. & Avérous, L. *Synthesis and evaluation of functional alginate hydrogels based on click chemistry for drug delivery applications*. Carbohydrate Polymers, 2018.

84] Mauri E., Papa S., Masi M., Veglianese P. and Rossi F. *Novel functionalization strategies to improve drug delivery from polymers*. Expert Opinion Drug Delivery, 2017.

[85] Christopher D. Hein,1 Xin-Ming Liu,1 and Dong Wang *Click Chemistry, A Powerful Tool for Pharmaceutical Sciences.* Pharmaceutical Research, Vol. 25, No. 10, 2008

[86] Ronald A. Siegel, Mahmood Falamarzian, Bruce A. Firestone and Bret C. Moxley *pH-controlled release from hydrophobic polyelectrolyte copolymer hydrogels*. Journal of Controlled Release, 1988

[87] Ji-Sheng Yang∗, Ying-Jian Xie, Wen He *Research progress on chemical modification of alginate: A review.* Carbohydrate polymers, 2011

[88] M. Leonarda, M. Rastello De Boissesona , P. Huberta , F. Dalenconb , E. Dellacheriea *Hydrophobically modified alginate hydrogels as protein carriers with specific controlled release properties.* Journal of Controlled Release, 2004

[89] Xi Chen, Qianzhen Wu, Lars Henschke, Günther Weber, Tanja Weil *An efficient and versatile approach for the preparation of a rhodamine B ester bioprobe library.* Dyes and Pigments, 2012

[90] Emanuele Mauri, *Shyntesis and characterization of RGD functionalized hydrogels for cell adhesion*. master thesis in Chemical Engineering, DCMIC, Politecnico di Milano, 2014

[91] M. M. Soledad Lencina, Noemí A. Andreucetti, César G. Gómez and Marcelo

A. Villar *Recent Studies on Alginates Based Blends, Composites, and Nanocomposites*. Advanced structured materials, 2013

[92] Morten Meldal, and Christian Wenzel Tornøe *Cu-Catalyzed Azide-Alkyne Cycloaddition.* Chem. Rev., 2008

[93] Sukdeb Saha, Mahesh U. Chhatbar, Prasenjit Mahato, L. Praveen, A. K. Siddhanta and Amitava Das *Rhodamine-alginate conjugate as self-indicating gel bead for efficient detection and scavenging of Hg2+ and Cr3+ in aqueous media*. Chemical Communications, 2011

[94] Xiao-Feng Yang, Xiang-Qun Guo, Yi-Bing Zhao *Novel spectrofluorimetric method for the determination of sulfite with rhodamine B hydrazide in a micellar medium*. Analytica Chimica Acta, 2002

[95] V. Dujols, F. Ford, A.W. Czarnik*A Long-Wavelength Fluorescent Chemodosimeter Selective for Cu(II) Ion in Water.* Journal of American Chemical Society, 1997

96] Mariana Beija, Carlos A. M. Afonso and Jose´ M. G. Martinho *Synthesis and applications of Rhodamine derivatives as fluorescent probes.* Chem. Society Review, 2009

[97] Frédéric Vallée, Christophe Müller, Alain Durand, Sarah Schimchowitsch, Edith Dellacherie, Christian Kelche, Jean Christophe Cassel, Michèle Leonard *Synthesis and rheological properties of hydrogels based on amphiphilic alginate-amide derivatives.* Carbohydrate Research, 2009

[98] Boris Polyak, Shimona Geresh, and Robert S. Marks *Synthesis and Characterization of a Biotin-Alginate Conjugate and Its Application in a Biosensor Construction.* Biomacromolecules, 2004

99] Khalil Abu-Rabeah, Boris Polyak, Rodica E. Ionescu, Serge Cosnier, and Rober *Synthesis and Characterization of a Pyrrole-Alginate Conjugate and Its Application in a Biosensor Construction.* Biomacromolecules, 2005

[100] Y L Li, W X Wang, Y Wang, W B Zhang, H M Gong, and M X Liu *Synthesis and Characterization of Rhodamine B-ethylenediamine-hyaluronan Acid as Potential Biological Functional Materials.* IOP Conference Series: Materials Science and Engineering, Volume 359, conference 1, 2018